

## **Copyright Warning & Restrictions**

The copyright law of the United States (Title 17, United States Code) governs the making of photocopies or other reproductions of copyrighted material.

Under certain conditions specified in the law, libraries and archives are authorized to furnish a photocopy or other reproduction. One of these specified conditions is that the photocopy or reproduction is not to be “used for any purpose other than private study, scholarship, or research.” If a user makes a request for, or later uses, a photocopy or reproduction for purposes in excess of “fair use” that user may be liable for copyright infringement,

This institution reserves the right to refuse to accept a copying order if, in its judgment, fulfillment of the order would involve violation of copyright law.

**Please Note: The author retains the copyright while the New Jersey Institute of Technology reserves the right to distribute this thesis or dissertation**

Printing note: If you do not wish to print this page, then select “Pages from: first page # to: last page #” on the print dialog screen

The Van Houten library has removed some of the personal information and all signatures from the approval page and biographical sketches of theses and dissertations in order to protect the identity of NJIT graduates and faculty.

## ABSTRACT

### Magnetohydrodynamic Behavior under Current Impulse Excitation

by  
Shi Wu

The effects of magnetic field on magnetohydrodynamic (MHD) channel flow between two parallel plates of infinite extent are investigated. The applied magnetic field is due to an infinite impulse current-carrying conductor located a small distance below the lower channel wall. Influence of the induced magnetic field, such that the magnetic Reynolds number ( $R_m$ ) is less than unity but greater than zero, is included. The solution is obtained using the perturbation theory in the expansion of the field components in a double-power series in  $R_m$  and  $I$ . Calculations for the magneto-fluid components were carried out using personal computer. The computer programming is focused on the component of induced magnetic field  $B_{x1}$ . It covers every single term of the tangential induced magnetic field component  $B_{x1}$  and the total component. The results can be used to develop applying impulse acceleration of exhaust plasma in a fusion-MHD power generator.

**Magnetohydrodynamic Behavior under  
Current Impulse Excitation**

**by  
Shi Wu**

**A Thesis  
Submitted to the Faculty of  
New Jersey Institute of Technology  
in Partial Fulfillment of the Requirements for the Degree of  
Master of Science in Electrical Engineering**

**Department of Electrical and Computer Engineering**

**October 1993**



**APPROVAL PAGE**

**Magnetohydrodynamic Behavior under  
Current Impulse Excitation**

**Shi Wu**

*8-20-93*

---

Dr. Khalil Denno, Thesis Advisor  
Distinguished Professor of Electrical and Computer Engineering, NJIT

*8/20/93*

---

Dr. Waild Hubbi, Committee Member  
Associate Professor of Electrical and Computer Engineering, NJIT

*August 20, 1993*

---

Dr. Edip Niver, Committee Member  
Associate Professor of Electrical and Computer Engineering, NJIT

## **BIOGRAPHICAL SKETCH**

**Author:** Shi Wu

**Degree:** Master of Science in Electrical Engineering

**Date:** October 1993

**Date of Birth:**

**Place of Birth:**

**Undergraduate and Graduate Education:**

- Master of Science in Electrical Engineering,  
New Jersey Institute of Technology, Newark, NJ, 1993
- Bachelor of Science in Industry Automation,  
Shanghai University of Technology, Shanghai, P. R. China, 1987

**Major:** Electrical Engineering

## **ACKNOWLEDGMENT**

The author wishes to express his sincere gratitude to his supervisor, the late Dr. Khalil Denno, for his guidance, friendship and moral support throughout this research.

Special thanks to Professor Walid Hubbi and Professor Edip Niver for serving as members of the committee. And the author appreciates the timely help and suggestions from Professor Hubbi.

And finally, a thank you to Joel Schneiderman for his help.



## TABLE OF CONTENTS

Chapter	Page
1 INTRODUCTION .....	1
1.1 Magnetohydrodynamic Flow Problems .....	1
1.2 Fundamental Limitation on Linearity .....	6
2 THEORY OF MHD .....	9
2.1 The Magneto-Fluid Equations .....	9
2.2 Derivation of the Induced Magnetic-Field Equations .....	15
3 PHASES OF COMPUTATIONS .....	17
3.1 Solution of the Induced Magnetic Field Equations .....	17
3.2 The Computer Programming and Calculation .....	26
4 DISCUSSION AND RESULTS .....	32
5 CONCLUSIONS .....	52
APPENDIX .....	56
REFERENCES .....	94

## LIST OF FIGURES

Figure	Page
1.1 Schematic of Magnetohydrodynamic Converter .....	7
1.2 Boundary Layer Development with Magnetic Field Generated by Impulse Current-carrying Conductor under Lower Electrode .....	8
3.1 Axial component of induced magnetic field $B_{x11}$ .....	29
4.1(a) Axial Component of Induced Magnetic Field 1, $y=1$ , $-100 < x < 100$ .....	56
4.1(b) Axial Component of Induced Magnetic Field 1, $y=1$ , $-2 < x < 2$ .....	56
4.2(a) Axial Component of Induced Magnetic Field 1, $y=5$ , $-100 < x < 100$ .....	57
4.2(b) Axial Component of Induced Magnetic Field 1, $y=5$ , $-8 < x < 8$ .....	57
4.3(a) Axial Component of Induced Magnetic Field 1, $y=10$ , $-100 < x < 100$ .....	58
4.3(b) Axial Component of Induced Magnetic Field 1, $y=10$ , $-20 < x < 20$ .....	58
4.4 Axial Component of Induced Magnetic Field 1, $y=50$ , $-100 < x < 100$ .....	59
4.5(a) Axial Component of Induced Magnetic Field 1, $y=100$ , $-100 < x < 100$ .....	59
4.5(b) Axial Component of Induced Magnetic Field 1, $y=100$ , $-150 < x < 150$ .....	60
4.6(a) Axial Component of Induced Magnetic Field 1, $y=200$ , $-100 < x < 100$ .....	60
4.6(b) Axial Component of Induced Magnetic Field 1, $y=200$ , $-300 < x < 300$ .....	61
4.7(a) Axial Component of Induced Magnetic Field 1, $y=500$ , $-100 < x < 100$ .....	61
4.7(b) Axial Component of Induced Magnetic Field 1, $y=500$ , $-700 < x < 700$ .....	62
4.8(a) Axial Component of Induced Magnetic Field 1, $y=1000$ , $-100 < x < 100$ ...	62
4.8(b) Axial Component of Induced Magnetic Field 1, $y=1000$ , $-1000 < x < 1000$ .....	63
4.9(a) Axial Component of Induced Magnetic Field 2, $y=1$ , $-100 < x < 100$ .....	63
4.9(b) Axial Component of Induced Magnetic Field 2, $y=1$ , $-2 < x < 2$ .....	64
4.10(a) Axial Component of Induced Magnetic Field 2, $y=5$ , $-100 < x < 100$ .....	64
4.10(b) Axial Component of Induced Magnetic Field 2, $y=5$ , $-4 < x < 4$ .....	65

<b>Figure</b>	<b>Page</b>
4.11(a) Axial Component of Induced Magnetic Field 2, $y=10$ , $-100 < x < 100$ .....	65
4.11(b) Axial Component of Induced Magnetic Field 2, $y=10$ , $-10 < x < 10$ .....	66
4.12(a) Axial Component of Induced Magnetic Field 2, $y=50$ , $-100 < x < 100$ .....	66
4.12(b) Axial Component of Induced Magnetic Field 2, $y=50$ , $-40 < x < 40$ .....	67
4.13 Axial Component of Induced Magnetic Field 2, $y=100$ , $-100 < x < 100$ .....	67
4.14(a) Axial Component of Induced Magnetic Field 2, $y=200$ , $-100 < x < 100$ ....	68
4.14(b) Axial Component of Induced Magnetic Field 2, $y=200$ , $-150 < x < 150$ ....	68
4.15(a) Axial Component of Induced Magnetic Field 2, $y=500$ , $-100 < x < 100$ ....	69
4.15(b) Axial Component of Induced Magnetic Field 2, $y=500$ , $-400 < x < 400$ .....	69
4.16(a) Axial Component of Induced Magnetic Field 2, $y=1000$ , $-100 < x < 100$ ...	70
4.16(b) Axial Component of Induced Magnetic Field 2, $y=1000$ , $-1000 < x < 1000$ .....	70
4.17(a) Axial Component of Induced Magnetic Field 3, $y=1$ , $-100 < x < 100$ .....	71
4.17(b) Axial Component of Induced Magnetic Field 3, $y=1$ , $-2 < x < 2$ .....	71
4.18(a) Axial Component of Induced Magnetic Field 3, $y=5$ , $-100 < x < 100$ .....	72
4.18(b) Axial Component of Induced Magnetic Field 3, $y=5$ , $-4 < x < 4$ .....	72
4.19(a) Axial Component of Induced Magnetic Field 3, $y=10$ , $-100 < x < 100$ .....	73
4.19(b) Axial Component of Induced Magnetic Field 3, $y=10$ , $-8 < x < 8$ .....	73
4.20(a) Axial Component of Induced Magnetic Field 3, $y=50$ , $-100 < x < 100$ .....	74
4.20(b) Axial Component of Induced Magnetic Field 3, $y=50$ , $-60 < x < 60$ .....	74
4.21 Axial Component of Induced Magnetic Field 3, $y=100$ , $-100 < x < 100$ .....	75
4.22 (a) Axial Component of Induced Magnetic Field 3, $y=200$ , $-100 < x < 100$ .....	75
4.22(b) Axial Component of Induced Magnetic Field 3, $y=200$ , $-150 < x < 150$ .....	76
4.23(a) Axial Component of Induced Magnetic Field 3, $y=500$ , $-100 < x < 100$ ....	76
4.23(b) Axial Component of Induced Magnetic Field 3, $y=500$ , $-400 < x < 400$ ....	77

<b>Figure</b>	<b>Page</b>
4.24(a) Axial Component of Induced Magnetic Field 3, $y=1000$ , $-100 < x < 100$ ...	77
4.24(b) Axial Component of Induced Magnetic Field 3, $y=1000$ , $-1000 < x < 1000$ .....	78
4.25(a) Axial Component of Induced Magnetic Field 4, $y=1$ , $-100 < x < 100$ .....	78
4.25(b) Axial Component of Induced Magnetic Field 4, $y=1$ , $-1 < x < 1$ .....	79
4.26(a) Axial Component of Induced Magnetic Field 4, $y=5$ , $-100 < x < 100$ .....	79
4.26(b) Axial Component of Induced Magnetic Field 4, $y=5$ , $-4 < x < 4$ .....	80
4.27(a) Axial Component of Induced Magnetic Field 4, $y=10$ , $-100 < x < 100$ .....	80
4.27(b) Axial Component of Induced Magnetic Field 4, $y=10$ , $-8 < x < 8$ .....	81
4.28(a) Axial Component of Induced Magnetic Field 4, $y=50$ , $-100 < x < 100$ .....	81
4.28(b) Axial Component of Induced Magnetic Field 4, $y=50$ , $-40 < x < 40$ .....	82
4.29(a) Axial Component of Induced Magnetic Field 4, $y=100$ , $-100 < x < 100$ ....	82
4.29(b) Axial Component of Induced Magnetic Field 4, $y=100$ , $-40 < x < 40$ .....	83
4.30(a) Axial Component of Induced Magnetic Field 4, $y=200$ , $-100 < x < 100$ ....	83
4.30(b) Axial Component of Induced Magnetic Field 4, $y=200$ , $-150 < x < 150$ ....	84
4.31(a) Axial Component of Induced Magnetic Field 4, $y=500$ , $-100 < x < 100$ ....	84
4.31(b) Axial Component of Induced Magnetic Field 4, $y=500$ , $-400 < x < 400$ ....	85
4.32(a) Axial Component of Induced Magnetic Field 4, $y=1000$ , $-100 < x < 100$ ...	85
4.32(b) Axial Component of Induced Magnetic Field 4, $y=1000$ . $-1000 < x < 1000$ .....	86
4.33(a) Axial Component of Induced Magnetic Field, $y=1$ , $-100 < x < 100$ .....	86
4.33(b) Axial Component of Induced Magnetic Field, $y=1$ , $-1 < x < 1$ .....	87
4.34(a) Axial Component of Induced Magnetic Field, $y=5$ , $-100 < x < 100$ .....	87
4.34(b) Axial Component of Induced Magnetic Field, $y=5$ , $-4 < x < 4$ .....	88
4.35(a) Axial Component of Induced Magnetic Field, $y=10$ , $-100 < x < 100$ .....	88
4.35(b) Axial Component of Induced Magnetic Field, $y=10$ , $-8 < x < 8$ .....	89

<b>Figure</b>	<b>Page</b>
4.36 Axial Component of Induced Magnetic Field, $y=50$ , $-100 < x < 100$ .....	89
4.37(a) Axial Component of Induced Magnetic Field, $y=100$ , $-100 < x < 100$ .....	90
4.37(b) Axial Component of Induced Magnetic Field 4, $y=100$ , $-40 < x < 40$ .....	90
4.38(a) Axial Component of Induced Magnetic Field 4, $y=200$ , $-100 < x < 100$ ....	91
4.38(b) Axial Component of Induced Magnetic Field 4, $y=200$ , $-150 < x < 150$ ....	91
4.39(a) Axial Component of Induced Magnetic Field 4, $y=500$ , $-100 < x < 100$ .....	92
4.39(b) Axial Component of Induced Magnetic Field 4, $y=500$ , $-400 < x < 400$ ....	92
4.40(a) Axial Component of Induced Magnetic Field 4, $y=1000$ , $-100 < x < 100$ ...	93
4.40(b) Axial Component of Induced Magnetic Field 4, $y=1000$ . $-1000 < x < 1000$ .....	93
5.1 Axial Component of Induced Magnetic Field .....	54
5.2 3-D Axial Component of Induced Magnetic Field .....	55

## **Chapter 1**

### **INTRODUCTION**

#### **1.1 MAGNETOHYDRODYNAMIC FLOW PROBLEMS**

The research of seeking new, primary, energy resource while at the same time establishing other power generating schemes that result in an eventual increase of efficiency has been done by many scientists. Conventional power generating systems depend on their primary energy source. Fossil fuel reserves are becoming increasingly limited in supply. This impending shortage is already acute in many areas. The inefficiency of fossil fuel that increases pollution and contributes to fuel supply problems must be addressed head on. Magnetohydrodynamic power generating cycles augmenting a cycle for conventional steam systems will result in an increase in conversion efficiency because of MHD cycle's operating at high temperature, resulting in increased thermal efficiency. It has been reported that with fossil fuels, MHD would bring about a saving in fuel of about one third. And MHD affords the opportunity of reducing thermal pollution and related undesirables. More rigorous studies are needed in order to prove the feasibility of open cycle MHD on a commercial level. Problems to be solved relate to optimum channel dimensions, protection of channel walls from the hot conducting plasma, and fuel preparation. Other problems concern thermal efficiency of the channel, air preheating, and electrode distribution and orientation. The MHD generator has the following distinct advantages over conventional electric power generation methods. 1) It can handle extremely high temperatures. 2) It can handle very high power levels. 3) It has no moving parts or close tolerances. 4) It can start and reach full power very rapidly. Solutions for the following magnetofluid components have to be obtained: 1) Total axial and transverse

magnetic fields (applied and induced). 2) Induced electric fields. 3) Total gas velocity components. 4) Pressure gradient and total pressure components. 5) Magnetic pressure gradient and magnetic pressure components. 6) Induced current densities. This paper is focusing on the first part " Axial and transverse magnetic fields (induced)."

Early work of the magnetohydrodynamic (MHD) effects in inviscid flow fields with large electrical conductivity and strong applied magnetic fields were investigated by several researchers. Among the dimensionless important groups in every magneto-fluid dynamic flow are 1) The magnetic Reynolds number  $R_m$ , which expresses the ratio of the induced magnetic induction to the applied field, and 2) the magnetic force coefficient, which is the ratio of the electromagnetic force per unit volume to the inertia forces per unit volume in the fluid. One-dimensional MHD flow has been researched by Resler and Sears (1958). Two-dimensional perturbation flows at infinite, and at large but finite magnetic Reynolds numbers have been discussed by Resler and Seras (1959); they showed that the vortex and current sheet that lies on the surface of a solid body in steady plane or axisymmetric aligned-fields flow of an ideal inviscid conductor become, at large but finite  $R_m$ , a boundary layer of large vorticity and distinct sizable current density. If this magnetohydrodynamic number is very small, this boundary layer consists of an inviscid boundary layer whose thickness is very small, underlain by a much thinner viscous sublayer within which the significant magnetic-field components are essentially constant. The viscous sublayer is described by the same equation as the viscous boundary layer at low  $R_m$ . And many general solutions for finite magnetic Reynolds number and finite magnetic force coefficient have been obtained by Williams (1960). Hains has described a general method of characteristics for use in supersonic flow under these conditions: magneto-fluid flows in which the

magnetic Reynolds number is very small, and the applied magnetic field remains unperturbed by currents produced in the fluid, where he considered small values of the magnetic force coefficient, and obtained solutions for both subsonic and supersonic flow. Ludford has studied the case in which  $R_m$  is small, the magnetic force coefficient is very large and only pressure and magnetic forces are present. The geometrical configurations to be studied were suggested by Scherman, in which a steady two-dimensional, uniform, slightly conducting, incompressible flow passes through a channel; at which a two dimensional uniform magnetic field, is applied to the flow and has the general defect of obstructing it. In a particular case studied by Scherman the magnetic field was due to a current flowing in a straight conductor lying outside the channel and perpendicular to the flow.

In 1970s, Denno did significant research on MHD and got solutions for the induced magnetic field on plasma flow depending on different levels of ionization degree and the field strength. His studies included the cases of infinite and non-zero magnetic Reynolds number ( $R_m$ ) corresponding to situations of highly conducting and weakly ionized plasma, respectively. Since the most important of these features is the small value of the magnetic Reynolds number, the emphasis in his work was to derive expressions for the pressure gradient along the channel wall and to establish criteria for boundary layer separation where  $0 \leq R_m \leq 1$ . The effect of the induced field must be considered in the treatment of inviscid MHD channel flow. In Denno's paper also, MHD effects in an MHD channel flow are considered for the case where the fluid properties are such that the Reynolds number is less than unity but cannot be neglected. So that the induced magnetic field is taken into account. In [1], he described the magnetic flow between infinite parallel plates of arbitrary separation. Solution of the induced magnetic field perturbation



equation, the flow-field perturbation equations and that for the total pressure gradient and the magnetic pressure gradient were solved. The study was also confined where  $R_m$  is of the order of 0.10 or greater, the induced magnetic field effects must be taken into account in any treatment of inviscid MHD channel flow resulting with boundary layer separation. For  $R_m$  equals or greater than 0.1, an increase in the adverse pressure gradient along the channel is observed to result in a considerable improvement in boundary layer separation, and providing protection to the channel from the high temperature fluid. As the channel height increases, the influence of the induced magnetic field increases, and the maximum magnitude of the total and magnetic pressure gradients due to the induced magnetic field along the wall increase with the channel height. A comprehensive analytical study of the magnetic and flow fields in an MHD channel using the principles of the theory of perturbation coupled to the concept of the magnetic boundary layer was developed in [1]. Denno used a close mathematical form using the perturbation theory and the existence of magnetic boundary layer approximation for solution of the magnetic and flow field perturbations for incompressible and inviscid plasma problems in a paralleled plate channel. It was established that perturbation in total plasma pressure is directly connected to channel height. As the channel height increases, total pressure may be reduced, while magnetic pressure continuous increase. Continuous increase in the magnetic pressure can be taken as a measure of power dissipation in the MHD flow. Few years later, the behavior of the weakened fusion plasma with its electrical conductivity changing linearly along the MHD channel length was investigated. The results showed that fusion plasma with extremely high temperature and with high degree of ionization, if subjected to an applied magnetic field, will lead to a situation of aligned flow, with total boundary layer separation from channel wall; The

present trend for utilizing fusion plasma in MHD generation field is by mixing it with a weakly ionized plasma to a level at which the mixture will attain a certain desirable level of ionization, although weakening a perfectly conducting fluid may not be the best approach. And Denno showed that to reduce the perfect conductivity of fusion plasma is a disadvantage. He indicated that an excellent conducting fluid for using MHD induction type generator is a challenge.

Since the separation of the hot conducting fluid from the channel walls results in protecting the channel from the high-temperature, high-speed plasma, several investigators explored various schemes to use the MHD effects to reduce the amount of heat transfer from the fluid to the MHD channel. Investigations were conducted on an inviscid, incompressible flow under conditions of small magnetic Reynolds number to the extent that the induced magnetic field is neglected. In this thesis, the MHD effects in an MHD channel flow are considered for the case where the fluid properties are such that the magnetic Reynolds numbers is less than unity but cannot be neglected. Therefore, the induced magnetic field is taken into account. The fluid is assumed to be incompressible, inviscid, electrically conductivity such that  $0 < R_m < 1$ .

## 1.2 STATEMENT OF THE PROBLEM

The principle of MHD generation of electricity is that when a conducting fluid moves across a magnetic flux an e.m.f. is induced in it. When this gas is passed through the magnetic field an e.m.f. is induced, mutually perpendicular to the magnetic field direction and to direction of the gas flow. If suitable electrodes are placed in the appropriate position and connected to an external load, then this e.m.f. will produce a current capable of performing useful work.

The generation of electricity in the MHD converter is based upon the Faraday effect: that is, a voltage is generated across a conductor that is caused to move through a magnetic field. Figure 1-1 shows the essential features. To simplify electrodynamics of MHD generators, many line conductors form current sheet under the low plate electrode.

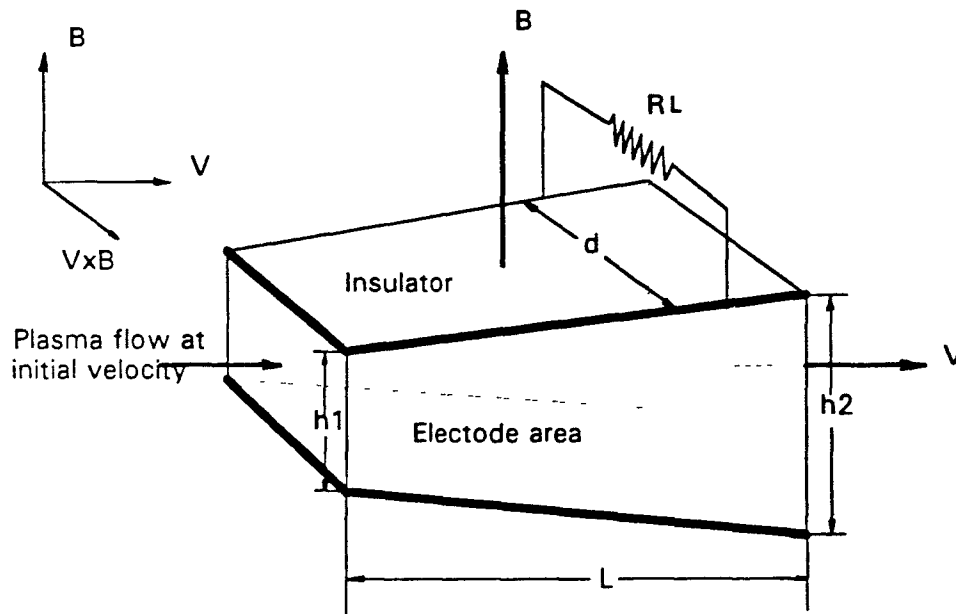


Figure 1-1 Schematic of magnetohydrodynamic converter

Figure 1-2 shows a conducting fluid flowing between two infinite parallel plates of arbitrary separation. At the channel entrance, the plasma is of zero viscosity and incompressible. The applied magnetic field is due to an infinite length of current-carrying conductor located a small distance  $y_0$  below the lower channel wall. In one line conductor, the current equation is:  $i(t) = I\delta(t)$ .

1) The problem is: To solve for the induced magnetic field and variations in the flow field (work in two dimensions) within the MHD channel, due to impulse excitation.

2) The problem objectives physically and mathematically: To develop clear impact of magnetic field perturbation on boundary layer separation. Let the infinite conductor be located at  $X = 0$ ,  $Y = -y_0$  and carry a current  $I\delta(0, -y_0, t)$ .

$I\delta(0, -y_0, t)$  is a function of  $x$ ,  $y$  and  $t$ . And it only happens at  $x=0, y=-y_0$ ,  $t$  can be any time. The field produced by current impulse conductor is identified as applied field  $B_0$ . The components of the applied magnetic field in dimensionless form is used to find the induced magnetic field  $B_{x1}$ :

$$B_{y_0} = \frac{I}{2\pi} \frac{x}{x^2 + (y + y_0)^2} \delta(0, -y_0, t) \quad (1)$$

$$B_{x_0} = \frac{I}{2\pi} \frac{(y + y_0)}{x^2 + (y + y_0)^2} \delta(0, -y_0, t) \quad (2)$$

In equation (1) and (2),  $t$  does not effect  $B_{x_0}, B_{y_0}$  themselves. So that these two equations can be written as:

$$B_{y_0} = \frac{I}{2\pi} \frac{x}{x^2 + (y + y_0)^2} \delta(0, -y_0)$$

$$B_{x_0} = \frac{I}{2\pi} \frac{(y + y_0)}{x^2 + (y + y_0)^2} \delta(0, -y_0)$$

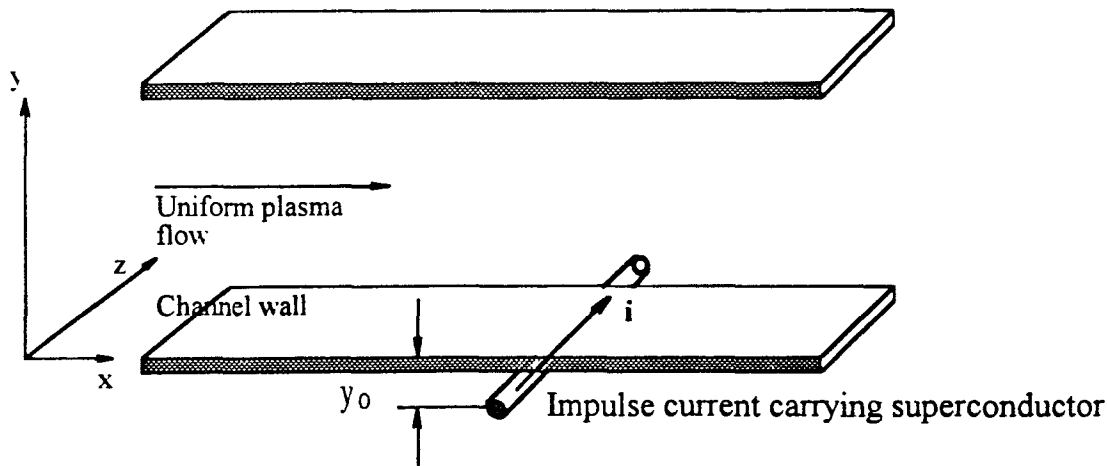


**Figure 1-2** Boundary layer development with magnetic field generated by impulse current-carrying conductor under lower electrode

Derivation of the equations representing distortion in the magnetic field and in the flow field is presented in Chapter 2 of this paper; their solution is given in Chapter 3.

The treatment involves the use of perturbation theory in the expansion of the magnetic-field and flow-field components in a double-power series in  $R_m$  and  $I$ , the magnetic Reynolds number and the magnetic interaction parameter, respectively. The effect of the induced magnetic field is to be determined.

## Chapter 2

### THEORY OF MHD

#### 2.1 THE MAGNETO -FLUID EQUATIONS

Various authors have given the basic equations for the flow field equations and electromagnetic field equations. The following equations (3) through (12) are very approximate and valid when the fluid is treated as a whole continuity as indicated in "Energy Conversion" by E. Walsh, Ronald Press (1967).

Consider a volume element in the coordinate system shown in Figure 1-2. The fluid is assumed as a whole continuum. If the fluid is moving with a certain velocity, and a scalar conductivity, then the current per unit area induced by the motion of the gas through a magnetic field of strength  $B$  is :

$$j = \sigma(VB - E) \quad (3)$$

where  $E$  is the internal electric field due to the load. It is customary to define a loading parameter  $K$ :

$$K = \frac{E}{VB} \quad (4)$$

So it can be written as:

$$j = (1 - K)\sigma VB \quad (5)$$

Then the power  $P$  delivered to the load, per unit volume of the generator, is:

$$P_0 = jE = K(1 - K)\sigma V^2 B^2 \quad (6)$$

The electric field and the power may be rearranged to give the output voltage and power per unit cube as a function of current. The results are:

$$E = VB - \frac{j}{\sigma} \quad (7)$$

$$P_0 = jVB - \frac{j^2}{\sigma} \quad (8)$$

that is the voltage varies linearly and the power quadratically with current just as is the case with most electric power sources. Of course in the MHD generator, as in conventional rotating machinery, these rules are not followed exactly if  $V$ ,  $B$ , or  $\sigma$  vary with current.

The force  $F$  on a unit cube of the gas will be opposed to the gas motion and given by:

$$F = jB = (1 - K)\sigma V B^2 \quad (9)$$

In order for the gas to move through the generator against this force, there must be a pressure difference  $\Delta p$  between the entrance and exit given approximately by

$$\Delta p = FL = (1 - K)\sigma V B^2 L \quad (10)$$

where  $L$  is the flow length of the generator.

The rate at which the gas does work pushing itself through the magnetic field is:

$$P_p = FV = (1 - K)\sigma V^2 B^2 \quad (11)$$

The ratio between the power output and the push work is the electrical efficiency  $\eta_e$ , ( $k$  is a constant):

$$\eta_e = \frac{P_o}{P_p} = k \quad (12)$$

Because the joule dissipation in this device occurs within the working fluid rather than in an external conductor, it is not lost energy, but it does represent a departure from thermodynamic reversibility.

In MHD energy conversion the conditions encountered and the approximations used are quite different from those associated with fusion and astrophysical research. One of the more important differences is the value of a dimensionless quantity known as the magnetic Reynolds number  $R_m$  where:

$$R_m = \mu_o \sigma_g VL \quad (13)$$

where  $\mu_0$  = permeability of free space

$\sigma_g$  = gas conductivity

$V$  = gas velocity

$L$  = length characteristic of problem

In general,  $R_m$  is large compared with unity in fusion research and astrophysics, but equal to or less than unity in MHD conversion power generation. In engineering magnetohydrodynamics a modification of  $R_m$ , the mixed magnetic Reynolds number  $R_{mx}$ , also becomes important.

A. Electromagnetic field equations

1) The Charge Continuity Equations:

$$\nabla \cdot \bar{j} + \frac{\partial \rho_e}{\partial t} = 0 \quad (14)$$

where  $\rho_e$  = electric charge density,  $j$  = current density.

2) Ampere's Law:

$$\nabla \times \bar{B} = \mu_0 \bar{j}_t \quad (15)$$

$$\nabla \cdot \bar{B} = 0 \quad (16)$$

where  $B$  = magnetoc flux density,  $\mu_0$  = permeability of space

3) Faraday's Equations:

$$\nabla \times \bar{E} = - \frac{\partial \bar{B}}{\partial t} \quad (17)$$

where  $E$  = electric field strength and the assumption is made that, in MHD flows, electron and ion densities are equal.

4) Ohm's Law:

$$\bar{j}_e = \sigma(\bar{E}_a + \bar{V} \times \bar{B}) \quad (18)$$

where  $\sigma$  = electrical conductivity,  $V$  = fluid velocity.

5) The Energy Equation:



$$W_{em} = \overline{E}_a \cdot \overline{j}_i - \frac{\overline{j}_e^2}{\sigma} \quad (19)$$

For an MHD flow having the properties of being incompressible, inviscid, and steady, and with no applied electric field, the MHD equations in nondimensional parameters are:

$$\begin{aligned} \nabla \cdot \overline{V} &= 0 \\ \nabla \cdot \overline{B} &= 0 \\ \nabla \times \overline{B} &= R_m (\overline{V} \times \overline{B}) \\ (\overline{V} \cdot \nabla) \overline{V} &= -\nabla \overline{P} + I (\overline{V} \times \overline{B}) \times \overline{B} \end{aligned} \quad (20)$$

where

$$\overline{V} = \frac{V}{V_{ref}}$$

$$\overline{B} = \frac{B}{B_{ref}}$$

$V_{ref}, B_{ref}$  are reference values of velocity, magnetic flux density.

$$R_m = \mu_0 \sigma_0 V_{ref} y_0$$

B: Flow field equations

6) The momentum equation:

$$\frac{1}{\rho} \nabla p + (\overline{q} \cdot \nabla) \overline{q} = \frac{\mu (\overline{J} \times \overline{B})}{\rho} \quad (21)$$

It can be written

$$\frac{1}{\rho} \nabla p + (\overline{q} \cdot \nabla) \overline{q} = \frac{S (\overline{E} + \overline{q} \times \overline{B})}{\rho} \times \overline{B} \quad (22)$$

$R_m$  is magnetic Reynolds number, a measure of the ration of the induced magnetic field with respect to the applied field.  $q$  is velocity vector.

The magnetic and flow field components which satisfy

$$\overline{\nabla} \times \overline{B} = R_m (\overline{V} \times \overline{B}) \quad (23)$$

are in the form:

$$\bar{B} = \bar{B}_0 + \sum_{n+k=1}^{\infty} I_1^n R_m^k \overline{B^{(n,k)}}$$

$$\nabla \cdot \bar{B}_1 = 0 \quad (24)$$

$$\nabla \times \bar{B}_1 = \bar{V}_0 \times \bar{B}_0 \quad (25)$$

where  $n, k = 0, 1, 2, \dots$

$B$  is expressed in type form of a double power series in  $R_m$  and  $I$ . The fluid and magnetic properties are made dimensionless by referring them to undisturbed uniform values. Here  $S$  and  $R_m$  are the magnetic force coefficient and magnetic Reynolds number, based on these uniform values of density ( $\rho_e$ ), field strength ( $B$ ), velocity ( $V$ ) and a representative length  $l$ .

Imagine now a one-dimensional gas flow perpendicular to a magnetic field. In a generator  $E = (1/2)\sigma_g V B^2 L_g$ , so that the work done by unit volume of the gas in moving across the field a distance  $L_g$  is :

$$FL_g = (1/2)\sigma_g V B^2 L_g \quad (26)$$

The energy stored in the magnetic field per unit volume is  $B^2/2\mu_0$ . The ratio of these is:

$$R_m = \mu_0 \sigma_g V L_g = \frac{B_1}{B_0} = \frac{\text{Work done by the gas}}{\text{Energy stored in the field}} \quad (27)$$

The magnetic Reynolds number has another useful interpretation.  $R_m$  is a measure of the extent to which the gas motion can modify or deflect the field. In engineering applications it is important to know how much energy is dissipated in the solid conductors that create the applied magnetic field.

Consider a flowing fluid conductor in a uniform magnetic field  $B$ , an e.m.f. is set up at right angles to the velocity vector  $V$  and the field  $B$  as shown in Fig 1-1 and if the Hall number is very small then a current will flow parallel to the induced e.m.f. The induced e.m.f. is the charged particle separating force caused by the

magnetic field. If no electrodes are immersed in the fluid, open circuit conditions prevail, then the electrons will flow downwards and the positive particles will flow upwards. As the charges separate there results a distribution of charge that opposes the induced e.m.f. and eventually is sufficient to balance the tendency for charge separation, e.m.f., and further current flow is prevented,  $\bar{E} = -\bar{V} \times \bar{B}$ .

In order to allow the e.m.f. to drive a current through an external load it is necessary to reduce the strength of the electrostatic field. This is achieved by immersing electrodes, which are connected to a load, into the fluid as shown in Fig 1-1. A restricted flow of electrons then occurs from the cathode through the fluid to the anode returning to the cathode via the external load. The driving force on the electrons is equal to the difference between the induced e.m.f. and the electrostatic field  $E$  and is called the total e.m.f. The actual value of the total e.m.f. clearly depends on the value of  $E$  which depends, by Ohm's law, on the total ohmic resistance of electron circuit. If the external resistance is reduced to zero, there is an unrestricted flow of electrons from the cathode into the fluid and out via the anode. The electrostatic field  $E$  is now zero, with no charge separation occurring. This short-short-circuit condition has a current density equal to  $\sigma(V \times B)$ . The simple representation of a conducting fluid moving in a magnetic field becomes much more complicated when the fluid has an appreciable Hall Number great than 0.1.

## 2.2 DERIVATION OF THE INDUCED MAGNETIC-FIELD EQUATIONS AND BOUNDARY CONDITIONS

### Magnetic-Field Equations

Referring to (24) (25) where  $B_1$  is the induced magnetic field, and we have that

$$V_1, P_1 = 0$$

Let  $V_0 = a_x$  where  $\hat{a}_x$  is a unit vector in the  $x$  direction. Equation (24) becomes

$$\nabla \cdot \bar{B}_1 = 0$$

$$\nabla \times B_1 = a_x \times (a_x B_{x0} + a_y B_{y0}) = a_z B_{y0} \quad (28)$$

$B_{y0}$  is the  $y$  component of the external field  $B_0$  since  $B_{x0} = xI\delta(0, -y_0)/[x^2 + (1+y)^2]$  where it should be stated that this is the same as (1), in normalized form. therefore, (25) becomes

$$\frac{\partial B_{y1}}{\partial x} - \frac{\partial B_{x1}}{\partial y} = \frac{x}{x^2 + (1+y)^2} I\delta(0, -y_0) \quad (29)$$

$$\frac{\partial B_{y1}}{\partial y} + \frac{\partial B_{x1}}{\partial x} = 0 \quad (30)$$

When (29) is differentiated with respect to  $y$  and (30) with respect to  $x$ , and then subtracted, we get

$$\frac{\partial^2 B_{x1}}{\partial x^2} + \frac{\partial^2 B_{x1}}{\partial y^2} = \frac{2x(1+y)}{[x^2 + (1+y)^2]^2} I\delta(0, -y_0) \quad (31)$$

$\delta$ =current impulse singular function,  $I$ =magnetude.

Boundary Conditions:

The fluid will pass in a transition sub layer of extremely small thickness from the channel wall to an inviscid boundary layer, the thickness of which depends upon the value of the magnetic Reynolds number  $R_m$ . At the channel surface the flow velocity components  $V_y$  and  $V_x$  are zero, but the values of  $B_{x1}$  and  $B_{y1}$  are unknown. The viscous and the inviscid layers merge smoothly, and hence the outer boundary values of  $V_x$  and  $B_{x1}$  for the viscous layer are given by the values assumed at  $y=0$  in the inviscid layer. The same conditions exist in the viscous boundary layer for all values of the magnetic Reynolds number  $R_m$ . The thickness of the viscous layer is of the order of  $1/\sqrt{R_e}$ , where  $R_e$  is the true

Reynolds number. Now recall (16), since  $V_0$  is in the  $x$  direction and  $B_1$  is two dimensional:

$$\frac{\partial B_{y1}}{\partial y} - \frac{\partial B_{x1}}{\partial x} = a_z V_0 B_{y0} \quad (32)$$

In the viscous layer, the two velocity components are zero, and hence  $V_0$  will be replaced by zero; therefore, (32) becomes

$$\frac{\partial B_{y1}}{\partial y} - \frac{\partial B_{x1}}{\partial x} = 0 \quad (33)$$

and also in this layer, the quantity  $\partial/\partial y$  is of the order of  $1/\delta$  and  $\partial/\partial x$  is one of the order of 1, where  $\delta$  is the thickness of the viscous sub layer which is of the order of  $1/\sqrt{R_e}$ . Therefore, (33) becomes

$$B_{x1} = \frac{B_{y1}}{\sqrt{R_e}} \quad (34)$$

The quantity  $B_{y1}$  will have some finite value at the channel wall and  $R_e$  is usually a large number. Hence, at channel wall, we find

$$B_{x1} \approx 0 \text{ at } y=0, \text{ and } y=L$$

where  $L$ =arbitrary channel height. Therefore, the partial differential equation  $B_{x1}$ , together with the established boundary conditions, becomes

$$\frac{\partial^2 B_{x1}}{\partial x^2} + \frac{\partial^2 B_{x1}}{\partial y^2} = \frac{2x(1+y)}{[x^2+(1+y)^2]^2} I \delta(0, -y_0) \quad (35)$$

$$B_{x1} = 0 \text{ at } y=0, L \text{ and}$$

$$B_{x1} = 0 \text{ at } x=\pm\infty \quad (36)$$

## Chapter 3

### PHASES OF COMPUTATIONS

#### 3.1 SOLUTION OF THE INDUCED MAGNETIC FIELD PERTURBATION EQUATIONS

Chapter 2 presented the derivation the partial differential equation describing the component of the induced magnetic field to the first order in  $R_w$  (refer to Fig. 1-2) is given in Eq (35). with the boundary conditions expressed by Eq (36).

The right-hand part of the partial differential equation (35) is

$$\frac{2x(1+y)}{[x^2+(1+y)^2]^2} I\delta(0, -y_0)$$

If the numerator  $2x(1+y)I\delta(0, y_0)$  is divided by the denominator  $[x^2+(1+y)^2]^2$ , the Eq (35) can be written as follow:

$$\frac{\partial B_{x1}}{\partial x^2} + \frac{\partial B_{x1}}{\partial y^2} = I\delta(0, -y_0) \left[ \frac{2}{x^3} + \frac{2y}{x^3} - \frac{4(1+y)^2}{x^5} - \frac{4y(1+y)^2}{x^5} + \frac{6(1+y)^4}{x^7} + \frac{6y(1+y)^4}{x^7} - \frac{8(1+y)^6}{x^9} - \frac{8y(1+y)^6}{x^9} \right]$$

where  $y$  is any point across the two plates.

This partial differential equation can be analyzed by *Laplace transform*. The most useful properties of the Laplace transform is the way in which it operates on derivatives. This property shows that the transform of derivatives can be evaluated in terms of the transform of the function. The technique for solving partial differential equation is that using Laplace transform to change partial differential equation to the ordinary differential equation. Then the inverse Laplace transform gives the solution of the problem.

Now we will transform equation (37) for  $y$  keeping  $x$  as the variable along the channel axis: take Laplace transform with expecting to  $y$

Now we will transform equation (37) for  $y$  keeping  $x$  as the variable along the channel axis: take Laplace transform with expecting to  $y$

The left part of the equation becomes:

$$\frac{\partial^2 \overline{B_{x1}}}{\partial x^2} + s^2 \overline{B_{x1}} - s \overline{B_{x1}}(x, 0) - \overline{B_{x1}}(x, 0)$$

Assume that  $\overline{B_{x1}}(x, 0) = 0$ , (because from boundary conditions Eq (36):  $B_{x1} = 0$ , when  $y=0$ ), so that the equation only has two items which are:

$$\frac{\partial^2 \overline{B_{x1}}}{\partial x^2} + s^2 \overline{B_{x1}}$$

Taking Laplace transform of the right part of the Eq (37), we get a differential Equation in terms of  $x$  with  $s$  carried along as the transform variable.

$$L_y \left[ \frac{2\delta(0, -y_0)}{x^3} \right] = \frac{2}{x^3} e^{-y_0 s},$$

$$L_y \left[ \frac{2y\delta(0, -y_0)}{x^3} \right] = \frac{2}{x^3} \int y\delta(0, -y_0) e^{-ys} dy = 0$$

$$\int y\delta(0, -y_0) e^{-ys} dy = \int v du, \quad v = y, u = \int e^{-ys} \delta(0, -y_0) dy = e^{-y_0 s}$$

$$uv = ye^{-y_0 s}, \int u dv = \int e^{-y_0 s} dy = ye^{-y_0 s}$$

$$L_y \left[ \frac{4(1+y)^2}{x^5} \delta(0, -y_0) \right] = \frac{4}{x^5} e^{-y_0 s}, \quad L_y \left[ \frac{4y(1+y)^2}{x^5} \delta(0, -y_0) \right] = 0$$

$$L_y \left[ \frac{6(1+y)^2}{x^7} \delta(0, -y_0) \right] = \frac{6}{x^7} e^{-y_0 s}, \quad L_y \left[ \frac{6y(1+y)^2}{x^7} \delta(0, -y_0) \right] = 0$$

$$L_y \left[ \frac{8(1+y)^2}{x^9} \delta(0, -y_0) \right] = \frac{8}{x^9} e^{-y_0 s}, \quad L_y \left[ \frac{8y(1+y)^2}{x^9} \delta(0, -y_0) \right] = 0$$

So, Eq (37) becomes:

$$\frac{\partial^2 \overline{B_{x1}}}{\partial x^2} + s^2 \overline{B_{x1}} = \left[ \frac{2}{x^3} - \frac{4}{x^5} + \frac{6}{x^7} - \frac{8}{x^9} \right] e^{-y_0 s} \quad (37)$$

This is a linear differential equation for which the general homogeneous solution is known. The method that is used here can determine the complete solution. This method is depicted fully and clearly in chapter 1 "Particular solutions by variation of parameters" (p.25 - p.27) in "Partial differential equations". Suppose that the general homogeneous solution of the equation:

$$\frac{d^n y}{dx^n} + a_1(x) \frac{d^{n-1} y}{dx^{n-1}} + \dots + a_{n-1}(x) \frac{dy}{dx} + a_n(x) y = h(x) \quad (\text{A})$$

has been obtained in the form:

$$y_H = \sum_{k=1}^n c_k u_k(x) \quad (\text{B})$$

where the  $u$ 's are  $n$  linearly independent homogeneous solutions and the  $c$ 's are  $n$  arbitrary constants or "parameters." We will find that a particular solution of the complete equation can be obtained by replacing the constant parameters  $c_k$  in the solution of the associated homogeneous equation by certain functions of  $x$ . Thus, we assume that

$$y_p = \sum_{k=1}^n C_k(x) U_k(x) \quad (\text{C})$$

is a solution of the equation and attempt to choose the  $n$  functions  $c_k$  suitably. Since we have  $n$  functions to determine, and since the requirement that  $y_p$  satisfies the equation represents only one condition, we have  $n-1$  additional conditions at our disposal.

Differentiating Eq (c) and using primes to denote differentiation with respect to  $x$ , we obtain:

$$\frac{dy_p}{dx} = \sum_{k=1}^n C_k u_k' + \sum_{k=1}^n C_k' u_k \quad (\text{D1})$$

There then follow:



$$\frac{d^2 y_p}{dx^2} = \sum_{k=1}^n C_k u_k'' + \sum_{k=1}^n C_k'' u_k \quad (D2)$$

As the second condition, we require again that the sum of the terms involving derivatives of the  $C$ 's vanish.

$$\sum_{k=1}^n C_k' u_k' = 0 \quad (D3)$$

Proceeding in this way through the  $n$ th derivative, we have as our  $n$ th derivative is:

$$\frac{d^n y_p}{dx^n} = \sum_{k=1}^n C_k u_k^{(n)} + \sum_{k=1}^n C_k' u_k^{(n-1)}$$

By introducing the expressions for  $y_p$  and its derivatives into the left-hand side of Eq (A), we find that the final condition, that Eq (C) satisfy Eq (A), becomes:

$$L y_p = \sum_{k=1}^n C_k u_k^{(n)} + a_1(x) \sum_{k=1}^n C_k u_k^{(n-1)} + \dots + a_n(x) \sum_{k=1}^n C_k u_k + \sum_{k=1}^n C_k' u_k^{(n-1)} = h(x)$$

Since each function  $u_k$  satisfies Eq (A) with  $h(x)$  replaced by zero, and since each bracket in the first summation is precisely the result of replacing  $y$  in the left-hand side of Eq (A) by a function  $u_k$ , the first summation vanishes identically, and the final condition becomes:

$$\sum_{k=1}^n C_k' u_k^{(n-1)} = h(x) \quad (D4)$$

If the solutions  $C_1, \dots, C_n$  are integrated and the result put into the Eq (C), the result is a particular solution of Eq (A) for any choice of the  $n$  constants of integration. In particular, for a second-order linear equation of the form:

$$\frac{d^2 y}{dx^2} + a_1(x) \frac{dy}{dx} + a_2(x) y = h(x)$$

there follows:

$$y = C_1(x) u_1(x) + C_2(x) u_2(x)$$

where

$$C_1' = \frac{\begin{vmatrix} 0 & u_2 \\ h & u_2' \end{vmatrix}}{\begin{vmatrix} u_1 & u_2 \\ u_1' & u_2' \end{vmatrix}} = -\frac{h(x)u_2(x)}{W[u_1(x), u_2(x)]}$$

and, similarly,

$$C_2' = \frac{h(x)u_1(x)}{W[u_1(x), u_2(x)]}$$

Thus we can write:

$$C_1(x) = -\int \frac{h(x)u_2(x)}{W(u_1(x), u_2(x))} dx + c_1$$

$$C_2(x) = \int \frac{h(x)u_1(x)}{W(u_1(x), u_2(x))} dx + c_2$$

Getting back to the differential equation, assume two independent homogenous solutions are:

$$U_1(x) = \frac{e^{ix} + e^{-ix}}{2}, \quad U_2(x) = \frac{e^{ix} - e^{-ix}}{2i} \quad (38)$$

Wronskian is  $W(u_1(x), u_2(x)) = \begin{vmatrix} \frac{e^{ix} + e^{-ix}}{2} & \frac{e^{ix} - e^{-ix}}{2i} \\ \frac{\partial U_1(x)}{\partial x} & \frac{\partial U_2(x)}{\partial x} \end{vmatrix}$

$$= \frac{1}{2}(e^{ix} + e^{-ix}) \frac{1}{2i}(ie^{ix} + ie^{-ix}) - \frac{1}{2i}(e^{ix} - e^{-ix}) \frac{1}{2}(ise^{ix} - ise^{-ix})$$

$$= \frac{1}{4i}(2is + 2is) = s$$

General solution for Eq (37) can be written as:

$$\overline{B}_x = C_1(x)U_1(x) + C_2(x)U_2(x) \quad (39)$$

$$C_1(x) = -\int \frac{f(x)U_2(x)}{W(U_1(x), U_2(x))} dx + c_1 \quad (40)$$

$$C_2(x) = \int \frac{f(x)U_1(x)}{W(U_1(x), U_2(x))} dx + c_2 \quad (41)$$

$$\begin{aligned} C_1(x) &= -\int \frac{Ae^{-y_0s}}{s} \left( \frac{2}{x^3} - \frac{4}{x^5} + \frac{6}{x^7} - \frac{8}{x^9} \right) \left( \frac{e^{ix} - e^{-ix}}{2i} \right) dx + c_1 \\ &= -\frac{Ae^{-y_0s}}{s} \int \left( \frac{2}{x^3} - \frac{4}{x^5} + \frac{6}{x^7} - \frac{8}{x^9} \right) \left( \frac{e^{ix} - e^{-ix}}{2i} \right) dx + c_1 \\ &= -\frac{Ae^{-y_0s}}{s} \left( \int \frac{e^{ix}}{ix^3} - \int \frac{e^{-ix}}{ix^3} dx - \int \frac{2e^{ix}}{ix^5} dx + \int \frac{2e^{-ix}}{ix^5} dx \right. \\ &\quad \left. + \int \frac{3e^{ix}}{ix^7} dx - \int \frac{3e^{-ix}}{ix^7} dx - \int \frac{4e^{ix}}{ix^9} dx + \int \frac{4e^{-ix}}{ix^9} dx \right) + c_1 \\ C_1(x)U_1(x) &= -\frac{Ae^{-y_0s}}{s} \left( \frac{e^{-ix} + e^{ix}}{2} \right) \left( \int \frac{e^{ix}}{ix^3} dx - \int \frac{e^{-ix}}{ix^3} dx - \int \frac{2e^{ix}}{ix^5} dx + \int \frac{2e^{-ix}}{ix^5} dx \right. \\ &\quad \left. + \int \frac{3e^{ix}}{ix^7} dx - \int \frac{3e^{-ix}}{ix^7} dx - \int \frac{4e^{ix}}{ix^9} dx + \int \frac{4e^{-ix}}{ix^9} dx \right) + c_1 \left( \frac{e^{ix} + e^{-ix}}{2} \right) \\ C_2(x) &= \int \frac{Ae^{-y_0s}}{s} \left( \frac{2}{x^3} - \frac{4}{x^5} + \frac{6}{x^7} - \frac{8}{x^9} \right) \left( \frac{e^{ix} + e^{-ix}}{2} \right) dx + c_2 \\ &= \frac{Ae^{-y_0s}}{s} \int \left( \frac{2}{x^3} - \frac{4}{x^5} + \frac{6}{x^7} - \frac{8}{x^9} \right) \left( \frac{e^{ix} + e^{-ix}}{2} \right) dx + c_2 \\ &= \frac{Ae^{-y_0s}}{s} \left( \int \frac{e^{ix}}{x^3} dx + \int \frac{e^{-ix}}{x^3} dx - \int \frac{2e^{ix}}{x^5} dx - \int \frac{2e^{-ix}}{x^5} dx \right. \\ &\quad \left. + \int \frac{3e^{ix}}{x^7} dx + \int \frac{3e^{-ix}}{x^7} dx - \int \frac{4e^{ix}}{x^9} dx - \int \frac{4e^{-ix}}{x^9} dx \right) + c_2 \\ C_2(x)U_2(x) &= \frac{Ae^{-y_0s}}{s} \left( \frac{e^{-ix} - e^{ix}}{2i} \right) \left( \int \frac{e^{ix}}{x^3} dx + \int \frac{e^{-ix}}{x^3} dx - \int \frac{2e^{ix}}{x^5} dx - \int \frac{2e^{-ix}}{x^5} dx \right. \\ &\quad \left. + \int \frac{3e^{ix}}{x^7} dx + \int \frac{3e^{-ix}}{x^7} dx - \int \frac{4e^{ix}}{x^9} dx - \int \frac{4e^{-ix}}{x^9} dx \right) + c_2 \left( \frac{e^{ix} - e^{-ix}}{2i} \right) \end{aligned}$$

$$\begin{aligned}
C_1(x)U_1(x) + C_2(x)U_2(x) &= -\frac{Ae^{-y_0s}}{s} \left( \frac{e^{-ix} + e^{ix}}{2} \right) \left( \int \frac{e^{ix}}{ix^3} dx - \int \frac{e^{-ix}}{ix^3} dx - \int \frac{2e^{ix}}{ix^5} dx + \int \frac{2e^{-ix}}{ix^5} dx \right. \\
&\quad \left. + \int \frac{3e^{ix}}{ix^7} dx - \int \frac{3e^{-ix}}{ix^7} dx - \int \frac{4e^{ix}}{ix^9} dx + \int \frac{4e^{-ix}}{ix^9} dx \right) + c_1 \left( \frac{e^{ix} + e^{-ix}}{2} \right) \\
&\quad + \frac{Ae^{-y_0s}}{s} \left( \frac{e^{-ix} - e^{ix}}{2i} \right) \left( \int \frac{e^{ix}}{x^3} dx + \int \frac{e^{-ix}}{x^3} dx - \int \frac{2e^{ix}}{x^5} dx - \int \frac{2e^{-ix}}{x^5} dx \right. \\
&\quad \left. + \int \frac{3e^{ix}}{x^7} dx + \int \frac{3e^{-ix}}{x^7} dx - \int \frac{4e^{ix}}{x^9} dx - \int \frac{4e^{-ix}}{x^9} dx \right) + c_2 \left( \frac{e^{ix} - e^{-ix}}{2i} \right)
\end{aligned}$$

Now Eq (39) becomes:

$$\begin{aligned}
C_1(x)U_1(x) + C_2(x)U_2(x) &= -\frac{Ae^{-y_0s}}{s} \left( \frac{e^{ix}}{2i} \right) \left( \int \frac{2e^{-ix}}{x^3} dx - \int \frac{4e^{-ix}}{x^5} dx + \int \frac{6e^{-ix}}{x^7} dx - \int \frac{8e^{-ix}}{x^9} dx \right) \\
&\quad + \frac{Ae^{-y_0s}}{s} \left( \frac{e^{-ix}}{2i} \right) \left( -\int \frac{2e^{ix}}{x^3} dx + \int \frac{4e^{ix}}{x^5} dx - \int \frac{6e^{ix}}{x^7} dx + \int \frac{8e^{ix}}{x^9} dx \right) \\
&\quad + c_1 \left( \frac{e^{ix} + e^{-ix}}{2} \right) + c_2 \left( \frac{e^{ix} - e^{-ix}}{2i} \right)
\end{aligned}$$

$$\begin{aligned}
\int \frac{2e^{-ix}}{x^3} dx &= -\frac{e^{-ix}}{x^2} - is \int \frac{e^{-ix}}{x^2} dx \\
&= -\frac{e^{-ix}}{x^2} - is \left[ \frac{e^{-ix}}{x} - is \int \frac{e^{-ix}}{x} dx \right] \\
&= -\frac{e^{-ix}}{x^2} + \frac{ise^{-ix}}{x} - s^2 \int \frac{e^{-ix}}{x} dx
\end{aligned}$$

$$\begin{aligned}
-\int \frac{4e^{-ix}}{x^5} dx &= \frac{e^{-ix}}{x^4} + is \int \frac{e^{-ix}}{x^4} dx \\
&= \frac{e^{-ix}}{x^4} + is \left[ -\frac{e^{-ix}}{3x^3} - \frac{is}{3} \int \frac{e^{-ix}}{x^3} dx \right] \\
&= \frac{e^{-ix}}{x^4} - \frac{ise^{-ix}}{3x^3} - \frac{s^2 e^{-ix}}{6x^2} + \frac{is^3 e^{-ix}}{6x} - \frac{s^4}{6} \int \frac{e^{-ix}}{x} dx
\end{aligned}$$

$$\int \frac{6e^{-15x}}{x^7} dx = -\frac{e^{-15x}}{x^6} - is \int \frac{e^{-15x}}{x^6} dx$$

$$= \frac{e^{-15x}}{x^6} + \frac{is e^{-15x}}{5x^5} + \frac{s^2 e^{-15x}}{20x^4} - \frac{is^3 e^{-15x}}{60x^3} - \frac{s^4 e^{-15x}}{120x^2} + \frac{is^5 e^{-15x}}{120x} - \frac{s^6}{120} \int \frac{e^{-15x}}{x} dx$$

$$-\int \frac{8e^{-15x}}{x^9} dx = \frac{e^{-15x}}{x^8} + is \int \frac{e^{-15x}}{x^8} dx$$

$$= \frac{e^{-15x}}{x^8} - \frac{is e^{-15x}}{7x^7} - \frac{s^2 e^{-15x}}{42x^6} + \frac{is^3 e^{-15x}}{210x^5} + \frac{s^4 e^{-15x}}{840x^4} - \frac{is^5 e^{-15x}}{2520x^3} - \frac{s^6 e^{-15x}}{5040x^2} + \frac{is^7 e^{-15x}}{5040x} - \frac{s^8}{5040} \int \frac{e^{-15x}}{x} dx$$

$$-\int \frac{2e^{15x}}{x^3} dx = \frac{e^{15x}}{x^2} - is \int \frac{e^{15x}}{x^2} dx$$

$$= \frac{e^{15x}}{x^2} - is \left[ -\frac{e^{15x}}{x} + is \int \frac{e^{15x}}{x} dx \right]$$

$$= \frac{e^{15x}}{x^2} + \frac{is e^{15x}}{x} + s^2 \int \frac{e^{15x}}{x} dx$$

$$\int \frac{4e^{15x}}{x^5} dx = -\frac{e^{15x}}{x^4} + is \int \frac{e^{15x}}{x^4} dx$$

$$= -\frac{e^{15x}}{x^4} + is \left[ -\frac{e^{15x}}{3x^3} + \frac{is}{3} \int \frac{e^{15x}}{x^3} dx \right]$$

$$= -\frac{e^{15x}}{x^4} - \frac{is e^{15x}}{3x^3} + \frac{s^2 e^{15x}}{6x^2} + \frac{is^3 e^{15x}}{6x} + \frac{s^4}{6} \int \frac{e^{15x}}{x} dx$$

$$-\int \frac{6e^{15x}}{x^7} dx = \frac{e^{15x}}{x^6} - is \int \frac{e^{15x}}{x^6} dx$$

$$= \frac{e^{15x}}{x^6} + \frac{is e^{15x}}{5x^5} - \frac{s^2 e^{15x}}{20x^4} - \frac{is^3 e^{15x}}{60x^3} + \frac{s^4 e^{15x}}{120x^2} + \frac{is^5 e^{15x}}{120x} + \frac{s^6}{120} \int \frac{e^{15x}}{x} dx$$

$$\int \frac{8e^{15x}}{x^9} dx = -\frac{e^{15x}}{x^8} - is \int \frac{e^{15x}}{x^8} dx$$

$$= -\frac{e^{15x}}{x^8} - \frac{is e^{15x}}{7x^7} + \frac{s^2 e^{15x}}{42x^6} + \frac{is^3 e^{15x}}{210x^5} - \frac{s^4 e^{15x}}{840x^4} - \frac{is^5 e^{15x}}{2520x^3} + \frac{s^6 e^{15x}}{5040x^2} + \frac{is^7 e^{15x}}{5040x} + \frac{s^8}{5040} \int \frac{e^{15x}}{x} dx$$

$$\overline{B}_{x1} = C_1(x)U_1(x) + C_2(x)U_2(x)$$

$$\begin{aligned}
&= \frac{A e^{-y_0 s}}{2i} \left( \frac{2i}{x} - \frac{2i}{3x^3} + \frac{2is^2}{6x} + \frac{2i}{5x^5} - \frac{2is^2}{60x^3} + \frac{2is^4}{120x} - \frac{2i}{7x^7} + \frac{2is^2}{210x^5} - \frac{2is^4}{2520x^3} + \frac{2is^6}{5040x} \right) \\
&+ \frac{A e^{-y_0 s}}{2i} \left( -s e^{ix} \int \frac{e^{-ix}}{x} dx + s e^{-ix} \int \frac{e^{ix}}{x} dx - \frac{s^3}{6} e^{ix} \int \frac{e^{-ix}}{x} dx + \frac{s^3}{6} e^{-ix} \int \frac{e^{ix}}{x} dx \right) \\
&+ \frac{A e^{-y_0 s}}{2i} \left( -\frac{s^5}{120} e^{ix} \int \frac{e^{-ix}}{x} dx + \frac{s^5}{120} e^{-ix} \int \frac{e^{ix}}{x} dx - \frac{s^7}{5040} e^{ix} \int \frac{e^{-ix}}{x} dx + \frac{s^7}{5040} e^{-ix} \int \frac{e^{ix}}{x} dx \right) \\
&+ c_1 \left( \frac{e^{ix} + e^{-ix}}{2} \right) + c_2 \left( \frac{e^{ix} - e^{-ix}}{2i} \right) \\
&= e^{-y_0 s} \left[ \frac{1}{x} - \frac{1}{3x^3} + \frac{s^2}{6x} + \frac{5}{5x^5} - \frac{s^2}{60x^3} + \frac{s^4}{120x} - \frac{1}{7x^7} + \frac{s^2}{210x^5} - \frac{s^4}{2520x^3} + \frac{s^6}{5040x} \right] \\
&+ \frac{e^{-y_0 s}}{2i} \left[ -s^2 e^{ix} E_1(-ix) + s^2 e^{-ix} E_1(ix) - \frac{s^4}{6} e^{ix} E_1(-ix) + \frac{s^4}{6} e^{-ix} E_1(ix) \right] \\
&+ \frac{e^{-y_0 s}}{2i} \left[ -\frac{s^6}{120} e^{ix} E_1(-ix) + \frac{s^6}{120} e^{-ix} E_1(ix) - \frac{s^7}{5040} e^{ix} E_1(-ix) + \frac{s^7}{5040} e^{-ix} E_1(ix) \right] \\
&+ c_1 \left( \frac{e^{ix} + e^{-ix}}{2} \right) + c_2 \left( \frac{e^{ix} - e^{-ix}}{2i} \right) \tag{42}
\end{aligned}$$

Taking the inverse transform of Eq (42):

$$\begin{aligned}
B_{x1} &= \delta(y - y_0) \left( \frac{1}{x} - \frac{1}{3x^3} + \frac{1}{5x^5} - \frac{1}{7x^7} \right) + \frac{\partial^2}{\partial y^2} (\delta(y - y_0)) \left( \frac{1}{6x} - \frac{1}{60x^3} + \frac{1}{210x^5} \right) \\
&+ \frac{\partial^4}{\partial y^4} (\delta(y - y_0)) \left( \frac{1}{120x} - \frac{1}{2520x^3} \right) + \frac{\partial^6}{\partial y^6} (\delta(y - y_0)) \left( \frac{1}{5040x} \right) \\
&+ K_1 \delta(y + ix) + K_2 \delta(y - ix) \\
&+ \frac{-6x(y - y_0)^2 + 2x^3}{((y - y_0)^2 + x^2)^3} + \frac{-20x(y - y_0)^4 + 40x^3(y - y_0)^2 - 4x^5}{((y - y_0)^2 + x^2)^5} \\
&+ \frac{-42x(y - y_0)^6 + 210x^3(y - y_0)^4 - 126x^5(y - y_0)^2 + 6x^7}{((y - y_0)^2 + x^2)^7}
\end{aligned}$$

$$+ \frac{-72x(y-y_0)^8 + 672x^3(y-y_0)^6 - 1008x^5(y-y_0)^4 + 288x^7(y-y_0)^2 - 8x^9}{((y-y_0)^2 + x^2)^9} \quad (43)$$

By putting boundary condition into Eq (43), we found  $K_1, K_2 = 0$ .

$B_{y1}$  can be found from Eq (33):

$$\frac{\partial B_{y1}}{\partial y} - \frac{\partial B_{x1}}{\partial x} = 0 \quad (33)$$

Therefore,

$$B_{y1} = - \int \frac{\partial B_{x1}}{\partial x} dy + \Phi(x) \quad (44)$$

where  $\Phi(x)$  is a function of  $x$  only.

$$\begin{aligned} B_{y1} &= - \int \frac{\partial}{\partial x} \left[ \frac{-6x(y-y_0)^2 + 2x^3}{((y-y_0)^2 + x^2)^3} + \frac{-20x(y-y_0)^4 + 40x^3(y-y_0)^2 - 4x^5}{((y-y_0)^2 + x^2)^5} \right] dy \\ &\quad - \int \frac{\partial}{\partial x} \left[ \frac{-42x(y-y_0)^6 + 210x^3(y-y_0)^4 - 126x^5(y-y_0)^2 + 6x^7}{((y-y_0)^2 + x^2)^7} \right] dy \\ &\quad - \int \frac{\partial}{\partial x} \left[ \frac{-72x(y-y_0)^8 + 672x^3(y-y_0)^6 - 1008x^5(y-y_0)^4 + 288x^7(y-y_0)^2 - 8x^9}{((y-y_0)^2 + x^2)^9} \right] dy \\ &= \frac{-6x(y-y_0)^3 + x^4(y-y_0) + (y-y_0)^5}{x^2((y-y_0)^2 + x^2)^3} \\ &\quad + \frac{-30x^2(y-y_0)^5 + 30x^4(y-y_0)^3 - 2x^6(y-y_0) + 2(y-y_0)^7}{x^2((y-y_0)^2 + x^2)^5} \\ &\quad + \frac{-84x^2(y-y_0)^7 + 210x^4(y-y_0)^5 - 84x^6(y-y_0)^3 + 3x^8(y-y_0) + 3(y-y_0)^9}{x^2((y-y_0)^2 + x^2)^7} \end{aligned}$$

$$+ \frac{-180x^2(y-y_0)^9 + 840x^4(y-y_0)^7 - 728x^6(y-y_0)^5 + 180x^8(y-y_0)^3 - 4x^{10}(y-y_0) + 4(y-y_0)^{11}}{x^2((y-y_0)^2 + x^2)^9}$$

It can be easily shown, using the Weirstrass  $M$  test, that the infinite-series solution, justifies the process of differentiation. The term  $\Phi(x)$  is found by applying the boundary condition that  $B_{y_1}$  is bounded at  $x = \pm\infty$ . Thus,  $\Phi(x)=0$ . The total solution for  $B_{x_1}$  is given by the total magnetic field can be expressed as:

$$B_x = B_{x_0} + R_m B_{x_1}$$

$$B_y = B_{y_0} + R_m B_{y_1}$$

Results:

$$\begin{aligned} B_{x_1} = & \delta(y-y_0) \left( \frac{1}{x} - \frac{1}{3x^3} + \frac{1}{5x^5} - \frac{1}{7x^7} \right) + \frac{\partial^2}{\partial y^2} (\delta(y-y_0)) \left( \frac{1}{6x} - \frac{1}{60x^3} + \frac{1}{210x^5} \right) \\ & + \frac{\partial^4}{\partial y^4} (\delta(y-y_0)) \left( \frac{1}{120x} - \frac{1}{2520x^3} \right) + \frac{\partial^6}{\partial y^6} (\delta(y-y_0)) \left( \frac{1}{5040x} \right) \\ & + K_1 \delta(y+ix) + K_2 \delta(y-ix) \\ & + \frac{-6x(y-y_0)^2 + 2x^3}{((y-y_0)^2 + x^2)^3} + \frac{-20x(y-y_0)^4 + 40x^3(y-y_0)^2 - 4x^5}{((y-y_0)^2 + x^2)^5} \\ & + \frac{-42x(y-y_0)^6 + 210x^3(y-y_0)^4 - 126x^5(y-y_0)^2 + 6x^7}{((y-y_0)^2 + x^2)^7} \\ & + \frac{-72x(y-y_0)^8 + 672x^3(y-y_0)^6 - 1008x^5(y-y_0)^4 + 288x^7(y-y_0)^2 - 8x^9}{((y-y_0)^2 + x^2)^9} \quad (45) \end{aligned}$$

### 3.2 THE COMPUTER PROGRAMMING AND CALCULATION



Calculations for the magneto-fluid components were carried out using the personal computer. The computer programming and calculation is focused on the  $B_{x1}$  component.

Some functions of SIMULINK which have been used in this paper are discussed as following:

### 1) Function Functions:

Matrix operations are fundamental to SIMULINK. But a class of functions in SIMULINK work not with numerical matrices, but with mathematical functions.

These function functions include;

- Numerical integration
- Nonlinear equations and optimization
- Differential equation solution

Mathematical functions are represented in SIMULINK by function M-files.

For example, the function :

$$B_{x11} = \frac{-6x(y-y_0)^2 + 2x^3}{((y-y_0)^2 + x^2)^3}$$

is made available to SIMULINK by creating an M-file called Fig11.m:

```
function Bx11 = Fig(n,y)
```

```
Bx11 =((-6*x*(y-0.01).^2+2*x.^3)./(((y-0.01).^2+x.^2).^3));
```

A graph of the function is

```
x=-100:1:n;
```

```
plot (x,Bx11)
```

### 2) Graphing:

Scientific and engineering data are examined graphically in SIMULINK using "graph paper" commands to create plots on the screen. There are many different types of "graph paper" from which to choose:

- Plot: linear x-y plot
- loglog: loglog x-y plot
- semilogx: semi-log x-y plot (x-axis logarithmic)
- semilogy: semi-log x-y plot (y-axis logarithmic)
- polar: polar plot
- mesh: 3-dimensional mesh surface
- contour: contour plot
- bar: bar chart
- stairs: staircase graph

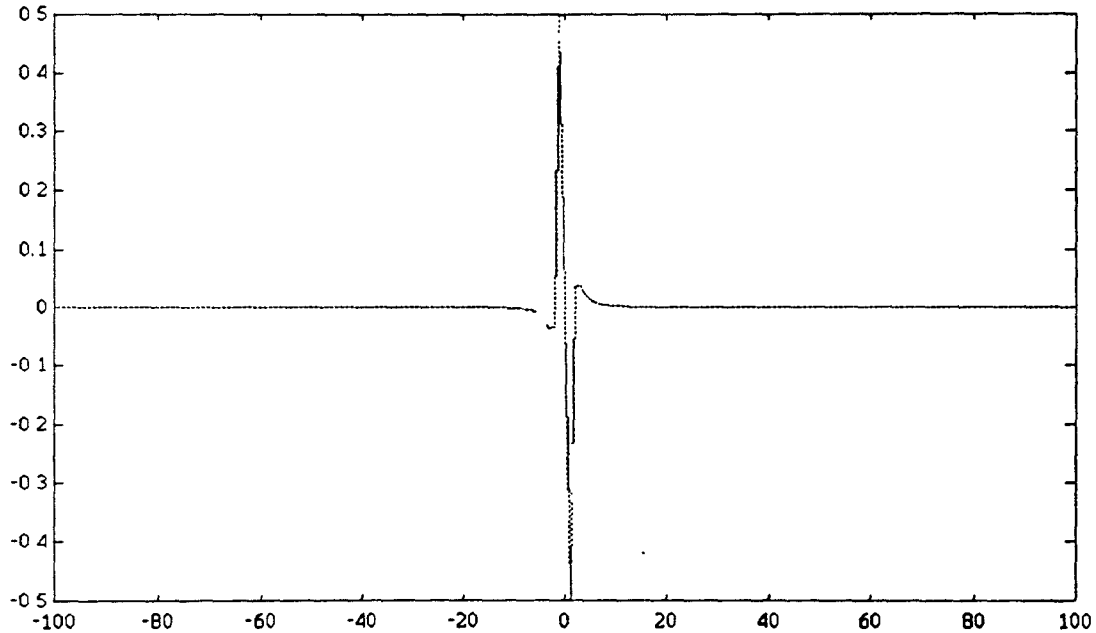


**Figure 3-1** Axial component of induced magnetic field  $B_{x11}$  (as an example)

Once a graph is on the screen, the graph may be labeled, titled, or have grid lines drawn in

- title: graph title
- xlabel: x-axis label
- ylabel: y-axis label

- text: arbitrarily positioned text
- gtext: mouse-positioned text
- grid: grid lines

The plot command creates linear  $x$ - $y$  plots. Once plot is mastered, logarithmic and polars are created by substituting the words loglog, semilog, semilogy, or polar for plot. all five commands are used the same way; they only affect how the axis is scaled and how the data are displayed. Notice that the data are auto-scaled and that  $x$ - and  $y$ -axes are drawn. As this point, depending upon the exact hardware you are using, the screen full of commands that you have typed in may have vanished to make way for the graph display. SIMULINK has two displays, a graph display and a command display. There are two ways to plot multiple lines on a single graph. The first is to give plot two arguments, as in plot ( $x,y$ ), where either  $x$ ,  $y$ , or both are matrices. Since we do not use matrices, we use the second, and easier, way to plot multiple lines on a single graph is to use plot with multiple arguments:

```
plot (x1, Bx11, x2, Bx12, x3, Bx13)
```

the variables  $x1$ ,  $Bx11$ ,  $x2$ ,  $Bx12$ ,  $x3$ ,  $Bx13$  etc. are pairs of vectors. Each  $x$ - $y$  pair is graphed, generating multiple lines on the plot. Multiple arguments have the benefit of allowing vectors of differing lengths to be displayed on the same graph. As before each pair uses a different line type. the linetypes used on a graph may be controlled if the defaults are not satisfactory. Point plots using various symbols may also be selected. For example,

```
plot (x1, Bx11, 'x')
```

draws a point plot using  $x$ -mark symbols while

```
plot (x1, Bx11, ':', x2, Bx12, '+')
```

uses a dotted line for the first curve and the plus symbol + for the second curve. Some systems that support color, line- and mark-colors may be specified in a manner similar to line- and mark-types. For example, the statements

```
plot(x, Bx11, 'r')
```

```
plot(x, Bx12, '+g')
```

use a red line on the first graph and green +marks on the second. Other colors are: red, green blue, white, invisible. If hard-copy does not support color, the various colors on the interactive display are mapped to different linetypes for output. In the next chapter, three demension plot is made, so the 3-D mesh surface and contour plots are introduced here: The statement mesh creates a three dimensional perspective plot of the elements in matrix Z. A mesh surface is defined by the Z coordinates of points above a rectangular grid in the x-y plane. The plot is formed by joining adjacent points with straight lines.

### 3) M-files: scripts and functions

SIMULINK are usually used in a command driven mode; when single-line commands are entered, they processes them immediately and displays the results. They are also capable of executing sequences of commands that are stored in files. Together, these two modes form an interpretive environment. Disk files that contain SIMULINK statements are called M-files because they have a file type of ".m" as the last part of the filename. An M-file consists of a sequence of normal SIMULINK statements, possibly including references to other M-files. An M-file can call itself recursively. One use of M-files is to automate long sequences of commands. Such files are called script files or just scripts. A scond type of M-file provides extensibility to SIMULINK. Called function files, they allow new functions to be added to the existing function. Much of the power of SIMULINK derives from this ability to create new functions that solve user-specific problems. Both types of M-files, scripts and functions, are ordinary ASCII text files, and are

created using an editor or word processor of your choice. In this paper, function files are used. If the first line of an M-file contains the word "function", the file is a function file. Here is a list of the function files which are used to plot curves:

- 1) *Figure 1.m*: it is used to graph  $Bx11$  (first term of  $Bx1$ ) *Figure 4-1a* to *Figure 4-8b*
- 2) *Figure 2.m*: it is used to graph  $Bx12$  (second term of  $Bx1$ ) *Figure 4-9a* to *Figure 4-17b*
- 3) *Figure 3.m*: it is used to graph  $Bx13$  (third term of  $Bx1$ ) *Figure 4-18a* to *Figure 4-25b*
- 4) *Figure 4.m*: it is used to graph  $Bx14$  (fourth term of  $Bx1$ ) *Figure 4-26a* to *Figure 4-33b*
- 5) *Figure 5.m*: it is used to graph total  $Bx1$  *Figure 4-34a* to *Figure 4-41b*
- 6) *Figure 6.m*: it is used to graph  $Bx16$  ( $\delta$ -function term) *Figure 4-42*
- 7) *Figure 7.m*: it is used to graph *Figure 5-1* (3-D total  $Bx1$ )

## Chapter 4

### DISCUSSION AND RESULTS

The tangential induced magnetic field component  $B_{x1}$  is given by the following equation:

$$\begin{aligned}
 B_{x1} = & \delta(y-y_0) \left( \frac{1}{x} - \frac{1}{3x^3} + \frac{1}{5x^5} - \frac{1}{7x^7} \right) \\
 & + \frac{-6x(y-y_0)^2 + 2x^3}{((y-y_0)^2 + x^2)^3} + \frac{-20x(y-y_0)^4 + 40x^3(y-y_0)^2 - 4x^5}{((y-y_0)^2 + x^2)^5} \\
 & + \frac{-42x(y-y_0)^6 + 210x^3(y-y_0)^4 - 126x^5(y-y_0)^2 + 6x^7}{((y-y_0)^2 + x^2)^7} \\
 & + \frac{-72x(y-y_0)^8 + 672x^3(y-y_0)^6 - 1008x^5(y-y_0)^4 + 288x^7(y-y_0)^2 - 8x^9}{((y-y_0)^2 + x^2)^9}
 \end{aligned}$$

Figure 4-1a illustrate the first term of the total induced magnetic field which is:

$$\frac{-6x(y-y_0)^2 + 2x^3}{((y-y_0)^2 + x^2)^3}, \text{ at } y=1, 100 < x < 100,$$

The plot indicate that the functional behavior is a doublet and symmetrical with respect to "0". When  $x=\pm\infty$ ,  $B_{x1}$  goes to zero, the value of  $B_{x1}$  changes from 0 to 2.0 almost linearly, while  $x$  changes from -2.0 to -0.5, it changes from +2.0 to -2.0 linearly, while  $x$  changes from -0.5 to +0.5, then  $B_{x1}$  changes form -2.0 to 0 while  $x$  changes from +0.5 to +2.0. The maximum deflection is at  $x=\pm 0.5$ . If we plot a curve whose  $x$  changes from -2 to +2, the maximum deflection will be much clear. Based on this plot, the following results were obtained: The field perturbation is sensitive to  $y$ . We consider that  $y$  can changes from 0 to infinity and the current

carrying conductor of infinite length is located at  $y = y_0$ . We assume that  $y_0 = 0.1$  ( $y_0$  is known as the reference length), which is very small. Compared with infinite number, 0.1 is a very small number (relatively approaching zero), so the point we are discussing is very close to the current carrying conductor. (We only discuss one current carrying conductor situation, we don't discuss the current sheet which is actually a boundary layer.) The differential equation for  $B_{x1}$  we had is:

$$\frac{\partial^2 B_{x1}}{\partial x^2} + \frac{\partial^2 B_{x1}}{\partial y^2} = \frac{2x(1+y)}{[x^2 + (1+y)^2]^2} I \delta(0, -y_0)$$

And its boundary conditions is :

$$B_{x1} = 0 \text{ at } y=0, L \text{ and}$$

$$B_{x1} = 0, x=\pm\infty$$

From Figure 4-1a, we see that  $B_{x1} = 0$  when  $x=\pm\infty$ . therefore, the solution that we got agrees with the established boundary conditions. We will discuss the other boundary condition later. Using Figure 4-1b, we can see much clear how the curve changes when  $x$  is very small.

To plot the same function using  $y=5$ , we obtain Figure 4-2a and Figure 4-2b that is also a doublet. Comparing this result with that  $y=1$ , we conclude that the maximum magnitude of the  $B_{x1}$  whose  $y=1$  is much less than that of  $y=0$ . Its width is the frequency span between the upper end lower half-power point is wider than the first one. The curve looks like been pulled open. The plots indicate that the curve is also a doublet and symmetrical with respect to "0". When  $x=\pm\infty$ ,  $B_{x1}$  goes to zero, the value of  $B_{x1}$  changes from 0 to 0.01, while  $x$  changes from -8.0 to -2.0, it changes from +0.01 to -0.01 almost linearly, while  $x$  changes from -2.0 to +2.0, then  $B_{x1}$  changes from -0.01 to 0 while  $x$  changes from +2.0 to +8.0. The maximum deflection is at  $x=\pm 2.0$ . If a curve whose  $x$  changes from -8.0 to +8.0 is

while  $x$  changes from  $+2.0$  to  $+8.0$ . The maximum deflection is at  $x=\pm 2.0$ . If a curve whose  $x$  changes from  $-8.0$  to  $+8.0$  is plotted, the maximum deflection will be much clear. The solution given here tells us that: When  $y$  changes from 1 to 5, the maximum field perturbation changes from 0.5 to 0.01. This means that : the larger the point from the current carrying conduct, the less the perturbation. So we assume that : with the increase of  $y$ , the maximum field perturbation will be smaller and smaller.

The sharp of the curve in Figure 4-3a is almost as same as that in Figure 4-2a. But the maximum magnitude of  $B_{x1}$  is much less then that in Figure 4-2a. The plot indicates that the curve is also a doublet and symmetrical with respect to "0." When  $x=\pm\infty$ ,  $B_{x1}$  go to zero, the value of  $B_{x1}$  changes from 0 to  $2\times 10^{-3}$ , while  $x$  changes from  $-20.0$  to  $-6.0$ , it changes from  $+2\times 10^{-3}$  to  $-2\times 10^{-3}$ , while  $x$  changes from  $-6.0$  to  $+6.0$ , then  $B_{x1}$  changes form  $-2\times 10^{-3}$ -0.01 to 0 while  $x$  changes from  $+6.0$  to  $+20.0$ . The maximum deflection is at  $x=\pm 6.0$ . If a curve is plotted whose  $x$  changes from  $-20.0$  to  $+20.0$ , the maximum deflection will be much clear. The bandwidth of the curve is wider than that of in Figure 4-2. Thus roughly speaking, we may say that the maximum magnetic field strength occurs far from the current carrying conductor and goes to smaller and smaller while  $y$  increases.

From Figure 4-4a,b, we see that that the curve is also a doublet and symmetrical with respect to "0".  $B_{x1}$  changes from 0 to  $1.5\times 10^{-5}$ , while  $x$  changes from  $-100.0$  to  $-20.0$ , it changes from  $+1.5\times 10^{-5}$  to  $-1.5\times 10^{-5}$ , while  $x$  changes from  $-20.0$  to  $+20.0$ , then  $B_{x1}$  changes form  $-1.5\times 10^{-5}$  to 0 while  $x$  changes from  $+20.0$  to  $+100.0$ . The maximum deflection is at  $x=\pm 20.0$ .

From Figure 4-5, we see that the curve is also a doublet and symmetrical with respect to "0".  $B_{x1}$  changes from  $0.5\times 10^{-6}$  to  $1.5\times 10^{-6}$ , while  $x$  changes from  $-100.0$  to  $-40.0$ , it changes from  $+1.5\times 10^{-6}$  to  $-1.5\times 10^{-6}$ , while  $x$  changes



from -40.0 to +40.0, then  $B_{x1}$  changes from  $-1.5 \times 10^{-6}$  to  $0.5 \times 10^{-6}$  while  $x$  changes from +40.0 to +100.0. The maximum deflection is at  $x = \pm 40.0$ .

From Figure 4-6, ( $y=200$ ), we see that the curve is changed to the one which looks like a  $\cos(x)$  function curve. The reason we got this is that we chose  $x$  whose range is from -100.0 to +100.0. If we use the range whose  $x$  changes from -500.0 to +500.0, we will get a curve very similar to these curves we got before. Now the maximum magnetic perturbation is getting very small that is only  $1.6 \times 10^{-7}$ .  $B_{x1}$  changes from  $+1.6 \times 10^{-7}$  to  $-1.6 \times 10^{-7}$ , while  $x$  changes from -100.0 to +100.0, and the change is as almost same as that of  $\cos(x)$  function.

Now lets take a look at the curve whose  $y=500.0$  (Figure 4-7a and Figure 4-7b). Like the preceding sections,  $x$  changes from -100.0 to +100.0. The solution given here is a special one. When  $x$  changes from -100.0 to +100.0, the magnetic field perturbation changes linearly from  $9.0 \times 10^{-9}$  to  $-9.0 \times 10^{-9}$ . The slope of the line is very small. But when we use the big  $x$ , we can get the curve that has the same sharp as others. The difference is the maximum magnetic perturbation is much less than those we discussed before.

The last plot we discuss about the first item is Figure 4-8. Using the same change of  $x$ , we got the same sharp of the curve of  $B_{x1}$ , the only difference is that the slopes of the lines. In Figure 4-8a, the unit of  $B_{x1}$  is  $2 \times 10^{-10}$ , but the unit of  $B_{x1}$  we used for Figure 4-7 is  $2 \times 10^{-10}$ . This curve happens when  $y=1000.0$ . Also, in Figure 4-8b which shows the change of  $B_{x1}$  while  $-1500 < x < 1500$ .

Figure 4-1a to Figure 4-8b illustrate the magnitude perturbation in the axial component of the induced magnetic field corresponding to a threshold value of the magnetic Reynolds number ( for the first term of the solution). The plots indicate that field perturbation is sensitive to  $y$ , with almost zero value at the surface of both electrodes. The location of electrodes is at  $y=0$ ,  $y=L$ , and the current carrying conductor is located at  $y = y_0$ . In the preceding section, different plots are

shown separately. Later we will put the curves with different  $y$  together, (select  $y=1, y=1.5, y=2.5$ ), see how the curve changes with different  $y$ .

Figure 4-9a to Figure 4-16b illustrate the second term of  $B_{x1}$ :

$$\frac{-20x(y-y_0)^4 + 40x^3(y-y_0)^2 - 4x^5}{((y-y_0)^2 + x^2)^5}$$

From Figure 4-9a, we see that  $B_{x1}=0$  when  $x=\pm\infty$ . therefore, the solution we that we have also agrees with the established boundary conditions. We will discuss the other boundary condition later. From the plot, we see that the curve is a doublet. When  $x=\pm\infty$ ,  $B_{x1}$  goes to zero, the value of  $B_{x1}$  changes from 0 to -0.05, while  $x$  changes from -1.5 to -0.5, it changes from -0.5 to 3.5 almost linearly, while  $x$  changes from -0.5 to +0.5, then  $B_{x1}$  changes from 3.5 to -3.5 while  $x$  changes from -0.5 to +0.5. The maximum deflection is at  $x=\pm 0.5$  which is  $\pm 3.5$ . Since the curve is a doublet, so that the right part is symmetrical as left part with respect to "0". Now we can compare this plot with Figure 4-1a which is the first term of  $B_{x1}$  whose  $y$  is also "1". When  $x$  is very large number, both field perturbations are infinite. The major change of curve in Figure 4-1b happens while  $x$  is between -1.5 and 1.5. And major change of curve in Fig 4-9b happens while  $x$  changes from -2.0 to 2.0. So that we can say that if the distance of point we measured to the point that the infinite current carrying conductor is small, both of them should be considered. First difference between these two is: the maximum magnitude of Figure 4-1b is about 1.5, and the one of Figure 4-9b is around 3.5. Second is that the curve in Figure 4-1b changes very smooth when  $x$  changes from  $-\infty$  to 0 and as same as when  $x$  goes from 0 to  $\infty$ . In Figure 4-9b, before the curve goes up, there is a small hollow; at the symmetry side before it goes to infinite, there is a small protruing. Before going any further, we guess

that the maximum field perturbations will be smaller and smaller while  $y$  be chosen larger and larger.

Figure 4-10 is obtained after putting  $y=5$  into that second term. As same as the other plots, when  $x=-\infty$ , the field perturbation is zero; when  $x=+\infty$ , it is zero also. The major change happens near where the current carrying conductor is located ( $-4 < x < 4$ ). That part of the curve is very similar to the function  $\sin(x)$ . Negligence of the part  $x < -4$ ,  $x > 4$ , the field perturbation of that term can be described as a sinusoidal function.

To plot the curve using  $y=10$ , we obtain Figure 4-11a and Figure 4-11b which are also doublets. Comparing this result with that  $y=5$ , we conclude that the maximum magnitude of the  $B_{x1}$  which  $y=10$  is much less than that of  $y=5$ . And its bandwidth is wider than the first one. It looks like that the curve has been pulled open. The plot indicate that the curve is also a doublet and symmetrical with respect to "0". When  $x=\pm\infty$ ,  $B_{x1}$  goes to zero, the value of  $B_{x1}$  changes from 0 to  $3 \times 10^{-5}$ , while  $x$  changes from -8.0 to -3.0, it changes from  $+3 \times 10^{-5}$  to  $-3 \times 10^{-5}$ , while  $x$  changes from -3.0 to +3.0, then  $B_{x1}$  changes from  $-3 \times 10^{-5}$  to 0 while  $x$  changes from +3.0 to +8.0. The maximum deflection is at about  $x=\pm 3.0$ . If we plot a curve whose  $x$  changes from -15.0 to +15.0, the maximum deflection will be much clear. The solution given here tells us that: When  $y$  changes from 5 to 10, the maximum field perturbation changes a lot, from 0.001 to  $3 \times 10^{-5}$ . This means that : the longer the distance from the point to the current carrying conduct, the less the field perturbation . That identical is agree to the presume which we assume before. With the increase of  $y$ , the maximum field perturbation will be smaller and smaller.

The sharp of the curve in Figure 4-12 ( $y=50$ ) is almost as same as that in Figure 4-11 and Figure 4-10, but the maximum magnitude of  $B_{x1}$  is much less than in Figure 4-11. The plot indicates that the curve is also a doublet and symmetrical

with respect to "0". When  $x=\pm\infty$ ,  $B_{x1}$  goes to zero, the value of  $B_{x1}$  changes from 0 to  $1\times 10^{-8}$ , while  $x$  changes from -30.0 to -15.0. The field magnitude changes from  $+1\times 10^{-8}$  to  $-1\times 10^{-8}$ , while  $x$  changes from -15.0 to +15.0, then  $B_{x1}$  changes from  $-1\times 10^{-8}$  to 0 while  $x$  changes from +15.0 to +30.0. The maximum deflection is at  $x=\pm 15.0$ . The bandwidth of the curve is wider than that of in Figure 4-11. Thus roughly speaking, we may say that the maximum magnetic field strength occurs far from the current carrying conductor and goes to smaller and smaller while  $y$  increases. From Figure 4-12, Figure 4-4, we see that the maximum of the magnetic field of the second term is much less than that of first term with the same  $y$  which is 50. If we put both curves in Figure 4-4, Fig 4-12 together, probably we can only see one curve which is the curve of the first term of  $B_{x1}$ , the other one is just a line. In that case, the second term need not be taken into account.

The curve of the second term whose  $y=100$  (Figure 4-13) is also a doublet and symmetrical with respect to "0".  $B_{x1}$  changes from 0 to  $3.2\times 10^{-10}$ , while  $x$  changes from -70.0 to -30.0.  $B_{x1}$  changes from  $+3.2\times 10^{-10}$  to  $-3.2\times 10^{-10}$ , while  $x$  changes from -30.0 to +30.0, then  $B_{x1}$  changes from  $-3.2\times 10^{-10}$  to 0 while  $x$  changes from +20.0 to +100.0. The maximum deflection is at  $x=\pm 30.0$ .

From Figure 4-14 ( $y=200$ ), we see that almost all of the change of the magnetic field  $B_{x1}$  occurs in a wide interval between  $-100 < x < 100$ , the maximum field perturbation occurs at  $x= \pm 50$ . But the maximum  $B_{x1}$  is only  $1.0\times 10^{-11}$ , even we did not plot the curves have big  $y$ , we can say that with the increasing of  $y$ , the maximum  $B_{x1}$  will be smaller.

Lets discuss two more curves for the second term of the field perturbation. The curve in Figure 4-15 shows change of  $B_{x1}$  with  $y=500.0$  and  $-100.0 < x < 100.0$ . From the curve, we see that  $B_{x1}$  goes from  $10\times 10^{-13}$  when  $x=-100.0$  down to  $-10\times 10^{-13}$  almost linearly. The reason we got this curve which is different from those we had before is that the bandwidth of the curve is very wide. It can not be seen

the whole change by using small  $-100 < x < 100$ . If we use big  $x$ , for instance,  $x$  changes from  $-300$  to  $300$ , we can get a curve like those curves we got in the preceding section. Here, a curve (Figure 4-15b) has different  $x$  value had been made which has the familiar sharp. And we are sure that  $B_{x1}$  is zero even Figure 4-15a does not show the value of  $x \rightarrow \pm\infty$ .

The last picture we discuss for this term is Figure 4-16 whose  $y$  is  $1000.0$ . We have the same situation as Figure 4-15 whose  $x$  was not chosen big enough to be seen the whole change of the  $B_{x1}$ . But choosing small  $x$ , we can see very clearly how the magnetic field changes when  $x$  is small, but  $y$  is big. Now the maximum  $B_{x1}$  is about  $2 \times 10^{-15}$ , so its a very small number which will not be taken into account.

Figure 4-12 ( $y=50$ ), Figure 4-13 ( $y=100$ ), Figure 4-14 ( $y=200$ ), Figure 4-15 ( $y=500$ ) and Figure 4-16 ( $y=1000$ ), the resulting patterns. After propagating  $y$ , curve spreads to wider. The plots were made for various values of  $y$  given in Fig 4-9 to Fig 4-16. When  $y=1$ , the sharp of curve is very similar to the curve in Figure 4-1, whose  $y=1$ , but in the opposite direction. Substituting  $y=5$  for the second term of  $B_{x1}$ , we obtain the curve in Figure 4-10, which is also very similar to curve in Figure 4-2 and in the opposite direction. Taking another  $y=10$ , we find some difference between this curve and the curve in Figure 4-3. It looks like a triplet. Before going up, it goes down first, and its symmetrical. By plot all those curves whose  $y$  changes from  $10$  to  $1000$ , Figure 4-9 to Figure 4-16 are obtained. When  $y$  varies from  $0$  to  $1000$ , the maximum values of  $B_{x1}$  goes to smaller and smaller. In Figure 4-16, the unit of  $B$  axis is  $5 \times 10^{-16}$  which is very small.

Similarly for third term of  $B_{x1}$ :

$$\frac{-42x(y-y_0)^6 + 210x^3(y-y_0)^4 - 126x^5(y-y_0)^2 + 6x^7}{((y-y_0)^2 + x^2)^7}, \quad 0 < y < 1000, -100 < x < 100$$

the sharp of the curves we get is very similar to that we got for the second term. But for every single curve, the magnitude of  $B_{x1}$  is smaller than the one for the second term that both of them has the same  $y$ .

Figure 4-17a illustrate the first term of the total induced magnetic field whose  $y=1$ ,  $-100 < x < 100$ , The plot indicate that the curve is a doublet and symmetrical with respect to "0". When  $x=\pm\infty$ ,  $B_{x1}$  goes to zero as others, the value of  $B_{x1}$  changes from 0 to 5.0, while  $x$  changes from -0.5 to -0.2, it changes form +5.0 to -5.0 almost linearly, while  $x$  changes from -0.2 to +0.2, then  $B_{x1}$  changes from -5.0 to 0 while  $x$  changes from +0.2 to +0.5. The maximum deflection is at  $x=\pm 0.2$ . If we plot a curve whose  $x$  changes from -6 to +6, the maximum deflection will be much clear. There is a difference between this one and the proceeding plots: Near the current carrying conductor, the magnetic field rises and falls, looks like a big boublet and a small doublet combined together. Weather it effects the whole function will be seen lately. We consider that  $y$  can changes from 0 to infinity and the current carrying conductor of infinite length is located at  $y = -y_0$ . We assume that  $y_0 = 0.1$ , which is very small. Compared with infinite number, 1.0 is a very small number, so the point we are discussing is very close to the current carrying conductor. (We only discuss one current carrying conductor situation.) From Figure 4-17a, we see that  $B_{x1}=0$  when  $x=\pm\infty$ . therefore, the solution we got agrees with the established boundary conditions. We will discuss the other boundary condition later.

To plot the curve using  $y=5$ , we obtain Figure 4-18 which is also a big doublet plus a small doublet. Comparing this result with that  $y=1$ , we conclude that the maximum magnitude of the  $B_{x1}$  which  $y=5$  is much less then that of  $y=1$ . And its bandwidth which is the frequency span between the upper end lower half-power points is wider then the first one. (Sounds like each term is the same). The curve looks like been pulled open. The plot indicate that the curve is symmetrical with

respect to "0". When  $x=\pm\infty$ ,  $B_{x1}$  goes to zero, the value of  $B_{x1}$  changes from 0 to  $7\times 10^{-5}$ , while  $x$  changes from -3.0 to -1.0, it changes from  $+7\times 10^{-5}$  to  $-7\times 10^{-5}$  while  $x$  changes from -1.0 to +1.0, then  $B_{x1}$  changes form  $-7\times 10^{-5}$  to 0 while  $x$  changes from +1.0 to +3.0. The maximum deflection is at  $x=\pm 1.0$ . If we plot a curve whose  $x$  changes from -10.0 to +10.0, the maximum deflection will be much clear. The solution given here tells us that: When  $y$  changes from 1 to 5, the maximum field perturbation changes from 5 to  $7\times 10^{-5}$ . This means that: the larger the point from the current carrying conduct, the less the perturbation. Even we changed  $y$  from 1 to 5, we got such a difference. So we assume that : with the increase of  $y$ , the maximum field perturbation will be much smaller and smaller. The sharp of the curve in Figure 4-19a is almost as same as that in Figure 4-18a. But the maximum magnitude of  $B_{x1}$  is much less that in Figure 4-18a. The plot indicates that the curve is also two doublet and symmetrical with respect to "0". When  $x=\pm\infty$ ,  $B_{x1}$  goes to zero, the value of  $B_{x1}$  changes from 0 to  $5\times 10^{-7}$ , while  $x$  changes from -5.0 to -2.5, it changes form  $+5\times 10^{-7}$  to  $-5\times 10^{-7}$ , while  $x$  changes from -2.5 to +2.5, then  $B_{x1}$  changes form  $-5\times 10^{-7}$  to 0 while  $x$  changes from +2.5 to +5.0. The maximum deflection is at  $x=\pm 2.5$ . The bandwidth of the curve is wider than that of in Figure 4-18. Thus roughly speaking, we may say that the maximum magnetic field strength occurs far from the current carrying conductor and goes to smaller and smaller while  $y$  increases. From Figure 4-20 ( $y=50$ ), we see that the sharp of the curve is as same as the of the one in Figure 4-19.  $B_{x1}$  changes from 0 to  $6.5\times 10^{-12}$ , while  $x$  changes from -22.0 to -10.0, it changes form  $+6.5\times 10^{-12}$  to  $-6.5\times 10^{-12}$ , while  $x$  changes from -10.0 to +10.0, then  $B_{x1}$  changes form  $-6.5\times 10^{-12}$  to 0 while  $x$  changes from +10.0 to +22.0. The maximum deflection is at  $x=\pm 10.0$ . Compared with the unit of Fig 3-3,  $2\times 10^{-12}$  is very small. So that we can say: For this term, when  $y$  goes to greater, it will not be taken account, because of the small magnitude. The following plots will have the same program. From Figure 4-21,

we see that the curve is also two doublets and symmetrical with respect to "0".  $B_{x1}$  changes from 0 to  $5 \times 10^{-14}$ , while  $x$  changes from -50.0 to -20.0, it changes from  $+5 \times 10^{-14}$  to  $-5 \times 10^{-14}$ , while  $x$  changes from -20.0 to +20.0, then  $B_{x1}$  changes from  $-5 \times 10^{-14}$  to 0 while  $x$  changes from +20.0 to +50.0. The maximum deflection is at  $x = \pm 20.0$ . From Figure 4-22a, ( $y=200$ ), we see that the curve's unit is changed to  $1 \times 10^{-16}$ , the maximum magnetic perturbation is getting very small which is only  $4.0 \times 10^{-16}$ .  $B_{x1}$  changes from 0 to  $4.0 \times 10^{-16}$ , while  $x$  changes from -100.0 to -40.0, and then it goes down from  $4.0 \times 10^{-16}$  to 0 and going to  $-4.0 \times 10^{-16}$  while  $x$  changes from -40.0 to 0 then to 40.0. This part shows the maximum deflection. After  $x > 40.0$ ,  $B_{x1}$  goes up again until it maintain "0". As we said before, the maximum magnitude of  $B_{x1}$  is very small.

Now lets take a look at the curve whose  $y=500.0$  (Figure 4-23). Like the preceding sections,  $x$  changes from -100.0 to +100.0. The solution given here is a special one. When  $x$  changes from -100.0 to +100.0, the magnetic field perturbation changes almost linearly from  $6.5 \times 10^{-19}$  to  $-6.5 \times 10^{-19}$ . The slope of the line is very small. If we use 100.0 as the unit of  $x$ , and use 1 unit of  $B_{x1}$ , this curve will not be seen.

The last plot we discuss about the third item is Figure 4-24a and Figure 4-24b. Using the same change of  $x$ , we got the same sharp of the curve of  $B_{x1}$ , the only difference is that the slopes of the lines. In Figure 4-24a, the unit of  $B_{x1}$  is  $1 \times 10^{-21}$ , but the unit of  $B_{x1}$  we used for Figure 4-23a is  $2 \times 10^{-19}$ . This curve happens when  $y=1000.0$ .

Figure 4-17a to Figure 4-24b illustrate the third term of the magnitude perturbation in the axial component of the induced magnetic field corresponding to a threshold value of the magnetic Reynolds number ( for the first term of the solution). The plots indicate that field perturbation is very sensitive to  $y$ . In the preceding section, different plots are shown separately. If we put the curves with



different  $y$  together, (select  $y=1$ ,  $y=10$ ,  $y=100$ ), see how the curve changes with different  $y$ . The result we have is : Only the one whose  $y=1$  could be seen from the plot. With this solution, we may say that for the third term of  $B_{x1}$ , only the ones have very small  $y$  need to be taken into account.

Figure 4-25a to Figure 4-32b illustrate the fourth term of  $B_{x1}$  :

$$\frac{-72x(y-y_0)^8 + 672x^3(y-y_0)^6 - 1008x^5(y-y_0)^4 + 288x^7(y-y_0)^2 - 8x^9}{((y-y_0)^2 + x^2)^9}$$

From Figure 4-25, we see that  $B_{x1}=0$  when  $x=\pm\infty$ . therefore, the solution we got also agrees with the established boundary conditions. From the plot, we see that the curve has two doublets. One of the doublets is bigger. When  $x=\pm\infty$ ,  $B_{x1}$  goes to zero, the value of  $B_{x1}$  changes from 0 to 7.0, while  $x$  changes from -0.5 to -0.2. It changes from 7.0 to -7.0 linearly, while  $x$  changes from -0.2 to +0.2, then  $B_{x1}$  changes from -7.0 to 0 while  $x$  changes from 0.2 to 0.5. The maximum deflection is at  $x=\pm 0.2$  which is  $\pm 7.0$ . Since the curve is a doublet, so that the right part is symmetrical as left part with respect to "0". When  $x$  is very large number, both field perturbations are zero. The major change of curve in Figure 4-25b happens while  $x$  is between -0.5 and 0.5. And major change of curve in Figure 4-1b to Figure 4-9b all happen at a narrow  $x$ . So we can say that if the four terms are together, every term needs to put into the curve. The curve should be the one that these four terms combined together. In Figure 4-25, before  $B_{x1}$  goes up, there is a small hollow; at the symmetry side before it goes to infinite, there is a small protruing. Before going any further, we guess that the maximum field perturbations will be smaller and smaller while  $y$  be chosen greater and greater.

Figure 4-26 is obtained after putting  $y=5$  into that fourth term. As same as the other plots, when  $x=-\infty$ , the field perturbation is zero; when  $x=+\infty$ , it is zero also. The major change happens near where the current carrying conductor is located (-

$2.0 < x < 2.0$ ). To plot the curve using  $y=5.0$ , we obtain Figure 4-26 which is also a doublet. Comparing this result with that  $y=5$ , we conclude that the maximum magnitude of the  $B_{x1}$  which  $y=5$  is much less than that of  $y=1$ . And its bandwidth is wider than the first one. It looks like that the curve has been pulled open just like the others. The plot indicates that the curve is also a doublet and symmetrical with respect to "0". When  $x=\pm\infty$ ,  $B_{x1}$  goes to zero, the value of  $B_{x1}$  changes from 0 to  $3.5 \times 10^{-6}$ , while  $x$  changes from -2.0 to -1.0, it changes from  $+3.5 \times 10^{-6}$  to  $-3.5 \times 10^{-6}$ , while  $x$  changes from -1.0 to +1.0, then  $B_{x1}$  changes from  $-3.5 \times 10^{-6}$  to 0 while  $x$  changes from +1.0 to +2.0. The maximum deflection is at about  $x=\pm 1.0$ . If we plot a curve whose  $x$  changes from -15.0 to +15.0, the maximum deflection will show very clear. The solution given here tells us that: When  $y$  changes from 1 to 5, the maximum field perturbation changes a lot, from 7.0 to  $3.5 \times 10^{-6}$ . This means that: the longer the distance from the point to the current carrying conduct, the less the field perturbation. That identical is agree to the presume which we assume before. With the increase of  $y$ , the maximum field perturbation will be smaller and smaller.

The sharp of the curve in Figure 4-27 ( $y=10$ ) is almost as same as that in Fig 4-25 and Figure 4-26, but the maximum magnitude of  $B_{x1}$  is much less than that in Fig 4-26. The plot indicates that the curve is also a doublet and symmetrical with respect to "0". When  $x=\pm\infty$ ,  $B_{x1}$  goes to zero, the value of  $B_{x1}$  changes from 0 to  $0.7 \times 10^{-8}$ , while  $x$  changes from -4.0 to -2.0. The field magnitude changes from  $+0.7 \times 10^{-8}$  to  $-0.7 \times 10^{-8}$ , while  $x$  changes from -2.0 to +2.0, then  $B_{x1}$  changes from  $-0.7 \times 10^{-8}$  to 0 while  $x$  changes from +2.0 to +4.0. The maximum deflection is at  $x=\pm 2.0$ . The bandwidth of the curve is wider than that of in Figure 4-26. Thus, we may say that the maximum magnetic field strength occurs far from the current carrying conductor and goes to smaller and smaller while  $y$  increases. From Figure 4-27, Figure 4-19 Figure 4-11 and Figure 4-3, we see that the maximum of

the magnetic field of the third term is much less than that of first term with the same  $y$  which is 10.0. If we put both curves in Figure 4-3, Figure 4-11, Figure 4-19, Figure 4-27 together, probably we can only see one curve which is the curve of the first term of  $B_{x1}$ , the other one is just a line. In that case, only the first need to be taken into account.

The curve of the second term whose  $y=50$  (Figure 4-28) is also a doublet and symmetrical with respect to "0".  $B_{x1}$  changes from 0 to  $3.2 \times 10^{-15}$ , while  $x$  changes from -18.0 to -8.0.  $B_{x1}$  changes from  $+3.2 \times 10^{-15}$  to  $-3.2 \times 10^{-15}$ , while  $x$  changes from -8.0 to +8.0, then  $B_{x1}$  changes from  $-3.2 \times 10^{-15}$  to 0 while  $x$  changes from +8.0 to +18.0. The maximum deflection is at  $x=\pm 8.0$ .

From Figure 4-29 ( $y=100$ ), we see that almost all of the change of the magnetic field  $B_{x1}$  occurs in a wide interval between  $-100 < x < 100$ , the maximum field perturbation occurs at  $x = \pm 18$ . But the maximum  $B_{x1}$  is only  $7.0 \times 10^{-18}$ , even we did not plot the curves have big  $y$ , we can say that with the increasing of  $y$ , the maximum  $B_{x1}$  will be smaller.

Lets discuss a couple of more curves for the fourth term of the field perturbation. The curve in Figure 4-30 shows change of  $B_{x1}$  with  $y=200.0$  and  $-100.0 < x < 100.0$ . From the curve, we see that  $B_{x1}$  goes from 0 to  $1.4 \times 10^{-20}$  when  $x=-75.0$  to  $-40.0$ . The maximum perturbation is very small  $1.4 \times 10^{-20}$ , this happens at  $x=-40.0$ .  $1.4 \times 10^{-20}$  is a very small number, this will not effect anything. Neither does Figure 4-31 and Figure 4-32. Before doing anything, we think that both curves in Figure 4-31 and Figure 4-32 has very small magnitude. They are too small to be taken into account.

Figure 4-31a shows the fourth term of  $B_{x1}$  when  $y=500$ . But from Figure 4-31a, we can not see the whole change of the field. We have to use big  $x$ , for instance,  $x$  changes from -300 to 300, we can get a curve like those curves we got in the preceding section. In Figure 4-31a, we can get the maximum magnitude ( $B_{x1}=3.5 \times$

$10^{-24}$ ) when  $x=75.0$ . Here, a curve (Figure 4-31b) has different  $x$  value had been made which has the familiar sharp. And we are sure that  $B_{x1}$  is zero even Figure 4-31a does not show the value of  $x \rightarrow \pm\infty$ .

The last picture we discuss is Figure 4-32a whose  $y$  is 1000.0. We have the same situation as Figure 4-32a whose  $x$  was not chosen big enough to be seen the whole change of the  $B_{x1}$ . But choosing small  $x$ , we can see very clearly how the magnetic field changes when  $x$  changes, but  $y$  is large. Now the maximum  $B_{x1}$  is about  $2 \times 10^{-27}$ , so its a very small number which will not be taken into account.

Figure 4-25 ( $y=1$ ), Figure 4-26 ( $y=5$ ), Figure 4-27 ( $y=10$ ), Figure 4-28 ( $y=50$ ), Figure 4-29 ( $y=100$ ), Figure 4-30 ( $y=200$ ), Figure 4-31 ( $y=500$ ) and Figure 4-32 ( $y=1000$ ) are the resulting patterns. After propagating  $y$ , curve spreads to wider.

Combining the four terms together, which is :

$$\begin{aligned} & \frac{-6x(y-y_0)^2 + 2x^3}{(y-y_0)^2 + x^2} + \frac{-20x(y-y_0)^4 + 40x^3(y-y_0)^2 - 4x^5}{((y-y_0)^2 + x^2)^5} \\ & + \frac{-42x(y-y_0)^6 + 210x^3(y-y_0)^4 - 126x^5(y-y_0)^2 + 6x^7}{((y-y_0)^2 + x^2)^7} \\ & + \frac{-72x(y-y_0)^8 + 672x^3(y-y_0)^6 - 1008x^5(y-y_0)^4 + 288x^7(y-y_0)^2 - 8x^9}{((y-y_0)^2 + x^2)^9} \end{aligned}$$

we obtain following curves. Figure 4-33a to Figure 4-40b are the plots for the total  $B_{x1}$ . Comparing these curves with the curves in Figure 4-1 to Figure 4-9, we can easily find that they almost have the same magnitude and same shape. The reason is very simple. Compared with other three terms, the first term has the largest unit of the  $B$  axis. For example, if we use the same  $y=5$ , the unit of  $B$  axis of Figure 1-3 is 0.005, but the unit of  $B$  axis of Fig 2-3 is 0.0008, the unit of  $B$  axis of Fig 3-3 is  $2 \times 10^{-5}$  and the unit of  $B$  axis of Fig 4-3 is  $1 \times 10^{-6}$ . So if we put all

these four terms together, only the first term is the main term whose curves show on Figure 4-33 to Figure 4-40.

From Figure 4-33a, we can see that  $B_{x1}=0$  when  $x=\pm\infty$ . therefore, the solution that we got agrees with the established boundary conditions of  $B_{x1}$ . The curve is a doublet with maximum magnitude 17.0. The value of  $B_{x1}$  changes from 0 to 17.0 when  $x$  changes from -1.0 to -.02. At  $x=-0.2$ ,  $B_{x1}$  gets the peak value which is 17.0. While  $x$  is changing from -0.2 to .02,  $B_{x1}$  is changing from peak value 17.0 to -17.0. Than it goes from -17.0 up to 0 when  $x$  changes from 0.2 to 1.0.

To plot the curve using  $y=5$ , we obtain Figure 4-34a and Figure 4-34b which are doublets. Comparing this result with that  $y=1$ , we conclude that the maximum magnitude of the  $B_{x1}$  whose  $y=5$  is much less then that of  $y=1$ . The maximum magnitude is about 0.012 which is only 1/1000 of that  $y=1$ . We can discover also that the  $x$  width that  $B_{x1}$  changes from 0 to maximum is wider then the first one ( $y=1$ ). The curve looks like been pulled open. The plot indicate that the curve is also a doublet and symmetrical with respect to "0". This means that : the more the distance from the point of  $y$  to current carrying conduct, the less the perturbation. So we assume that : with the increase of  $y$ , the maximum field perturbation will be smaller and smaller.

The sharp of the curves in Figure 4-35a and Figure 4-35b are almost as same as that in Figure 4-34 and Figure 4-33. But the maximum magnitude of  $B_{x1}$  is much less then that in Fig 5-1 (1/10000), even much less then that in Fig 5-2 (1/10). The plot indicates that the curve is also a doublet and symmetrical with respect to "0". When  $x=\pm\infty$ ,  $B_{x1}$  goes to zero, the value of  $B_{x1}$  changes from 0 to  $1.5\times 10^{-3}$ , while  $x$  changes from -20.0 to -4.0, it changes form  $+1.5\times 10^{-3}$  to  $-1.5\times 10^{-3}$ , while  $x$  changes from -4.0 to +4.0, then  $B_{x1}$  changes form  $-1.5\times 10^{-3}$  to 0 while  $x$  changes from +4.0 to +20.0. The maximum deflection is at  $x=\pm 4.0$ . If we plot a curve ( Figure 4-35b) whose  $x$  changes from -20.0 to +20.0, the maximum deflection will

be much clear. The bandwidth of the curve is wider than that of in Figure 4-34. We may say that the maximum magnetic field strength occurs far from the current carrying conductor and goes to smaller and smaller while  $y$  increases.

From Figure 4-36, we see that the curve is also a doublet and symmetrical with respect to "0".  $B_{x1}$  changes from 0 to  $1.5 \times 10^{-5}$ , while  $x$  changes from -100.0 to -20.0, it changes from  $+1.5 \times 10^{-5}$  to  $-1.5 \times 10^{-5}$ , while  $x$  changes from -20.0 to +20.0, then  $B_{x1}$  changes from  $-1.5 \times 10^{-5}$  to 0 while  $x$  changes from +20.0 to +100.0. The maximum deflection is at  $x = \pm 20.0$ .

Figure 4-37a and Figure 4-37b show the change of  $B_{x1}$  when  $y=100$ . There is no large difference between this curve and those others in sharp. The maximum magnetic perturbation is  $1.5 \times 10^{-6}$  which is 1/10 of that when  $y=50$ . In Figure 4-37a we can not see how  $B_{x1}$  is when  $x = \pm \infty$ , because that  $B_{x1}$  changes from 0 to maximum is out of range  $-100 < x < 100$  as we usually use. But the plot in Figure 4-37b shows us very clearly that  $B_{x1}$  always goes to 0, when  $x = \pm \infty$ .

From Figure 4-38a, ( $y=200$ ), we see that the curve is changed to the one which looks like a  $\cos(x)$  function curve. The reason we got this is that we chose the range of  $x$  from -100.0 to +100.0. If we use the range whose  $x$  changes from -400.0 to +400.0, we will get a curve (Figure 4-38b) very similar to these curves we got before. Now the maximum magnetic perturbation is getting very small which is only  $1.6 \times 10^{-7}$ .  $B_{x1}$  changes from  $+1.6 \times 10^{-7}$  to  $-1.6 \times 10^{-7}$ , while  $x$  changes from -100.0 to +100.0, and the change is as almost same as that of  $\cos(x)$  function.

Now lets take a look at the curve whose  $y=500.0$  (Figure 4-39a and Figure 4-39b). Like the preceding sections,  $x$  changes from -100.0 to +100.0. The solution given here is a special one. When  $x$  changes from -100.0 to +100.0, the magnetic field perturbation changes linearly from  $9.0 \times 10^{-9}$  to  $-9.0 \times 10^{-9}$ . The slope of the line is very small. But when we use the big  $x$ , we can get the curve (Figure 4-39b)

which has the same sharp as others. The difference is the maximum magnetic perturbation is much less than those we discussed before.

The last plot we discuss about  $B_{x1}$  is Figure 4-40a. Using the same change of  $x$ , we got the same sharp of the curve of  $B_{x1}$ , the only difference is that the slopes of the lines. In Figure 4-40a, the unit of  $B_{x1}$  is  $2 \times 10^{-10}$ , but the unit of  $B_{x1}$  we used for Figure 4-39 is  $2 \times 10^{-10}$ . This curve happens when  $y=1000.0$ . Also, in Figure 4-40b which shows the change of  $B_{x1}$  while  $-1500 < x < 1500$ .

Figure 4-33 to Figure 4-40 illustrate the magnitude perturbation in the axial component of the induced magnetic field corresponding to a threshold value of the magnetic Reynolds number ( for the first term of the solution). The plots indicate that field perturbation is sensitive to  $y$ , with almost zero value at the surface of both electrodes. The location of electrodes is at  $y=0$ , ,  $y=L$ , and the current carrying conductor is located at  $y = -y_0$ . In the preceding section, different plots are shown separately. Now we put the curves with different  $y$  together, (select  $y=1, y=1.5, y=2$ ), see how the curve changes with different  $y$ .

So far we have not discussed the fifth term yet which is a function of  $\delta$ :

$$\delta(y-y_0) \left( \frac{1}{x} - \frac{1}{3x^3} + \frac{1}{5x^5} - \frac{1}{7x^7} \right)$$

This  $\delta$  function will only be effective when  $y = y_0$ , with any value of  $x$  along the MHD channel, whether upstream or downstream. The magnitude of the  $\delta$  function is an infinite impulse. However, we chose the magnitude of the function as 1000 which can be used on the computer. Figure 4-41 shows this term. The curve is a doublet which has big magnitude, and it goes to 0 when  $x = \pm\infty$ . The physical picture shows a conducting fluid flowing between two infinite paralleled electrodes of an arbitrary height,  $L$ . The source of the magnetic field is an infinite conductor carrying current which has  $\delta$  function and located at a distance  $y_0$  below the lower channel wall. Those plots we already discussed indicate that field

perturbation is loosely sensitive to the distance between the position of any  $y$  and the position of the infinite conductor.  $y$  is channel height in all figures.

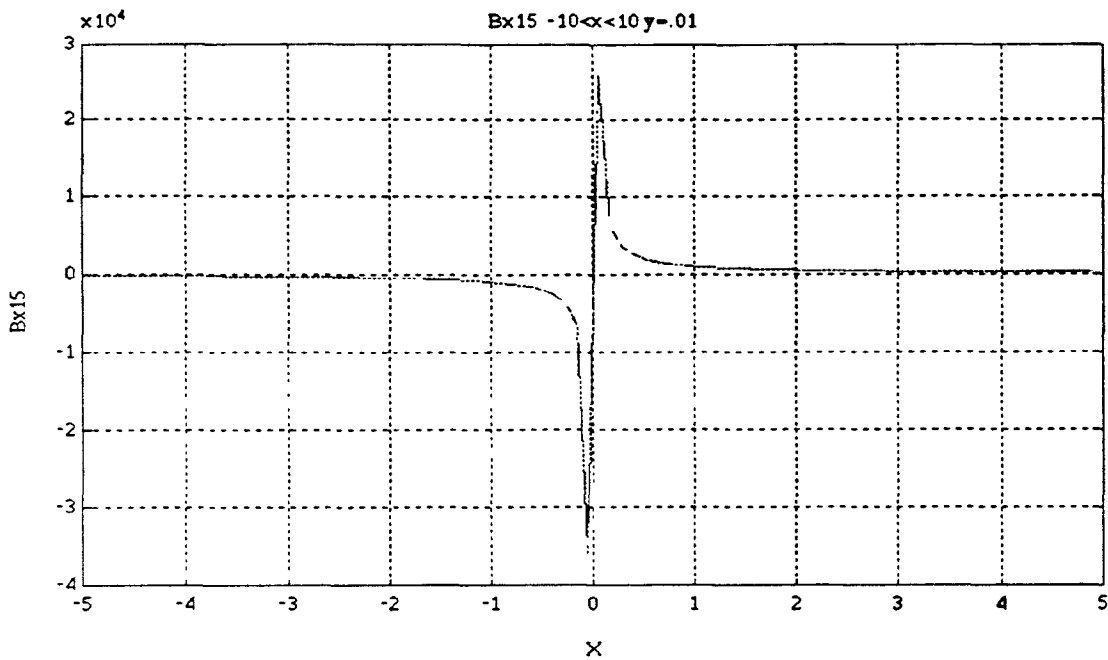


Figure 4-41 Axial component of total induced magnetic field 5,  $y=0.01$

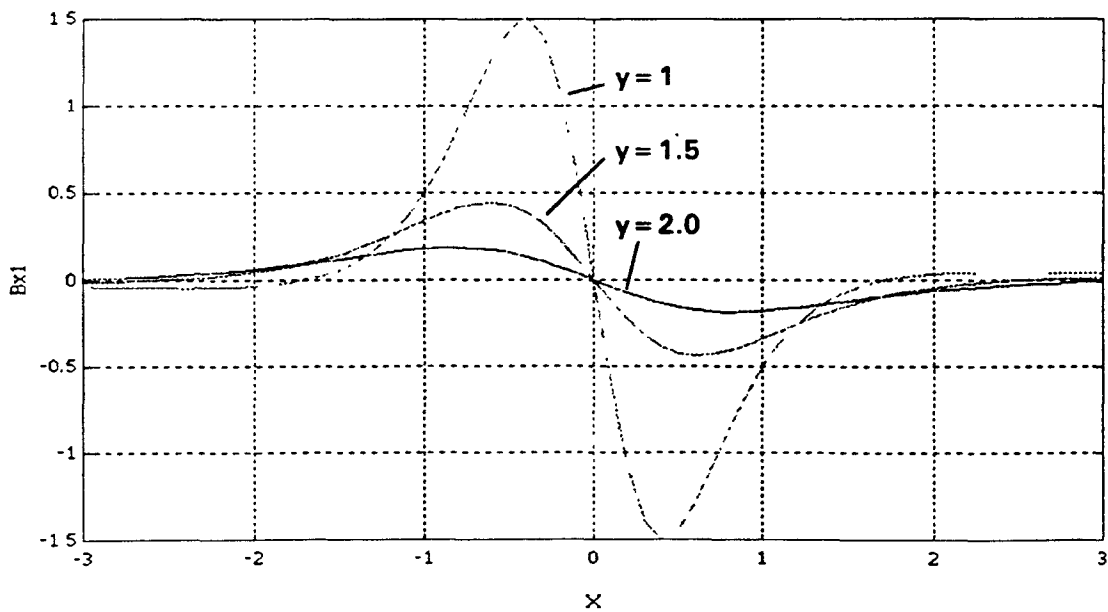


Figure 4-42 Axial component of total induced magnetic field,  $y=1.0, 1.5, 2.0$



## Chapter 5

### CONCLUSIONS

1) The solutions considered in the preceding chapter shows that solutions for magnetic and flow field perturbations for an incompressible and inviscid plasma in a parallel plate channel can be obtained in a closed mathematical form using the perturbation theory and the existence of magnetic boundary layer approximation. (A threshold value for the magnetic Reynolds number of 0.1 that corresponds to the beginning of boundary layer separation was assumed.

The induced magnetic field is due to an infinite linear superconductor carrying alternate current  $I\delta(0, -y_0)$  located a small distance  $y_0$  below the lower channel wall, and has only two components normal to the two electrodes. This geometrical configuration of the two parallel plates is actually an exact simulation for an MHD generator whose operational duct could be either the main divertor channel near the scrape-off region or the exhaust chamber of the tokamak fusion reactor. The source of external induction is centered on a coil wound around either the director duct or its exhaust chamber. The coil is biased with alternate field which is intended to contribute further to streamlining the feral magnetic field system in the reactor.

Solutions for the induced magnetic field were obtained by the method of mathematical perturbation and using the concept of magnetic boundary layer approximation, listed as follows:

$$B_{x1} = \delta(y - y_0) \left( \frac{1}{x} - \frac{1}{3x^3} + \frac{1}{5x^5} - \frac{1}{7x^7} \right) + \frac{-6x(y - y_0)^2 + 2x^3}{((y - y_0)^2 + x^2)^3} + \frac{-20x(y - y_0)^4 + 40x^3(y - y_0)^2 - 4x^5}{((y - y_0)^2 + x^2)^5}$$

$$\begin{aligned}
& + \frac{-42x(y-y_0)^6 + 210x^3(y-y_0)^4 - 126x^5(y-y_0)^2 + 6x^7}{((y-y_0)^2 + x^2)^7} \\
& + \frac{-72x(y-y_0)^8 + 672x^3(y-y_0)^6 - 1008x^5(y-y_0)^4 + 288x^7(y-y_0)^2 - 8x^9}{((y-y_0)^2 + x^2)^9}
\end{aligned}$$

The computer programming and calculation covered every single term of the tangential induced magnetic field component  $B_{x1}$  and the total tangential induced magnetic field component as given here. The software SIMULINK had been used in this paper. All M-files which are used to plot the functions of single term of induced magnetic field and total induced magnetic field can be updated in future. The result shows that when  $y$  is very small,  $B_{x1}$  is obtained as the equation as shown before; when  $y$  is greater than 5.0,  $B_{x1}$  can be expressed as the first term of total  $B_{x1}$ :

$$B_{x1} \approx \frac{-6x(y-y_0)^2 + 2x^3}{((y-y_0)^2 + x^2)^3}$$

This will cause the calculations much simple.

2) The computer simulation indicates that magnetic field perturbation is very small (almost zero ) value at the surface of the low electrode which is near the alternate current carrying conductor of infinite length. Then the magnetic field perturbation gets the greatest value when  $y$  is near 1.0. While  $y$  increases, the maximum magnetic field perturbation goes smaller and smaller, and the bandwidth of the curve becomes wider and wider. Roughly speaking, we may say that while  $y$  changes from 1.0 to infinite number, the curve of magnetic field perturbation becomes flatter. This change can be seen very clearly in the follow figure. (Figure 5-1):

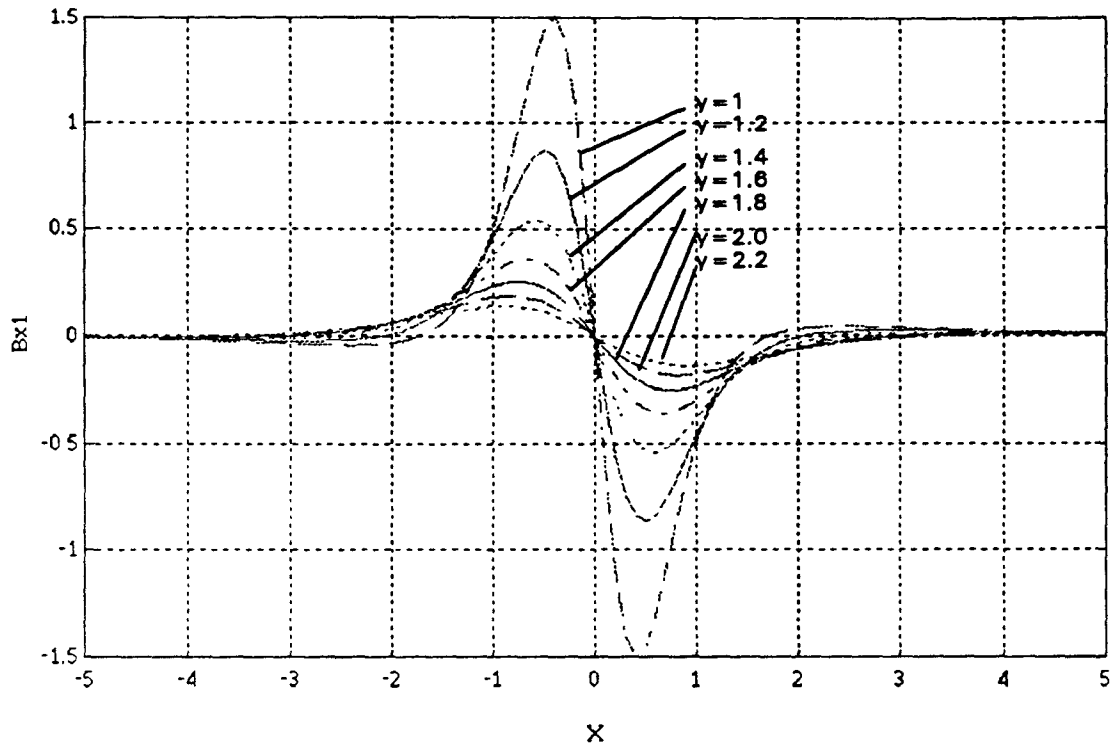


**Figure 5-1** Axial component of induced magnetic field

(Close  $y$  were chosen for plotting Figure 5-1. Because while  $y$  increases, the maximum magnetic field perturbation drops very fast. If  $y$  are too far apart, the big  $y$ 's curve will on top of another.)

The command of 3-D Mesh surface is used to create a 3-D plot as follow. This three dimension plot shows the change of  $x$ ,  $y$  and  $B_{x1}$  very clearly.

3) The solution which is obtained in this paper can be used to solve the induced magnetic field which is caused by alternate current carrying sheet. The method is that regarding the alternate current carrying sheet as many single current carrying conductors. Then using the process of summing :

$$B_{x1} = \sum_{x=x+a}^n B_{x1}$$

$a$  is the distance between each two conductors.  $B_{x1}$  is magnetic field of the current sheet.

4) The results can be used to develop applying pulsed acceleration of exhaust plasma in a fusion-MHD power generator. The external portion of the exhaust chamber for divertor of the PRDM fusion reactor could serve as an accelerator-induction generator channel. This can be accomplished by placing accelerating DC field on the AC ( current impulse singular function ) exciting field on the outward part. Determining the effectiveness of the magnetic field system for the AC induction generator in confining the poloidal field within the separatrix surface is required for designing the AC-MHD induction generator.

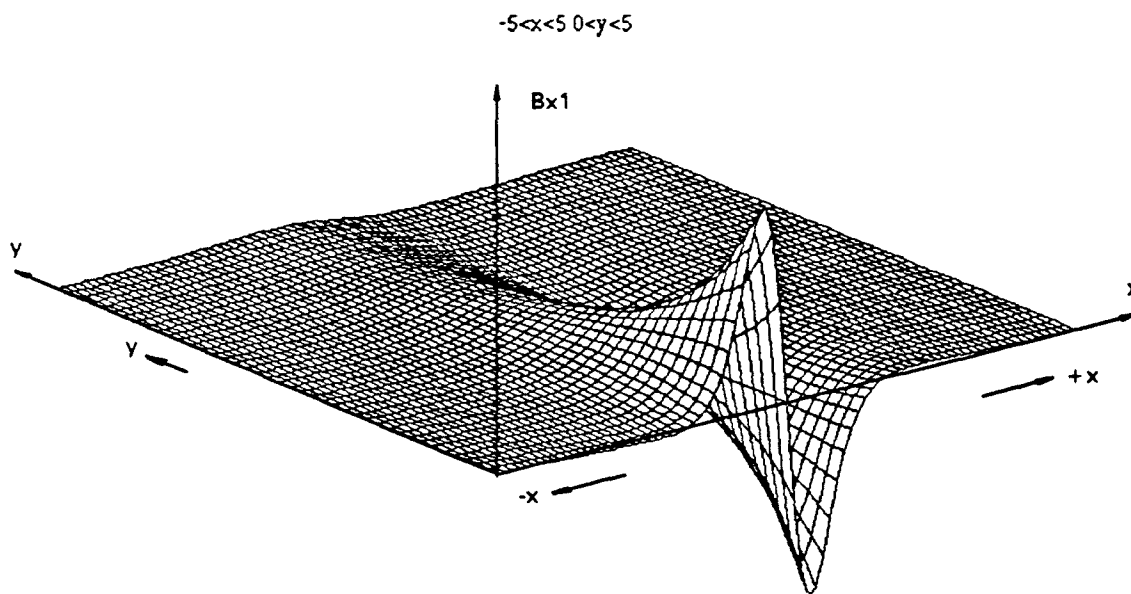


**Figure 5-2 3-D axial component of induced magnetic field**

# APPENDIX

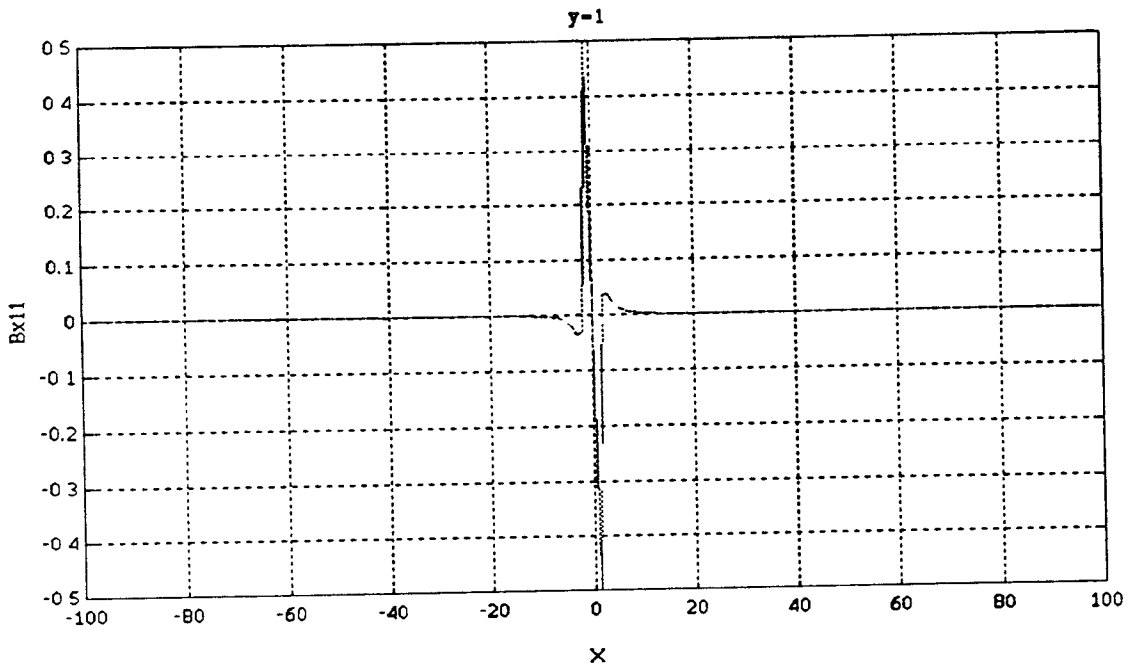


Figure 4-1a Axial component of induced magnetic field 1,  $y=1$ ,  $-100 < x < 100$

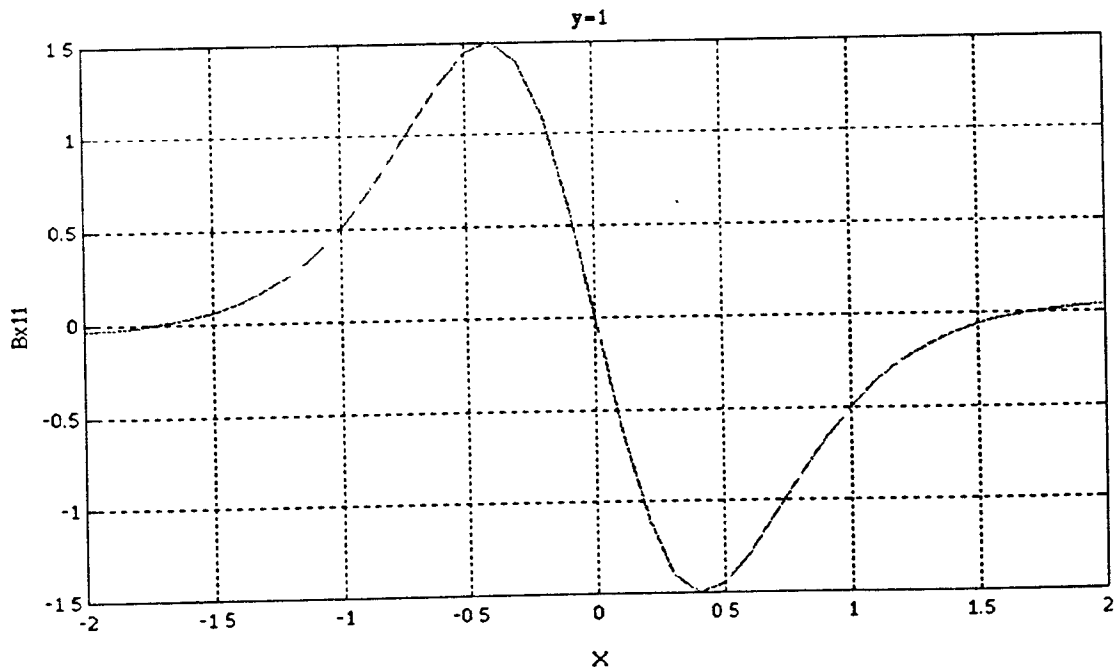


Figure 4-1b Axial component of induced magnetic field 1,  $y=1$ ,  $-2 < x < 2$

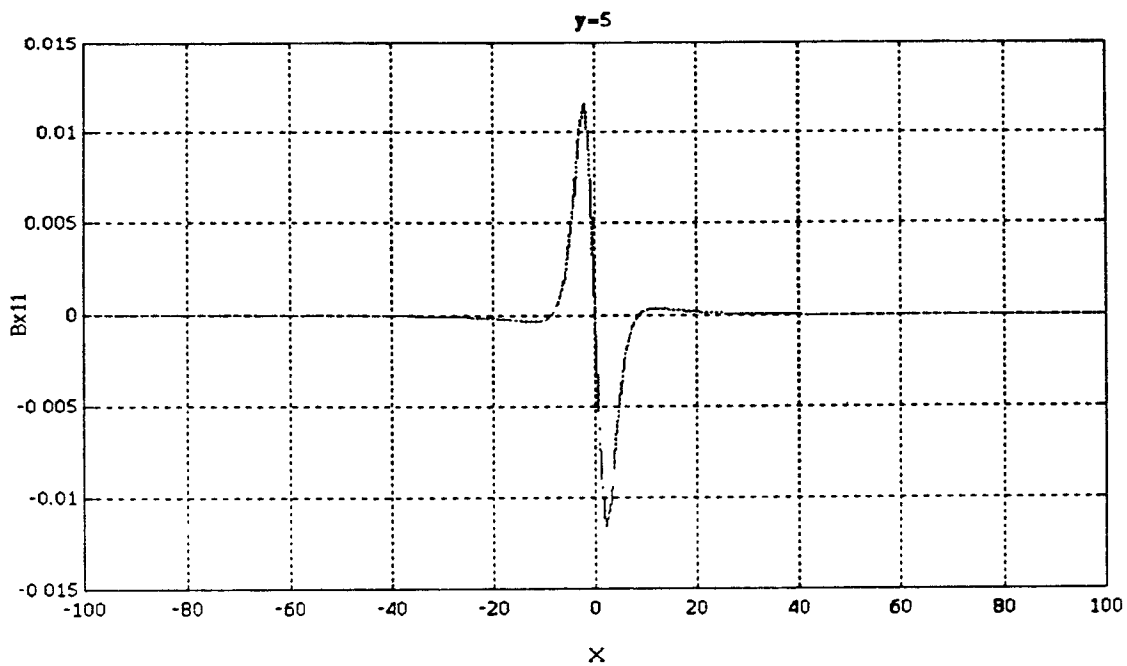


Figure 4-2a Axial component of induced magnetic field 1,  $y=5$ ,  $-100 < x < 100$

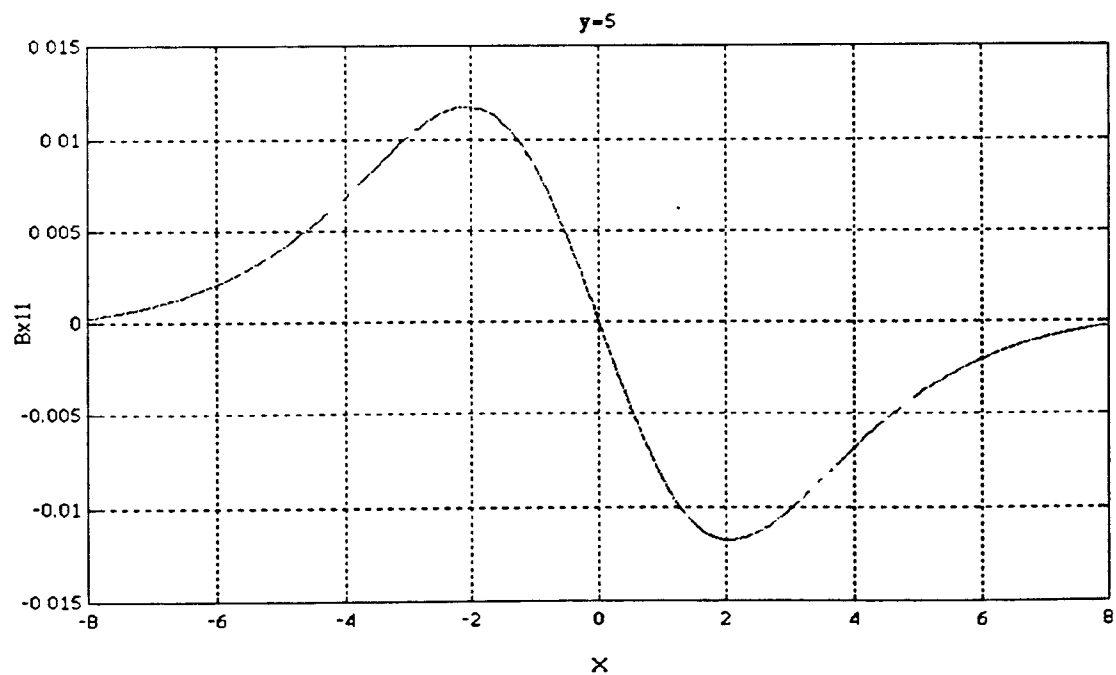


Figure 4-2b Axial component of induced magnetic field 1,  $y=5$ ,  $-8 < x < 8$

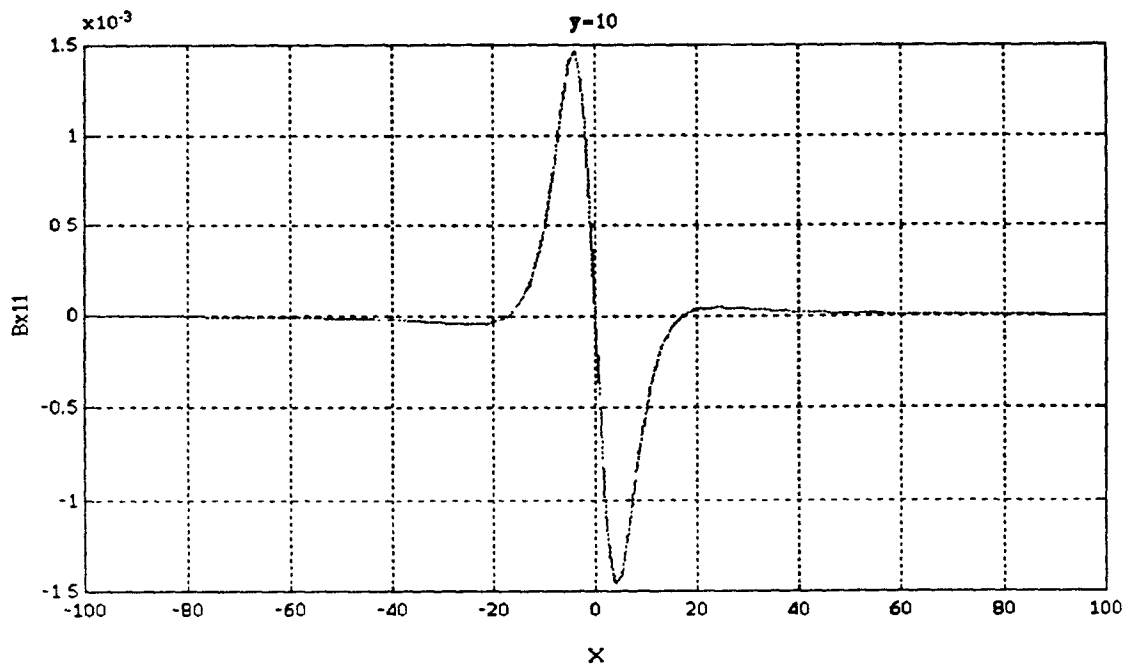


Figure 4-3a Axial component of induced magnetic field 1,  $y=10$ ,  $-100 < x < 100$

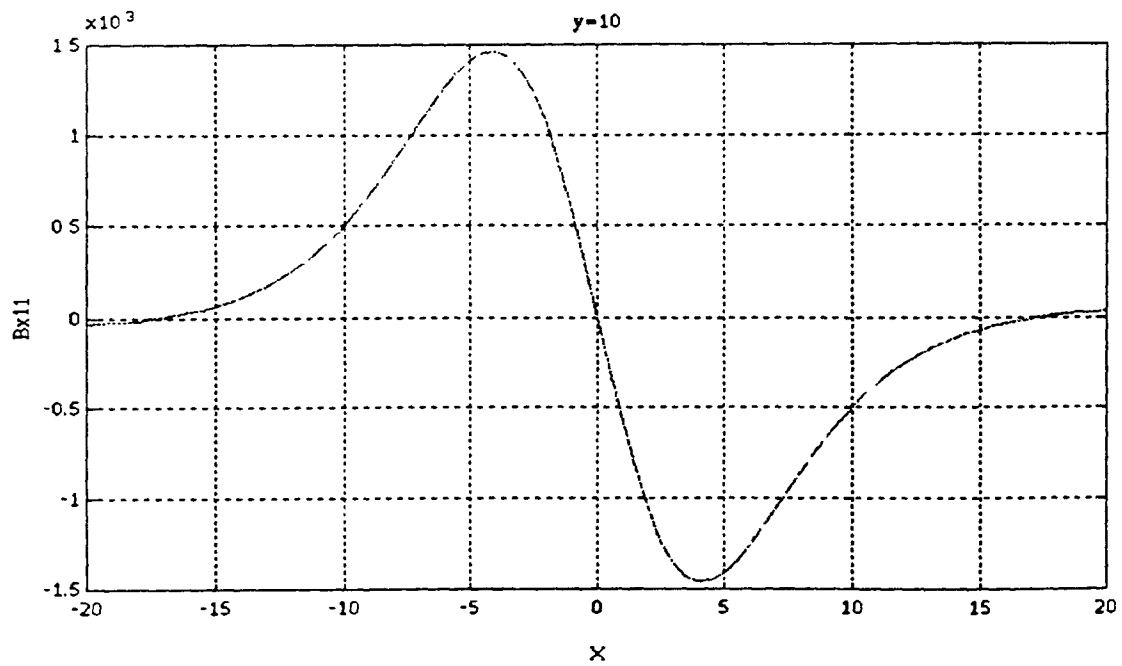


Figure 4-3b Axial component of induced magnetic field 1,  $y=10$ ,  $-20 < x < 20$

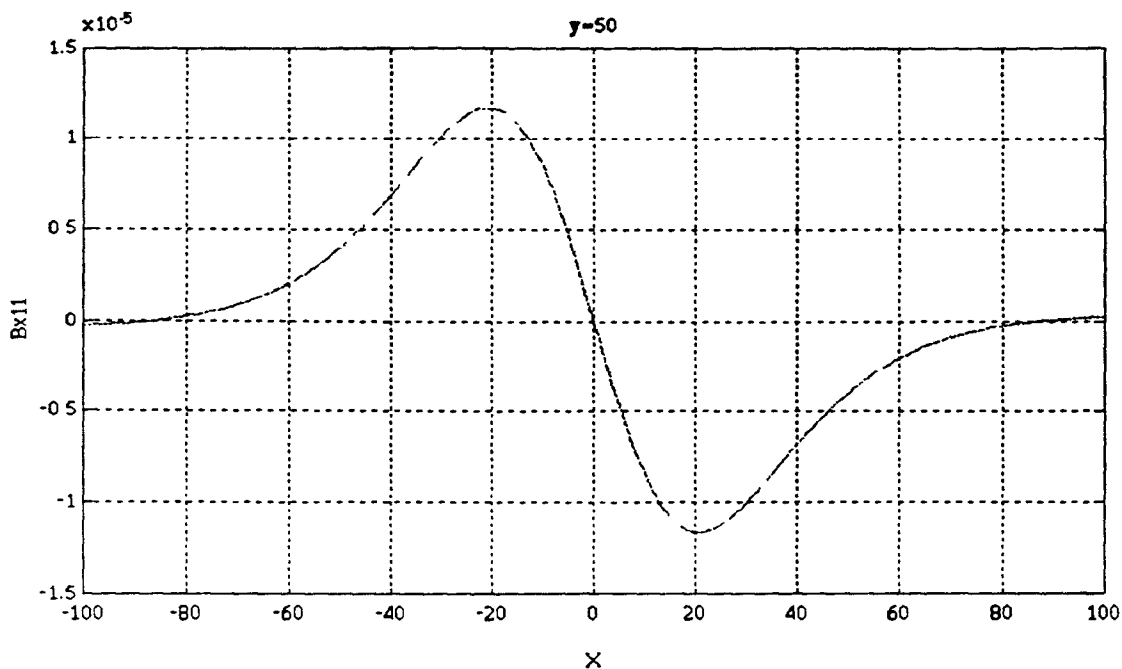


Figure 4-4 Axial component of induced magnetic field 1,  $y=50$ ,  $-100 < x < 100$

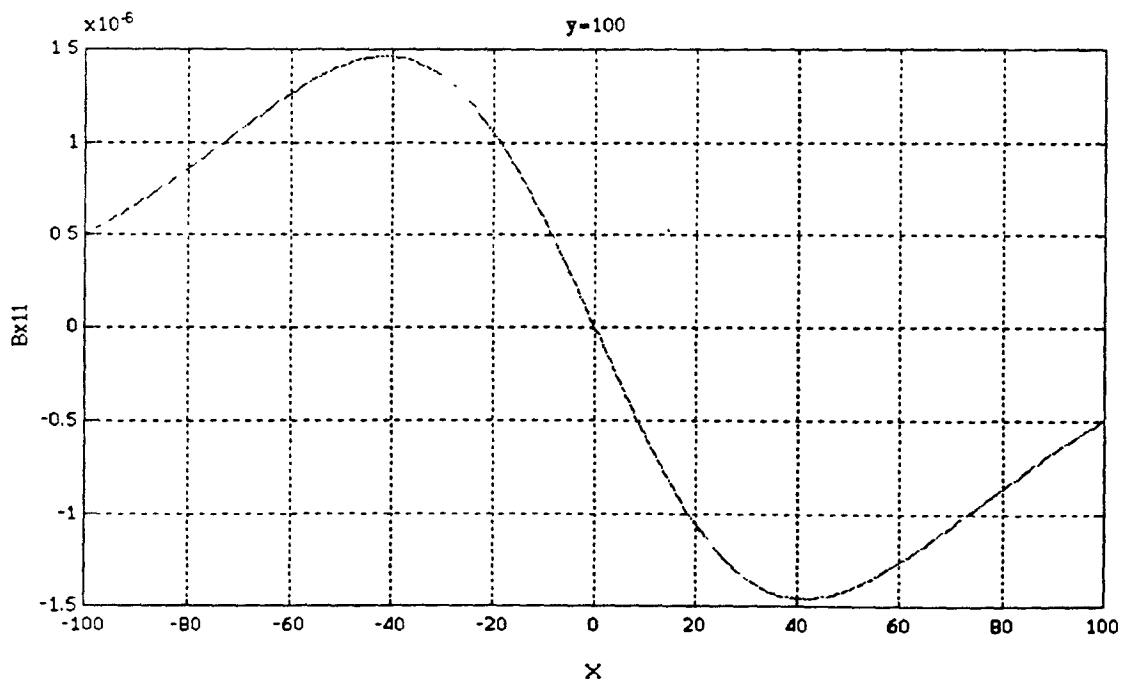


Figure 4-5a Axial component of induced magnetic field 1,  $y=100$ ,  $-100 < x < 100$



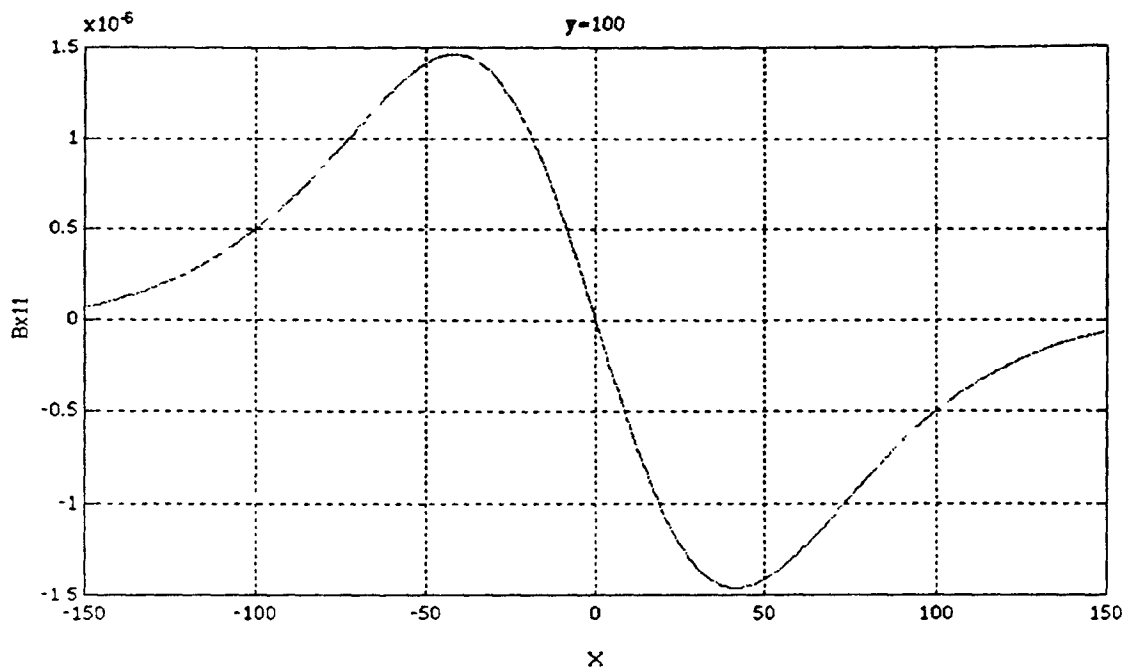


Figure 4-5b Axial component of induced magnetic field 1,  $y=100$ ,  $-150 < x < 150$

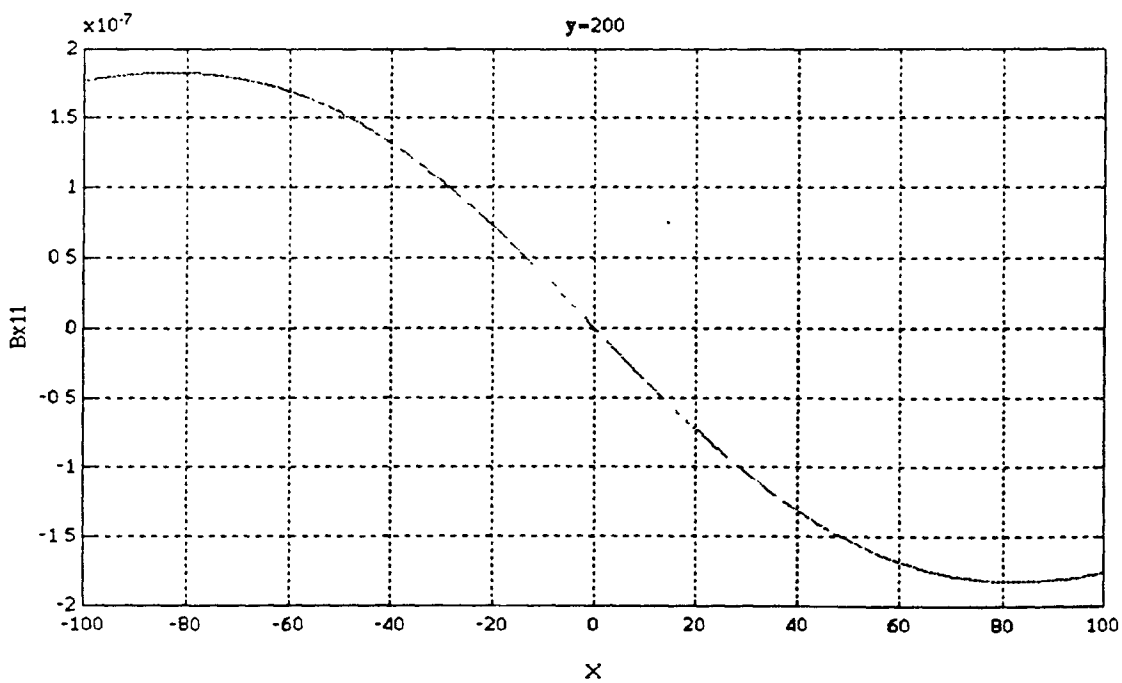


Figure 4-6a Axial component of induced magnetic field 1,  $y=200$ ,  $-100 < x < 100$

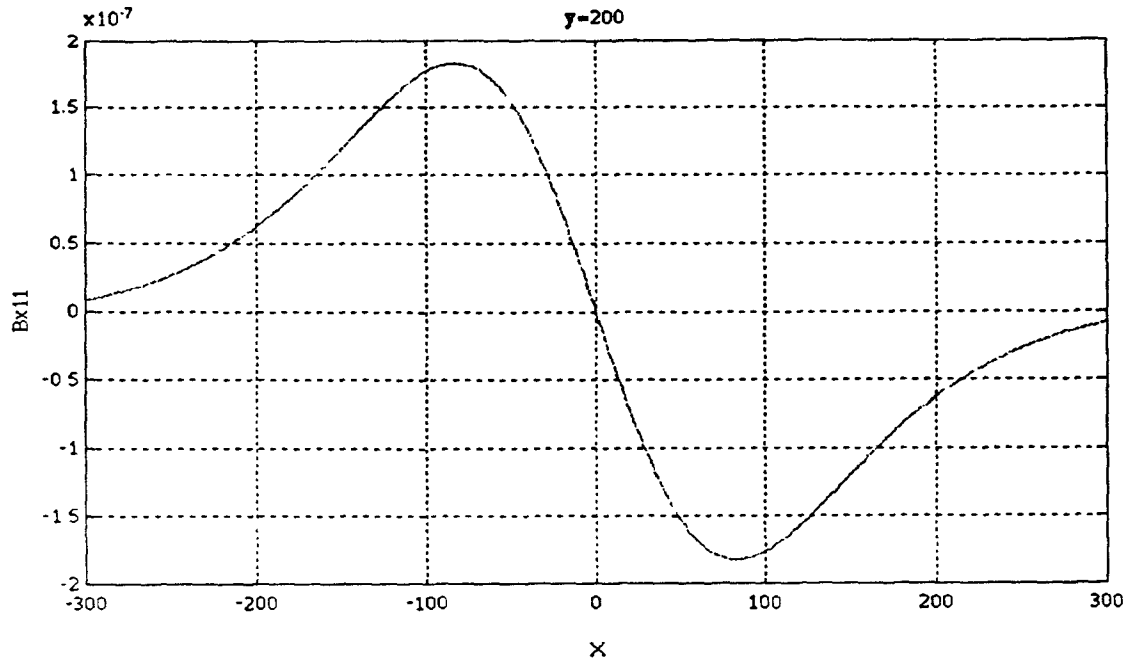


Figure 4-6b Axial component of induced magnetic field 1,  $y=200$ ,  $-300 < x < 300$

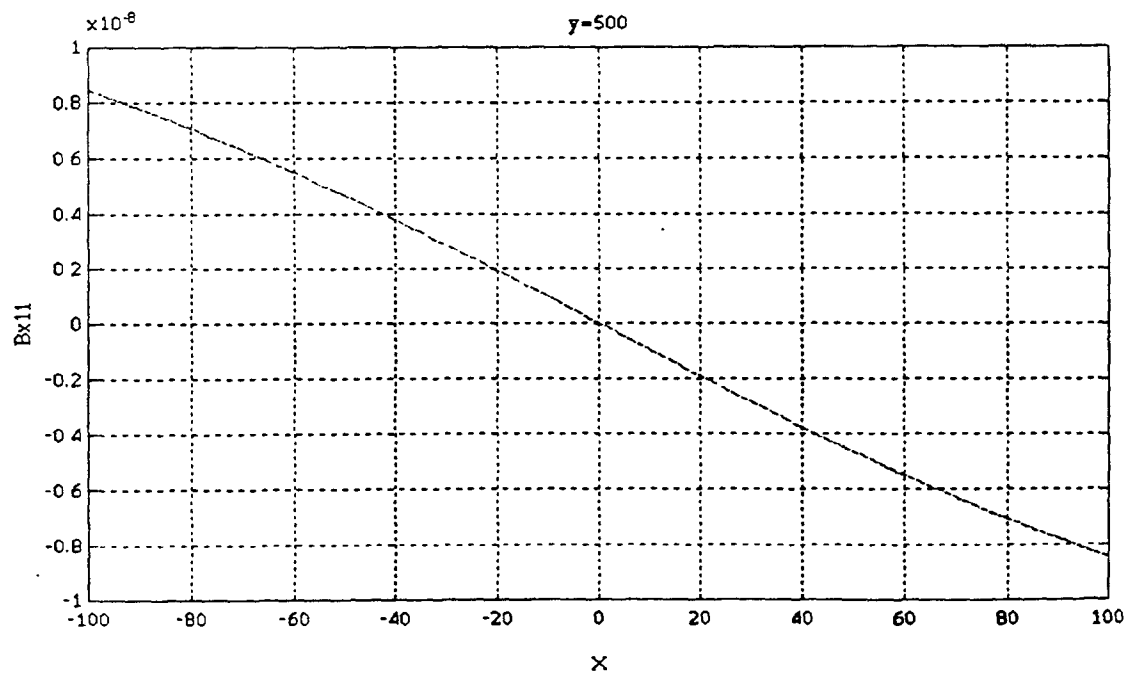


Figure 4-7a Axial component of induced magnetic field 1,  $y=500$ ,  $-100 < x < 100$

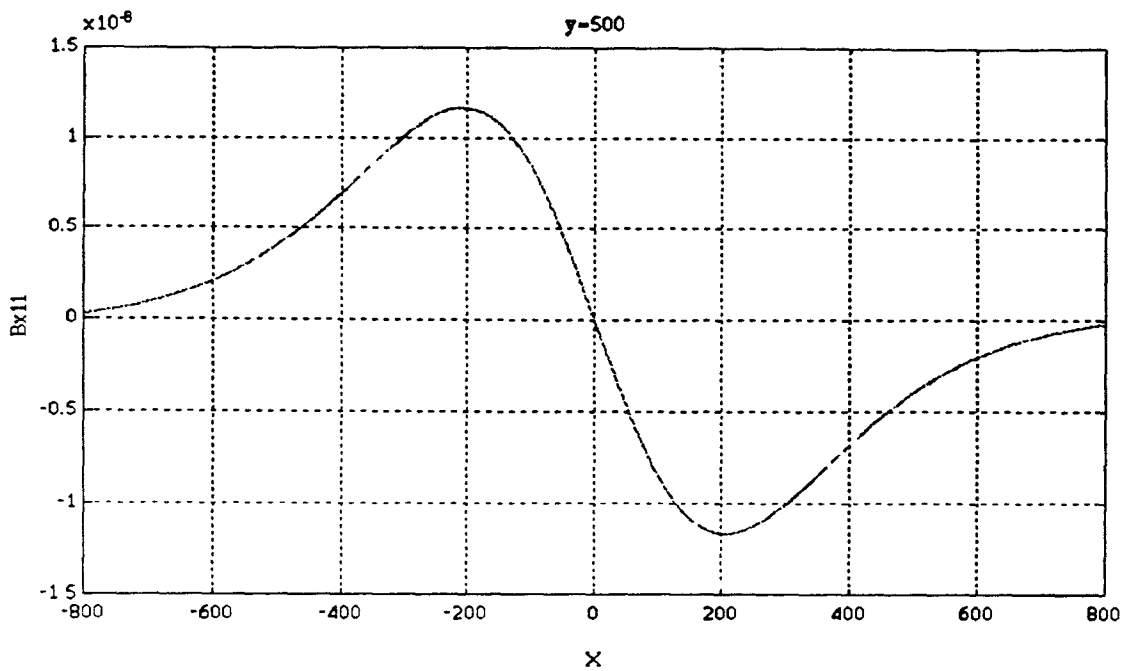


Figure 4-7b Axial component of induced magnetic field 1,  $y=500$ ,  $-700 < x < 700$

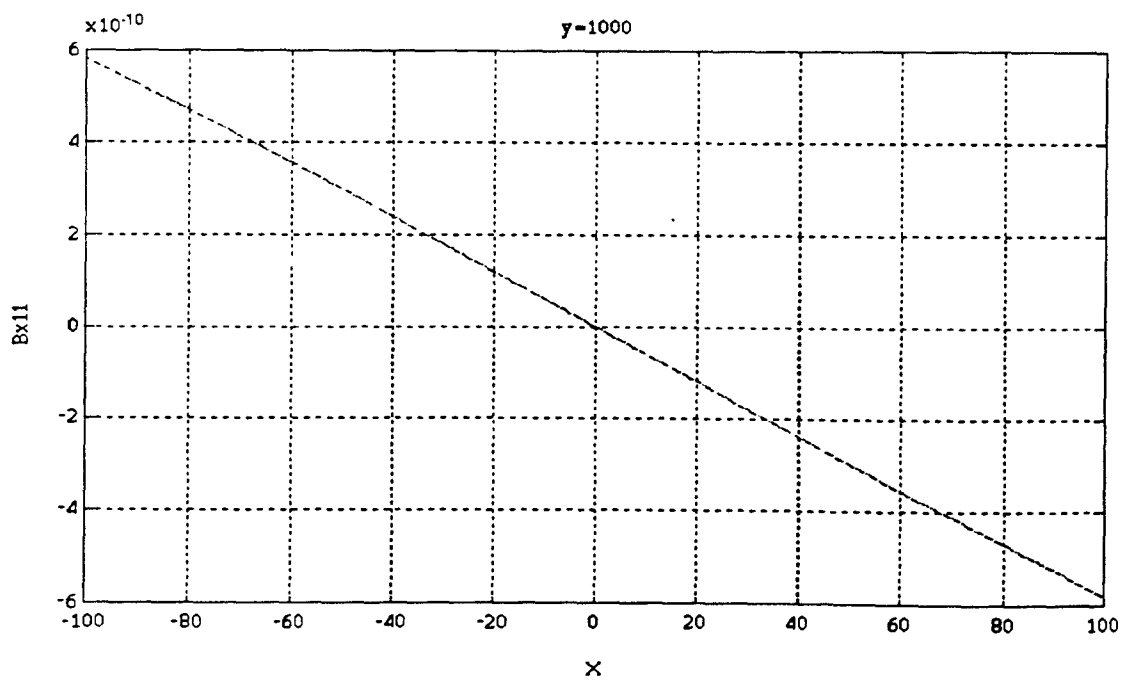


Figure 4-8a Axial component of induced magnetic field 1,  $y=1000$ ,  $-100 < x < 100$

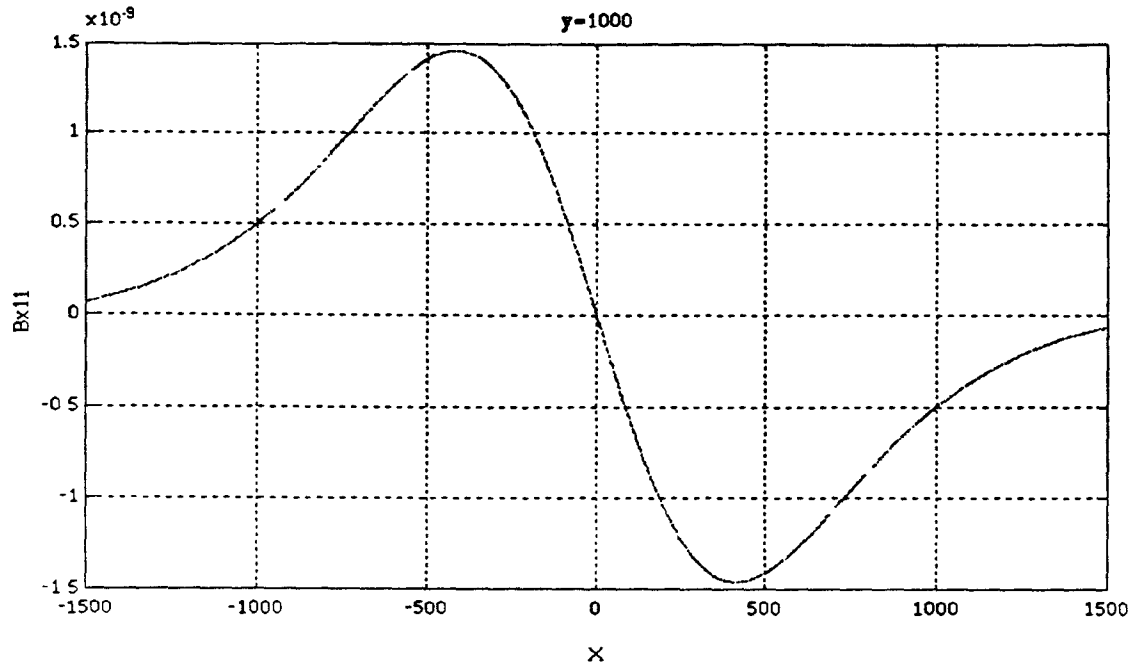


Figure 4-8b Axial component of induced magnetic field 1,  $y=1000$ ,  $-1000 < x < 1000$

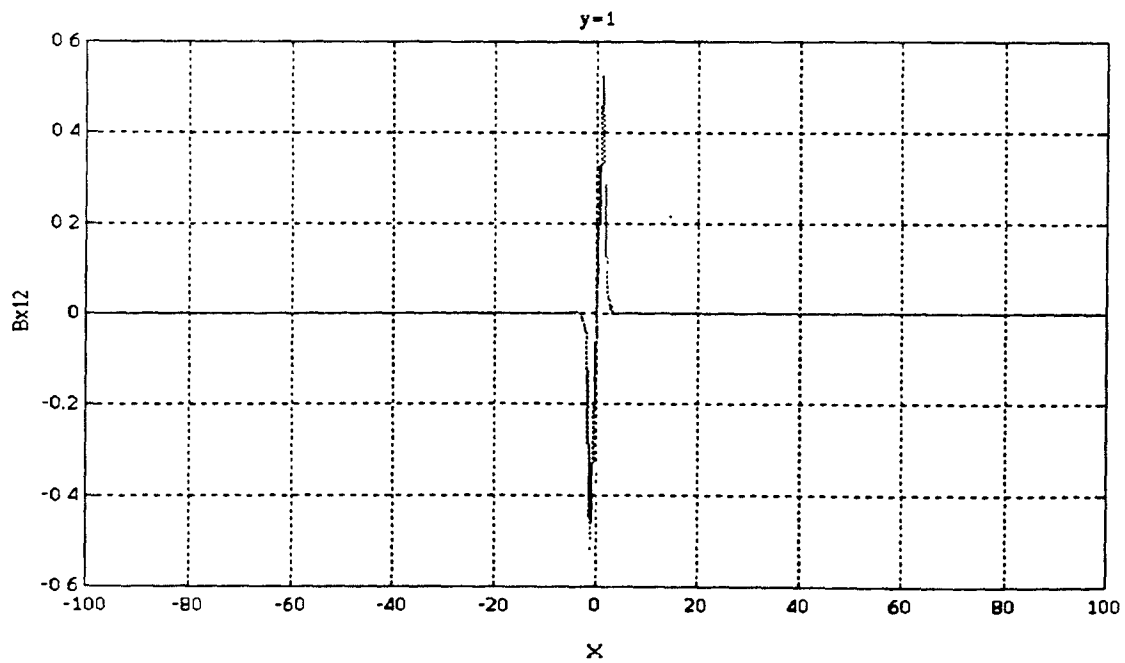


Figure 4-9a Axial component of induced magnetic field 2,  $y=1$ ,  $-100 < x < 100$

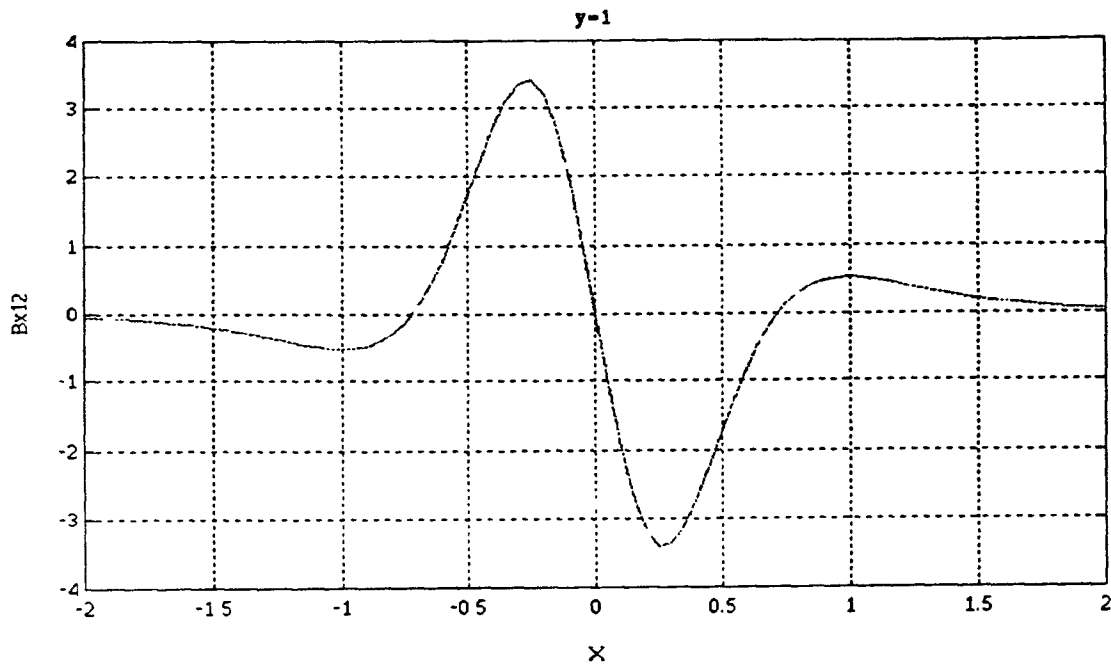


Figure 4-9b Axial component of induced magnetic field 2,  $y=1$ ,  $-2 < x < 2$

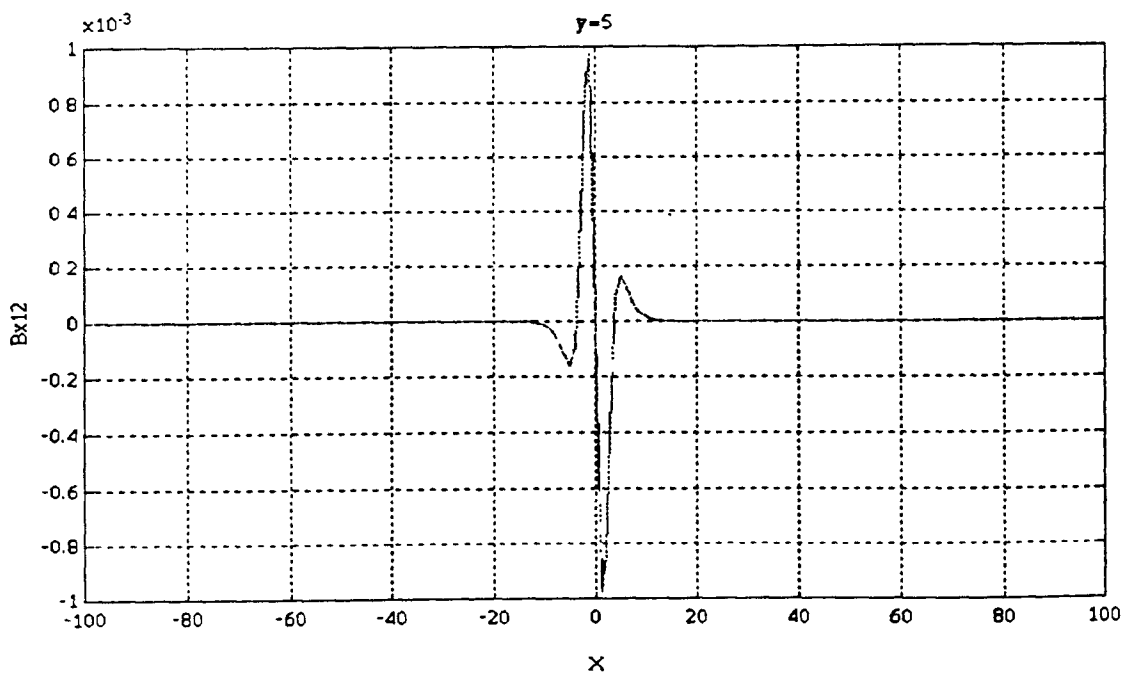


Figure 4-10a Axial component of induced magnetic field 2,  $y=5$ ,  $-100 < x < 100$

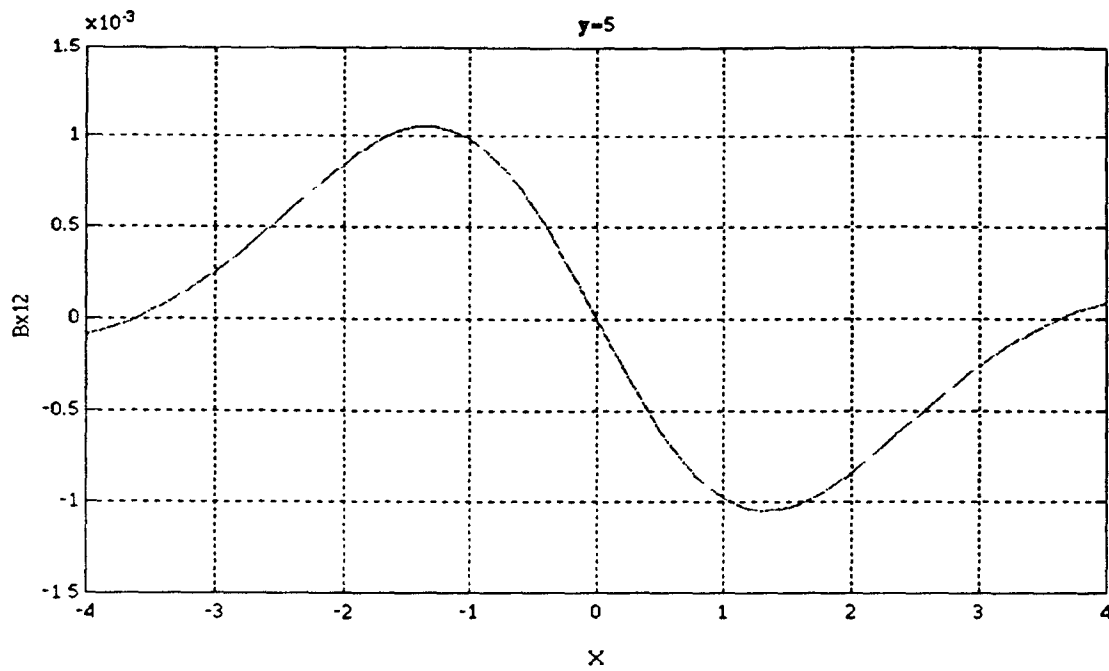


Figure 4-10b Axial component of induced magnetic field 2,  $y=5$ ,  $-4 < x < 4$

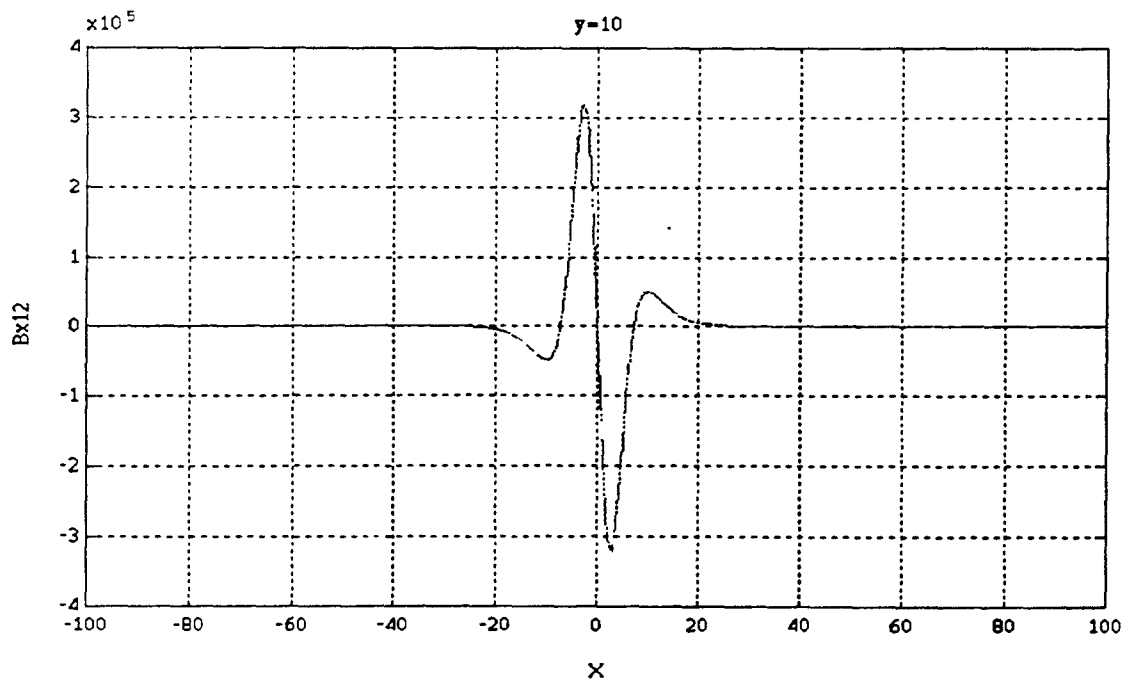


Figure 4-11a Axial component of induced magnetic field 2,  $y=10$ ,  $-100 < x < 100$

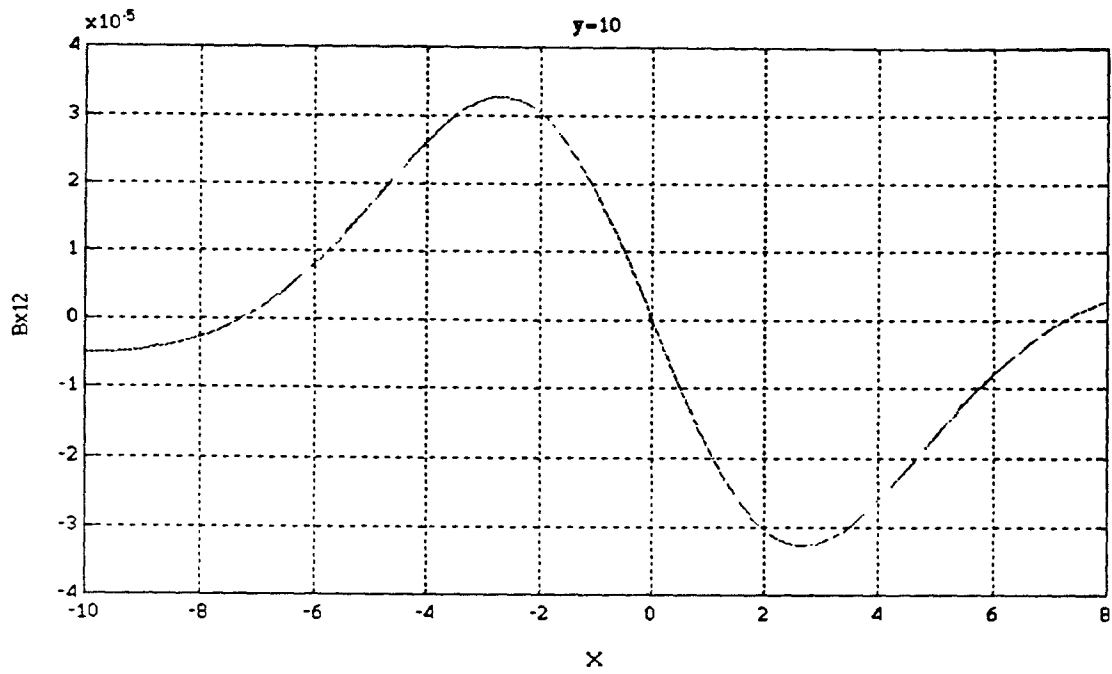


Figure 4-11b Axial component of induced magnetic field 2,  $y=10$ ,  $-10 < x < 10$

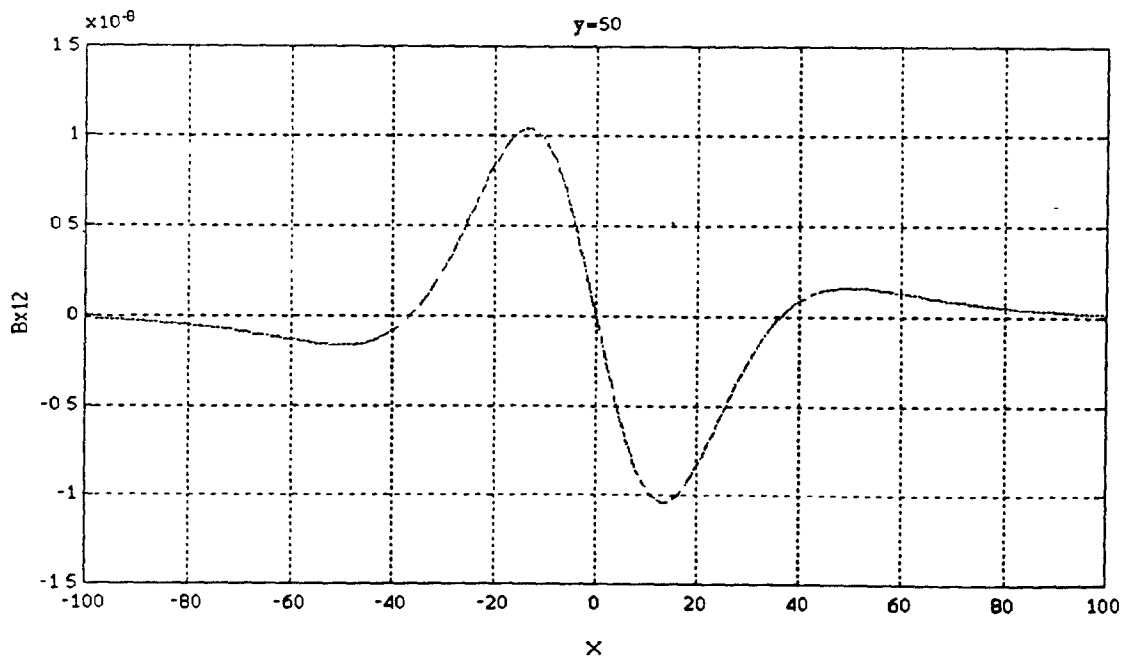


Figure 4-12a Axial component of induced magnetic field 2,  $y=50$ ,  $-100 < x < 100$

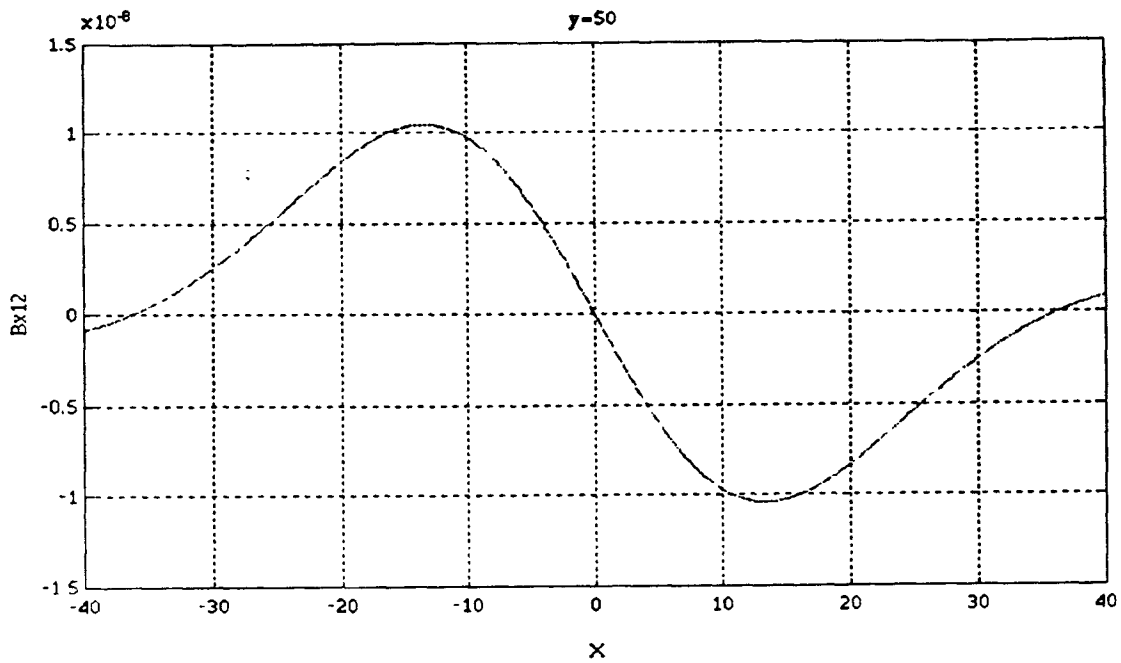


Figure 4-12b Axial component of induced magnetic field 2,  $y=50$ ,  $-40 < x < 40$

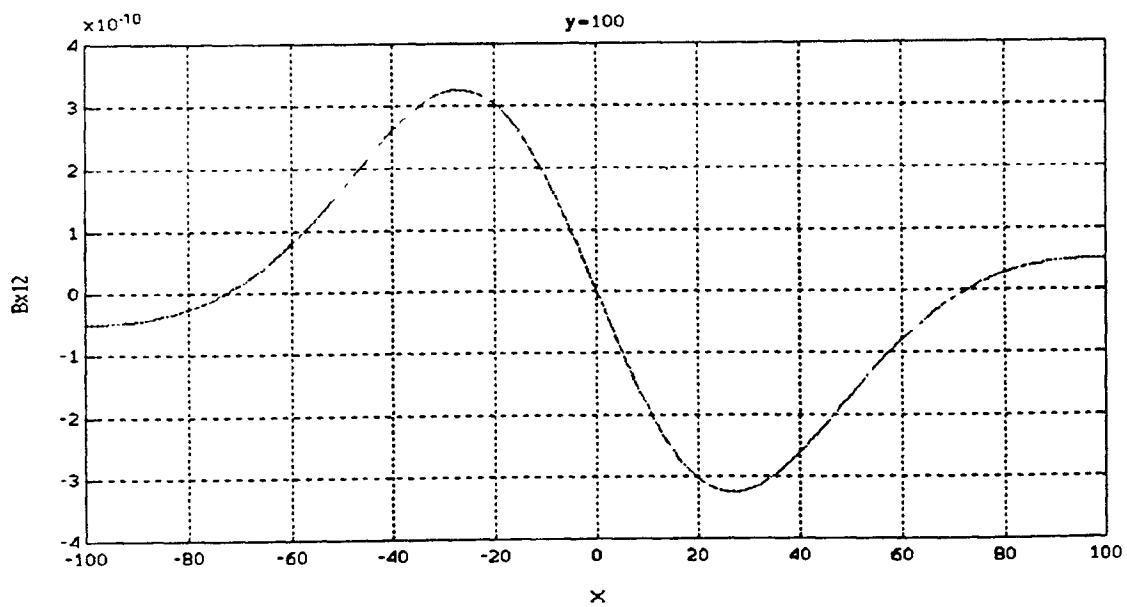


Figure 4-13 Axial component of induced magnetic field 2,  $y=100$ ,  $-100 < x < 100$



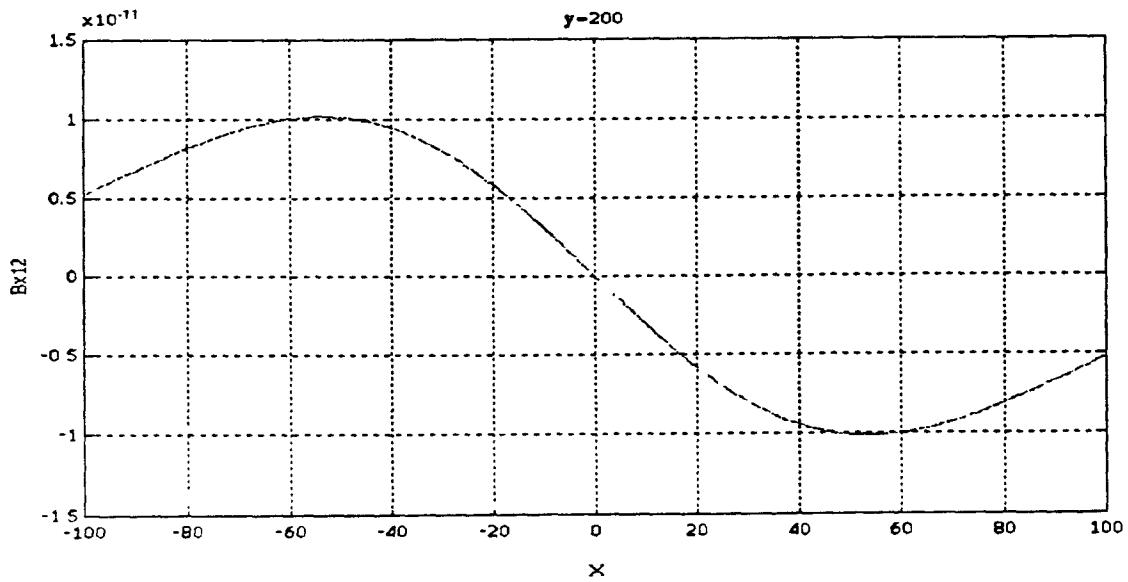


Figure 4-14a Axial component of induced magnetic field 2,  $y=200$ ,  $-100 < x < 100$

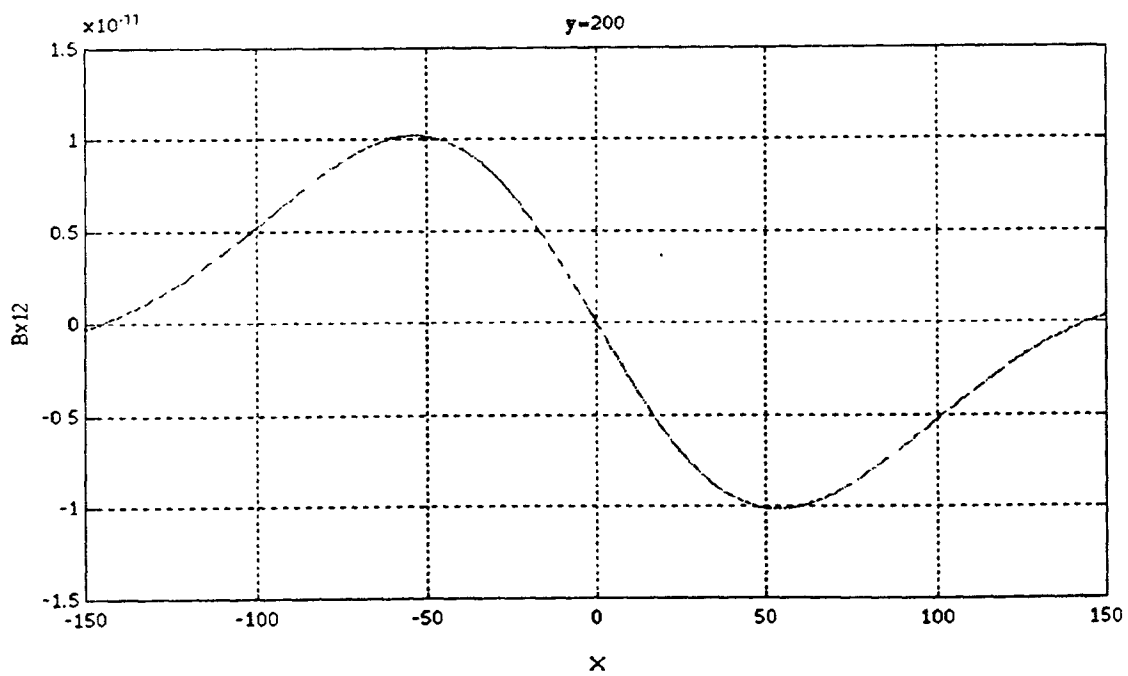


Figure 4-14b Axial component of induced magnetic field 2,  $y=200$ ,  $-150 < x < 150$

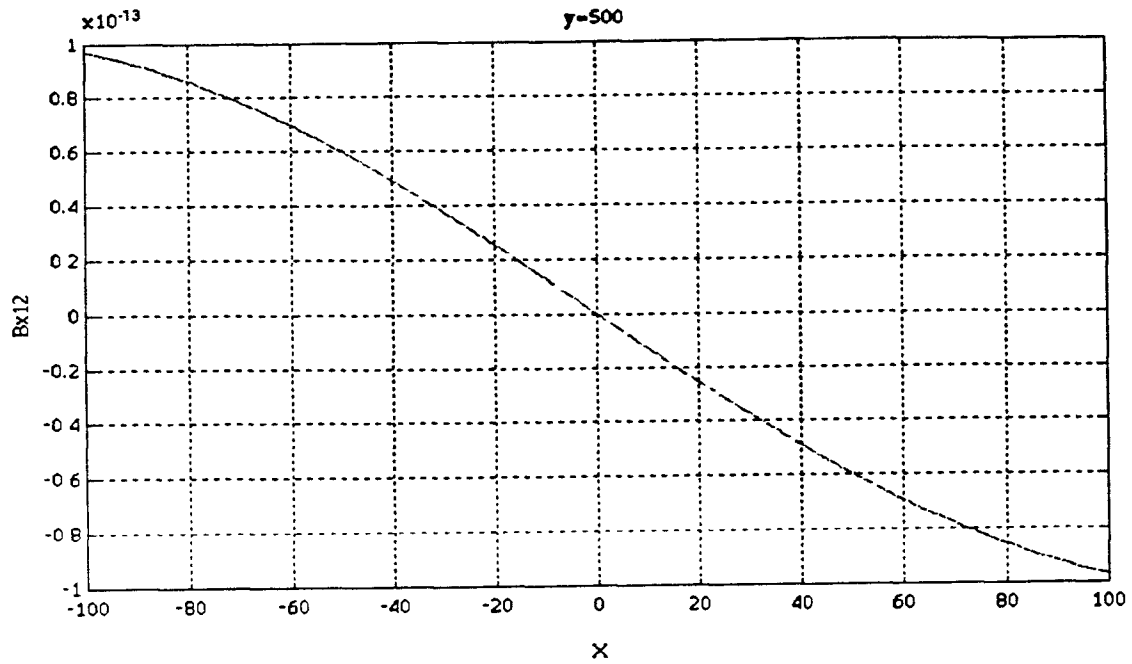


Figure 4-15a Axial component of induced magnetic field 2,  $y=500$ ,  $-100 < x < 100$

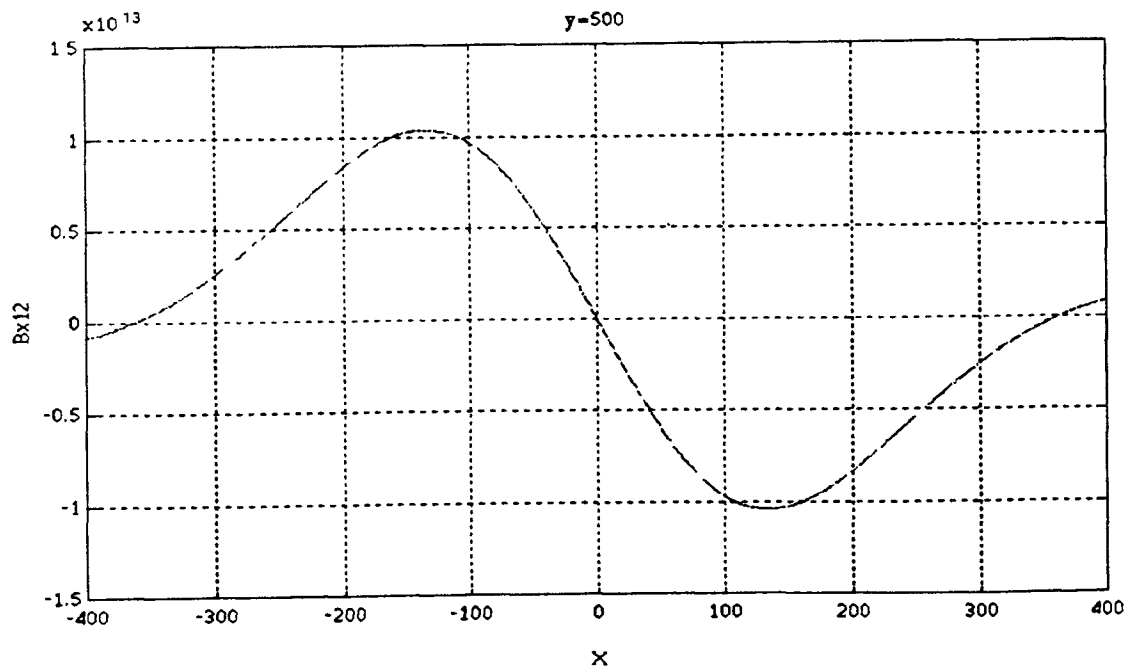


Figure 4-15b Axial component of induced magnetic field 2,  $y=500$ ,  $-400 < x < 400$

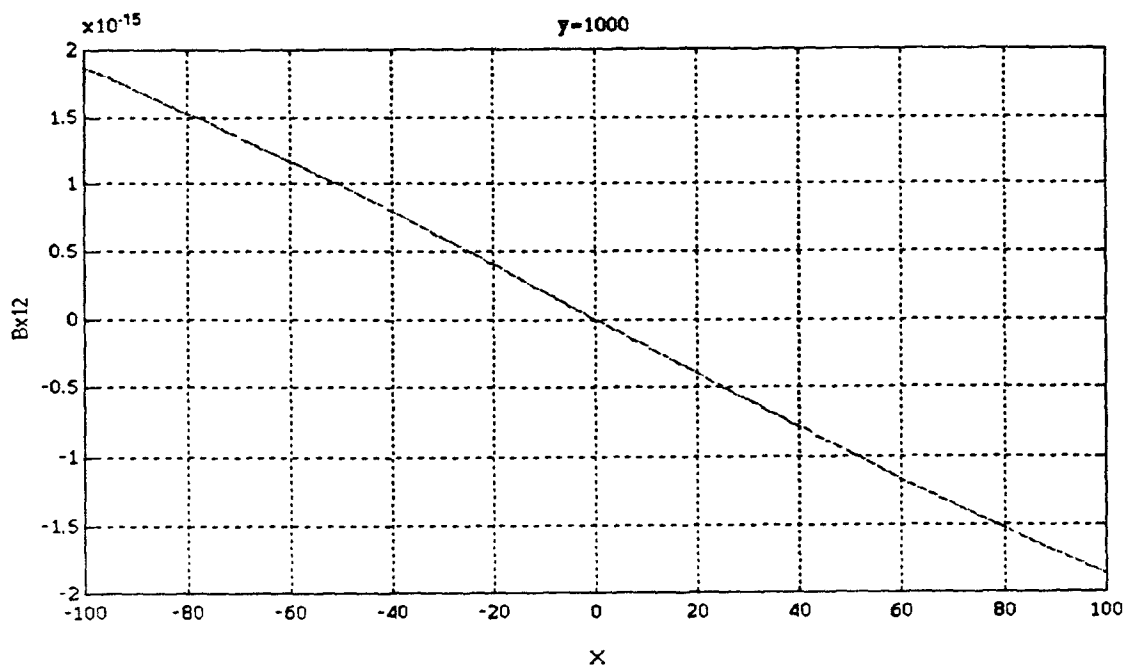


Figure 4-16a Axial component of induced magnetic field 2,  $y=1000$ ,  $-100 < x < 100$

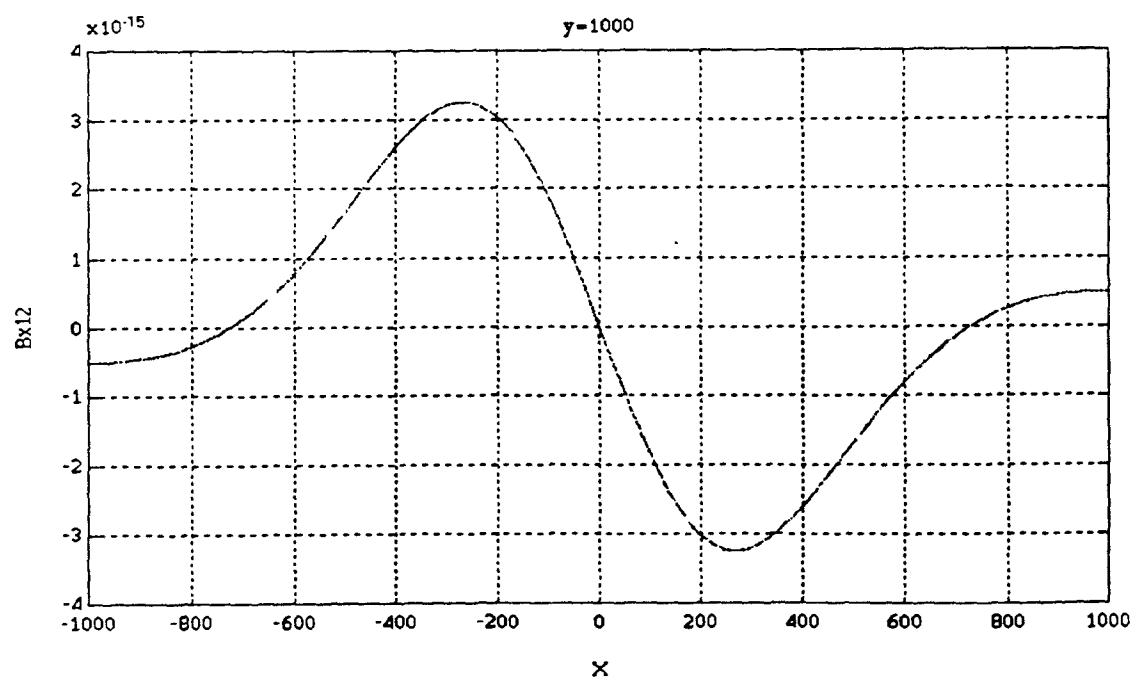


Figure 4-16b Axial component of induced magnetic field 2,  $y=1000$ ,  $-1000 < x < 1000$

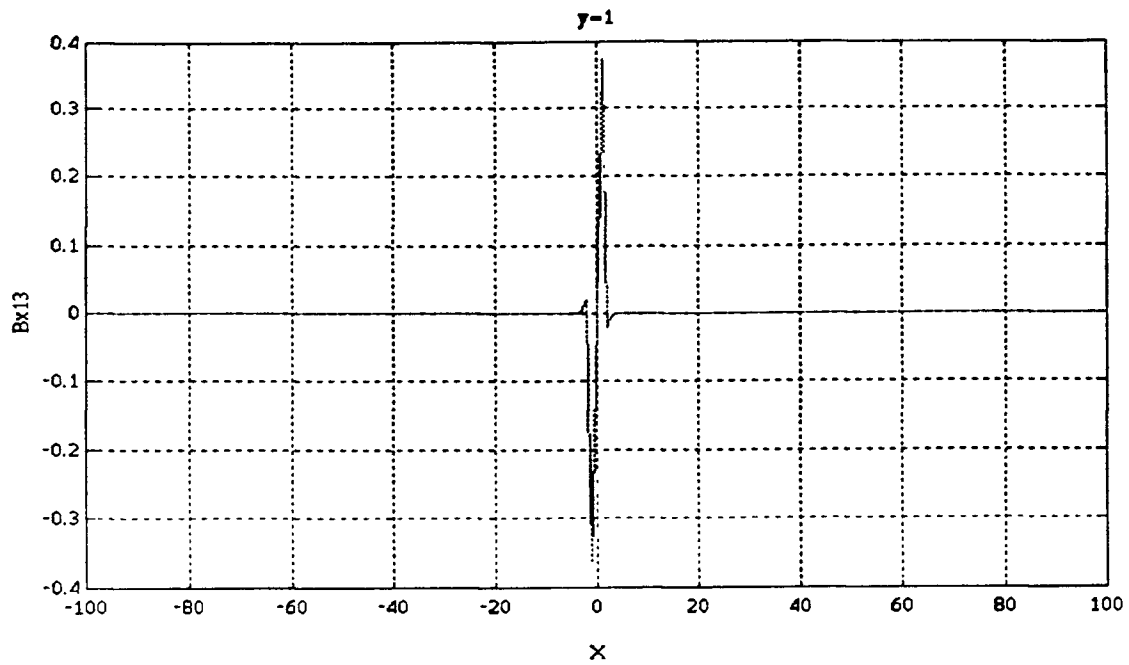


Figure 4-17a Axial component of induced magnetic field 3,  $y=1$ ,  $-100 < x < 100$

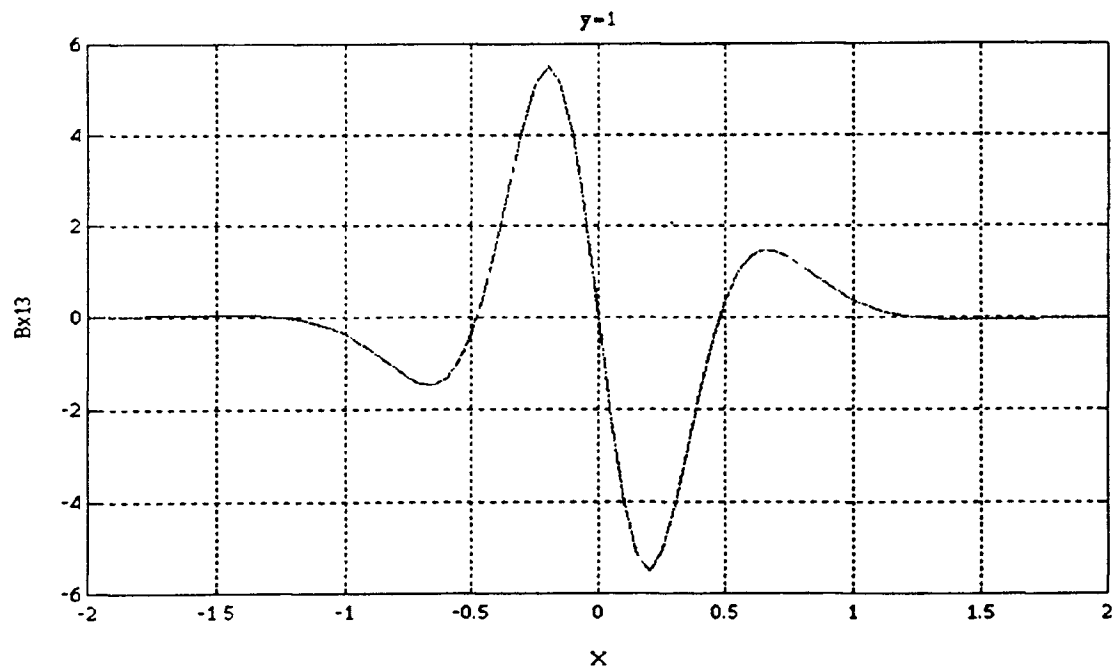


Figure 4-17b Axial component of induced magnetic field 3,  $y=1$ ,  $-2 < x < 2$

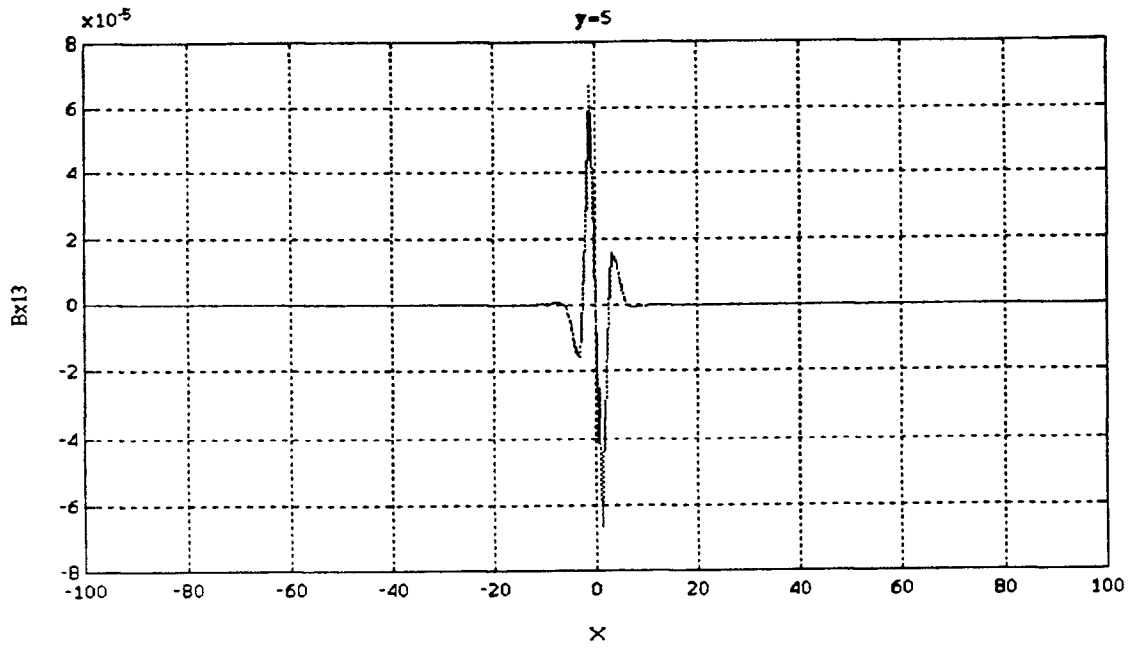


Figure 4-18a Axial component of induced magnetic field 3,  $y=5$ ,  $-100 < x < 100$

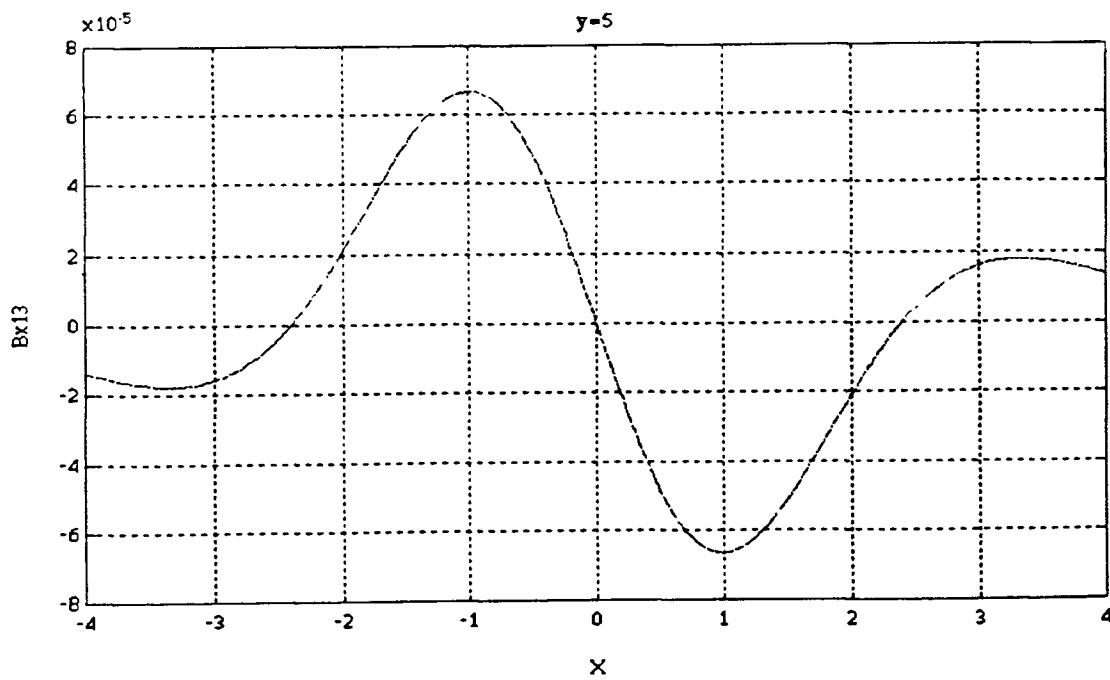


Figure 4-18b Axial component of induced magnetic field 3,  $y=5$ ,  $-4 < x < 4$

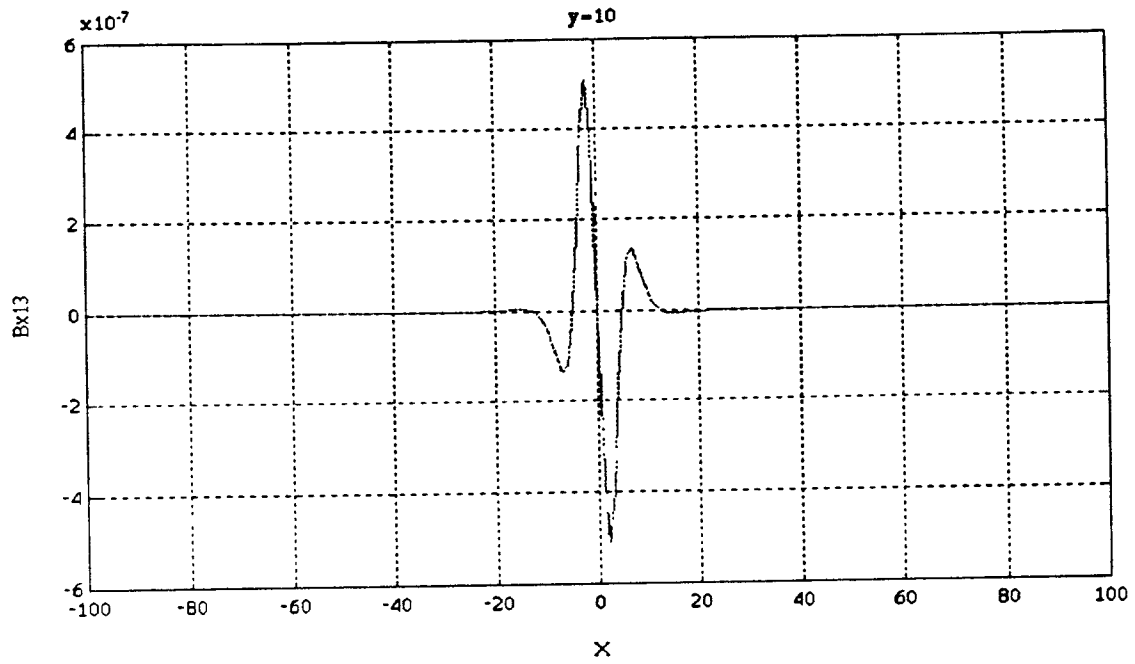


Figure 4-19a Axial component of induced magnetic field 3,  $y=10$ ,  $-100 < x < 100$

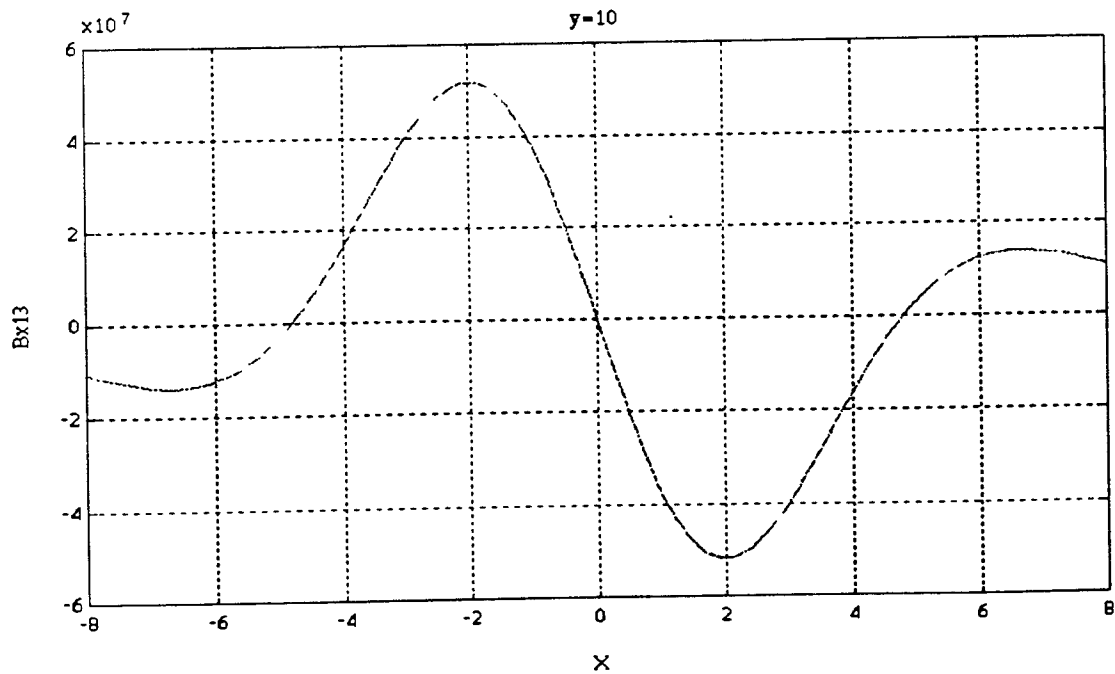


Figure 4-19b Axial component of induced magnetic field 3,  $y=10$ ,  $-8 < x < 8$

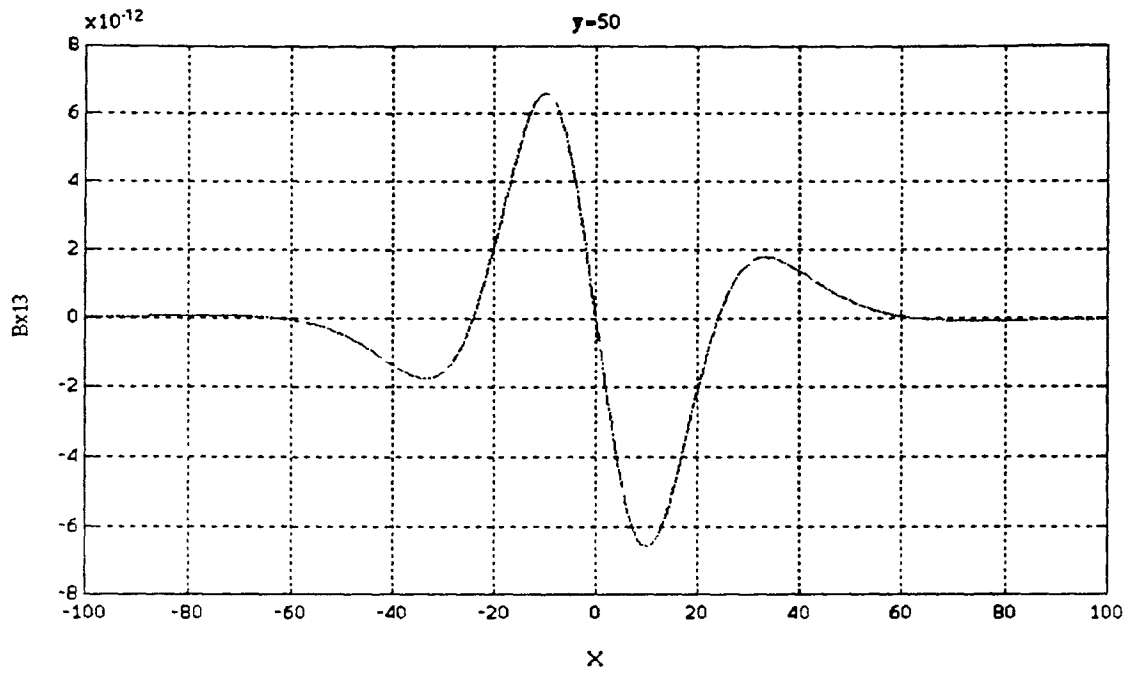


Figure 4-20a Axial component of induced magnetic field 3,  $y=50$ ,  $-100 < x < 100$

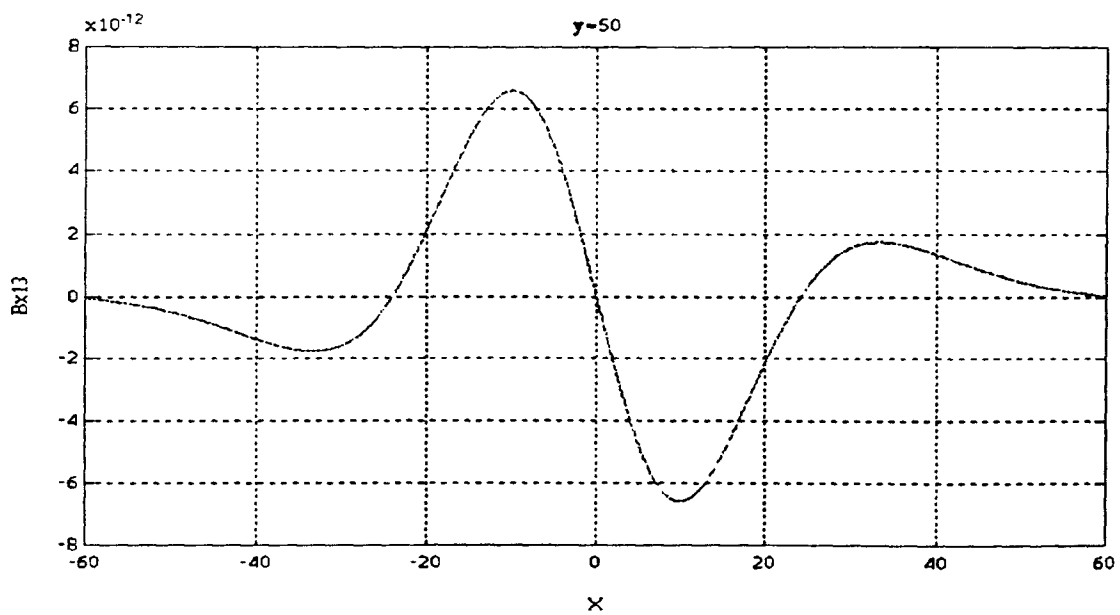


Figure 4-20b Axial component of induced magnetic field 3,  $y=50$ ,  $-60 < x < 60$

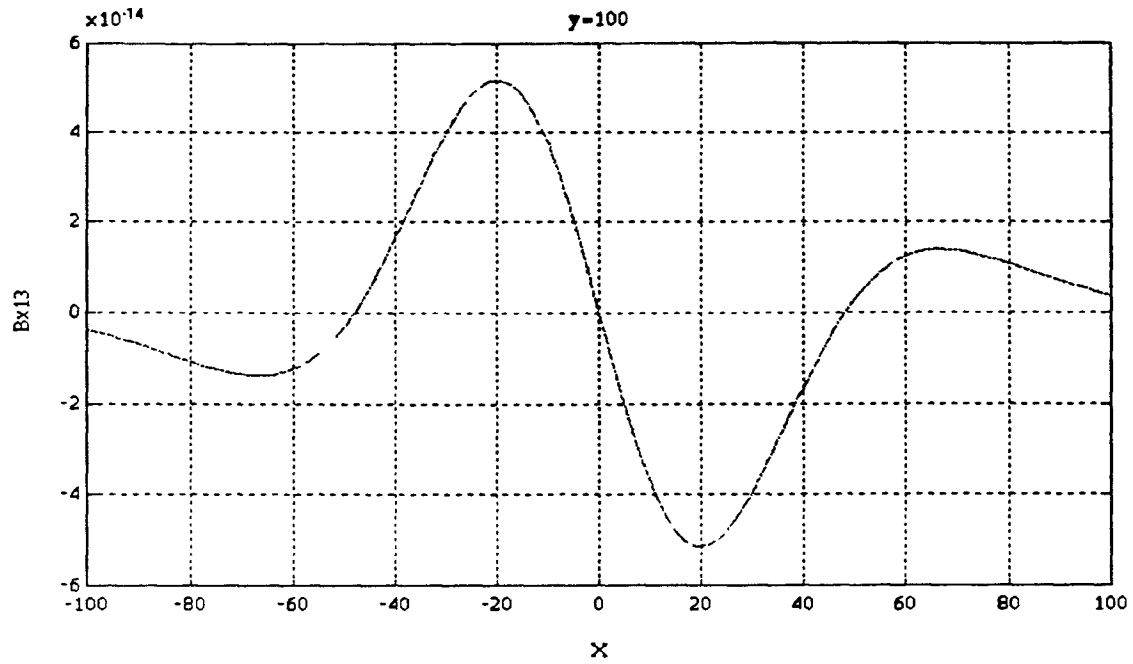


Figure 4-21 Axial component of induced magnetic field 3,  $y=100$ ,  $-100 < x < 100$

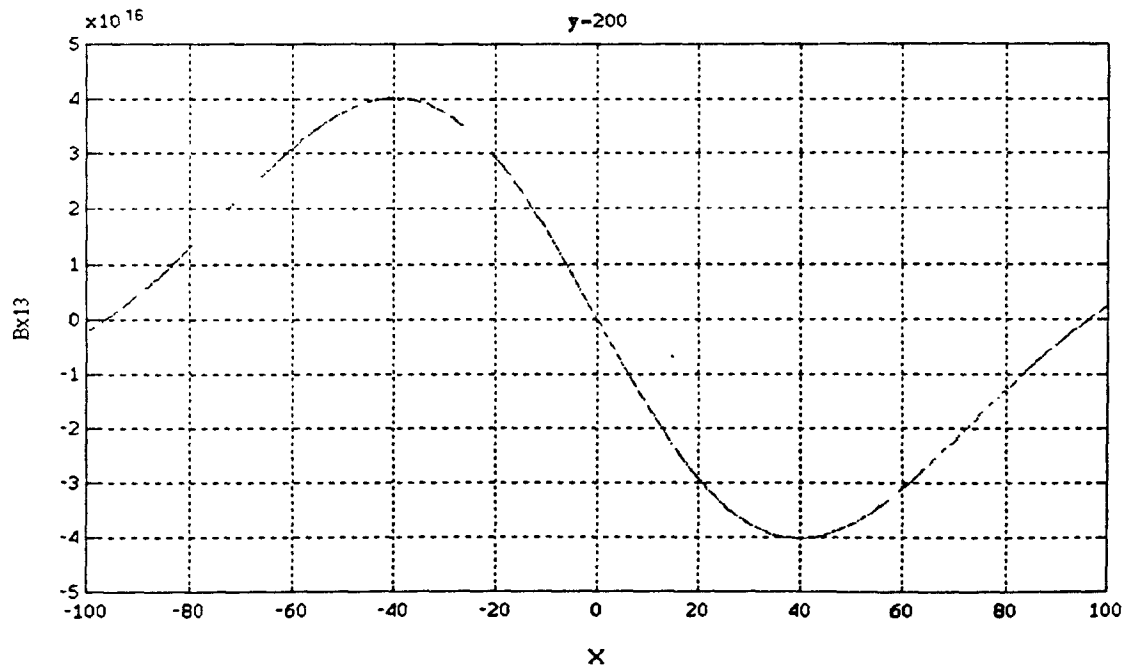


Figure 4-22a Axial component of induced magnetic field 3,  $y=200$ ,  $-100 < x < 100$



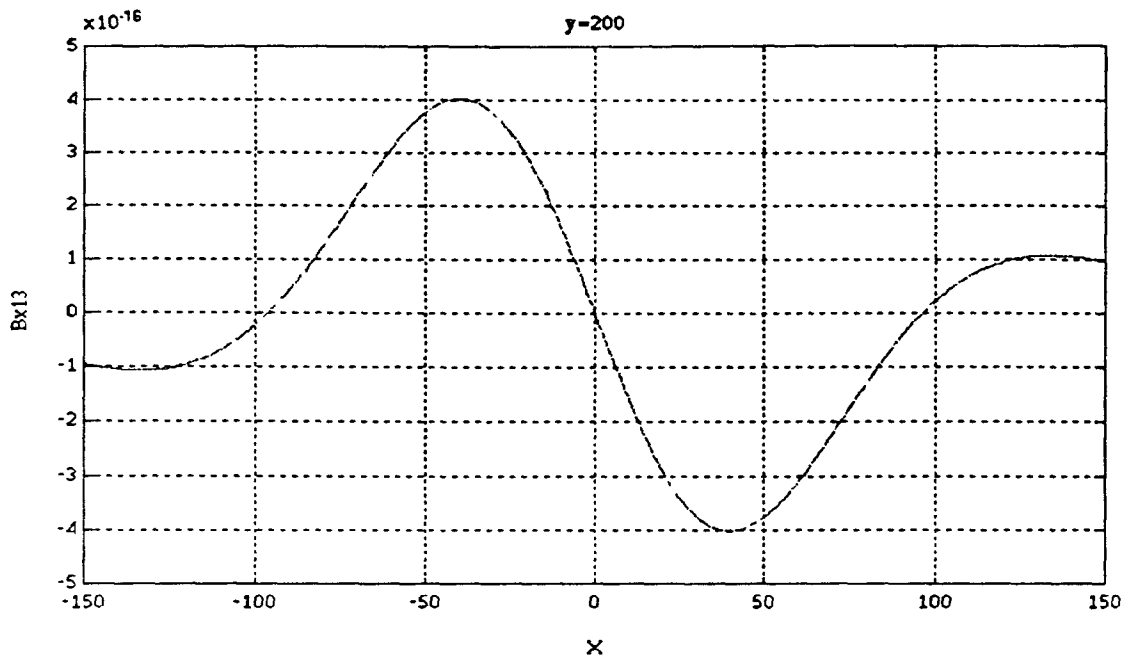


Figure 4-22b Axial component of induced magnetic field 3,  $y=200$ ,  $-150 < x < 150$

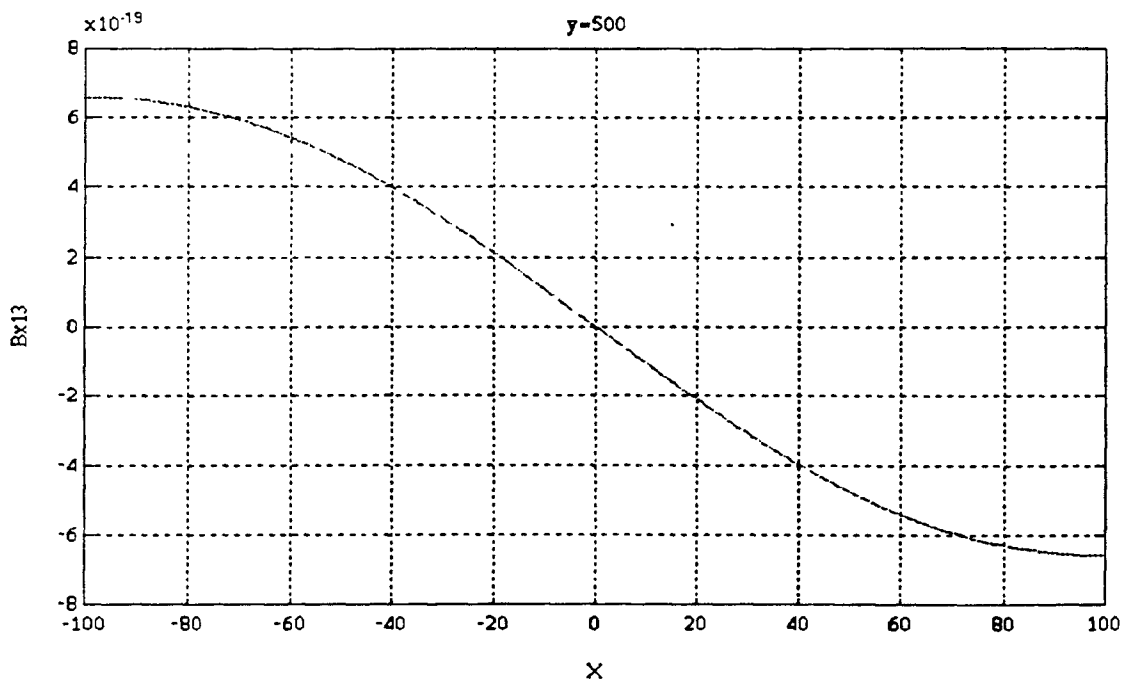


Figure 4-23a Axial component of induced magnetic field 3,  $y=500$ ,  $-100 < x < 100$

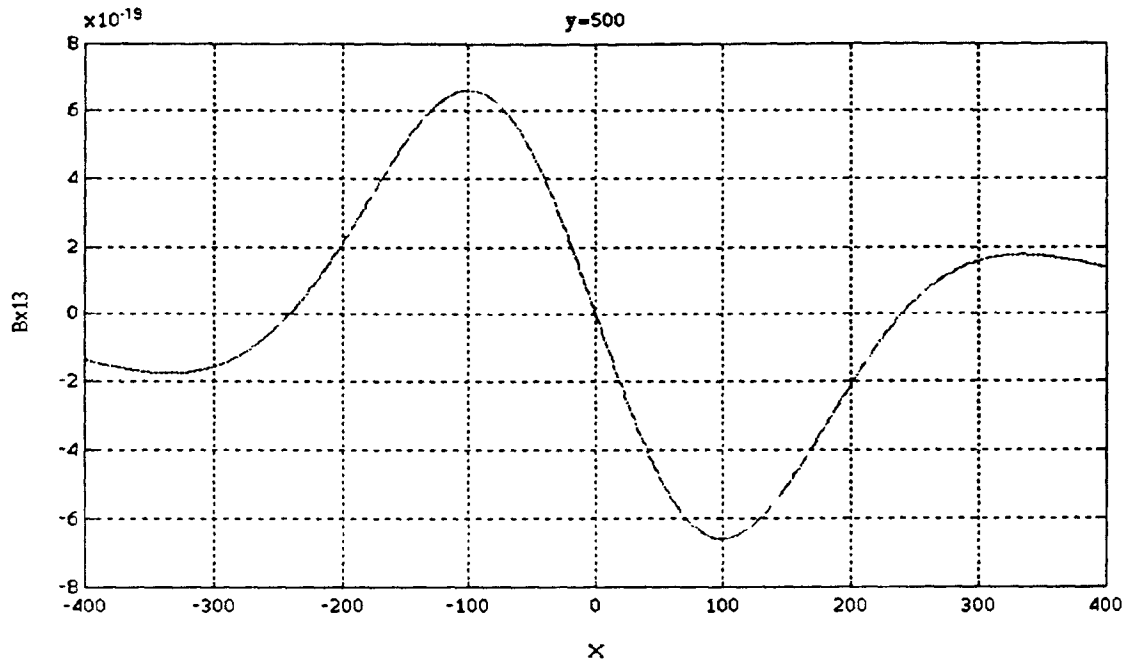


Figure 4-23b Axial component of induced magnetic field 3,  $y=500$ ,  $-400 < x < 400$

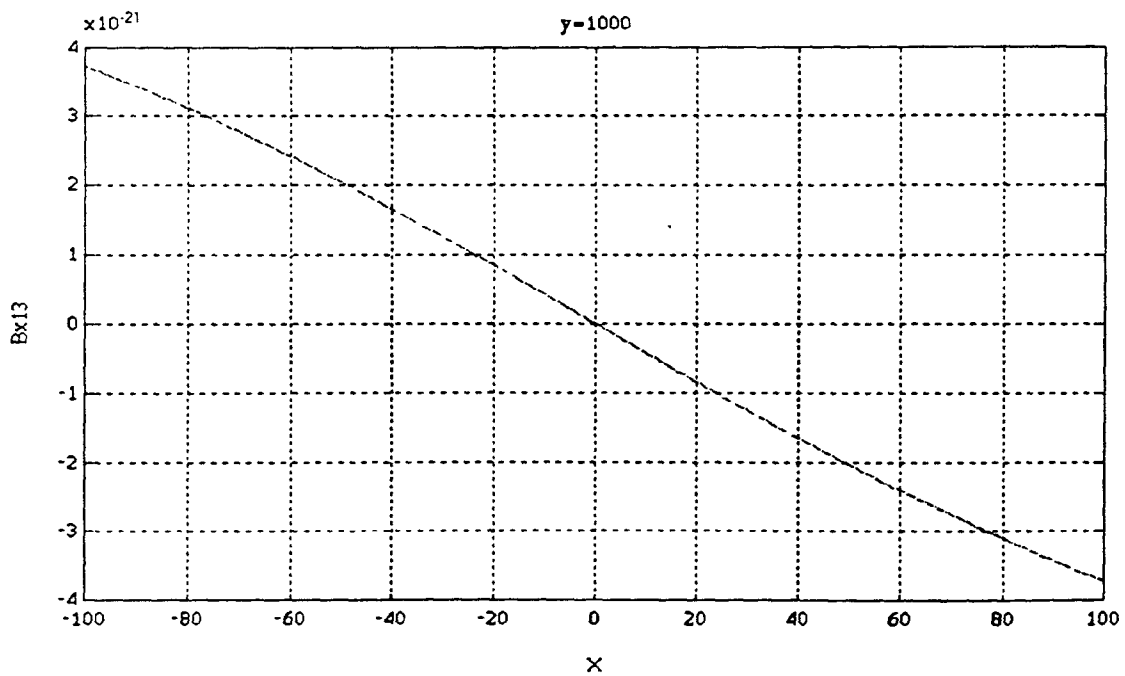


Figure 4-24a Axial component of induced magnetic field 3,  $y=1000$ ,  $-100 < x < 100$

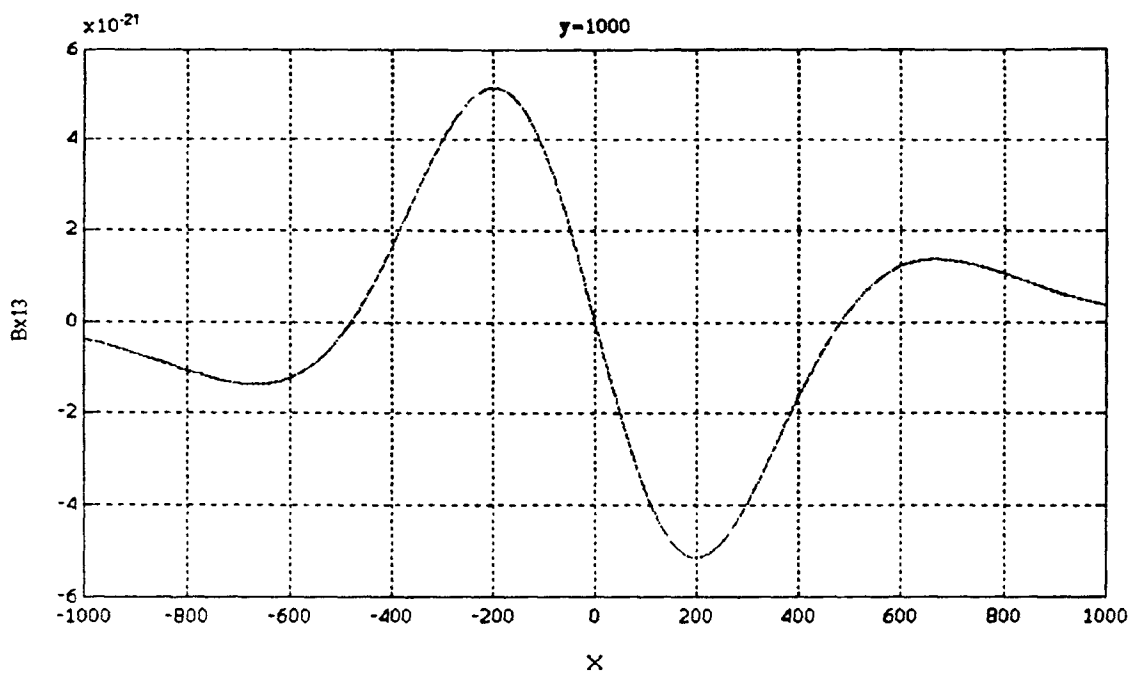


Figure 4-24b Axial component of induced magnetic field 3,  $y=1000$ ,  $-1000 < x < 1000$

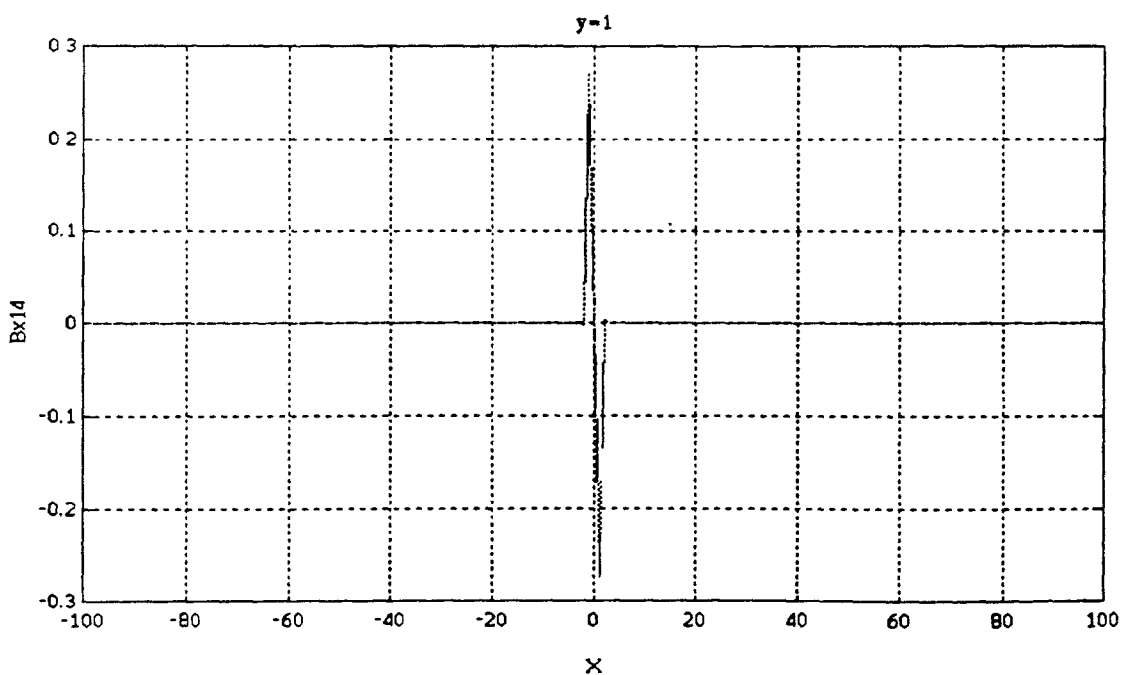


Figure 4-25a Axial component of induced magnetic field 4,  $y=1$ ,  $-100 < x < 100$

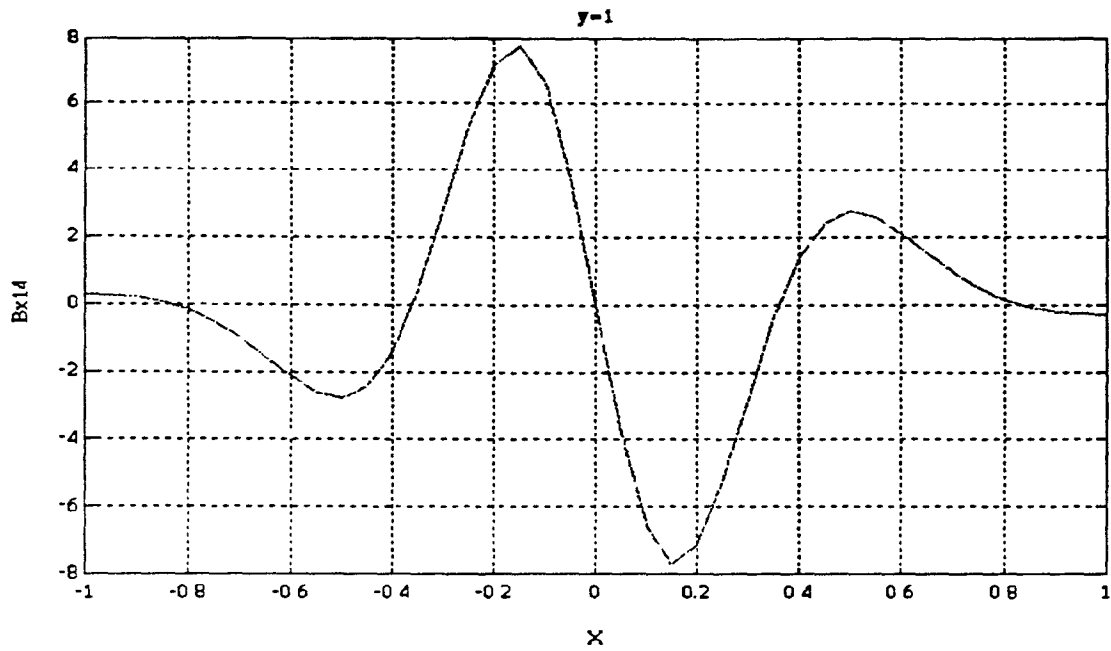


Figure 4-25b Axial component of induced magnetic field 4,  $y=1$ ,  $-1 < x < 1$

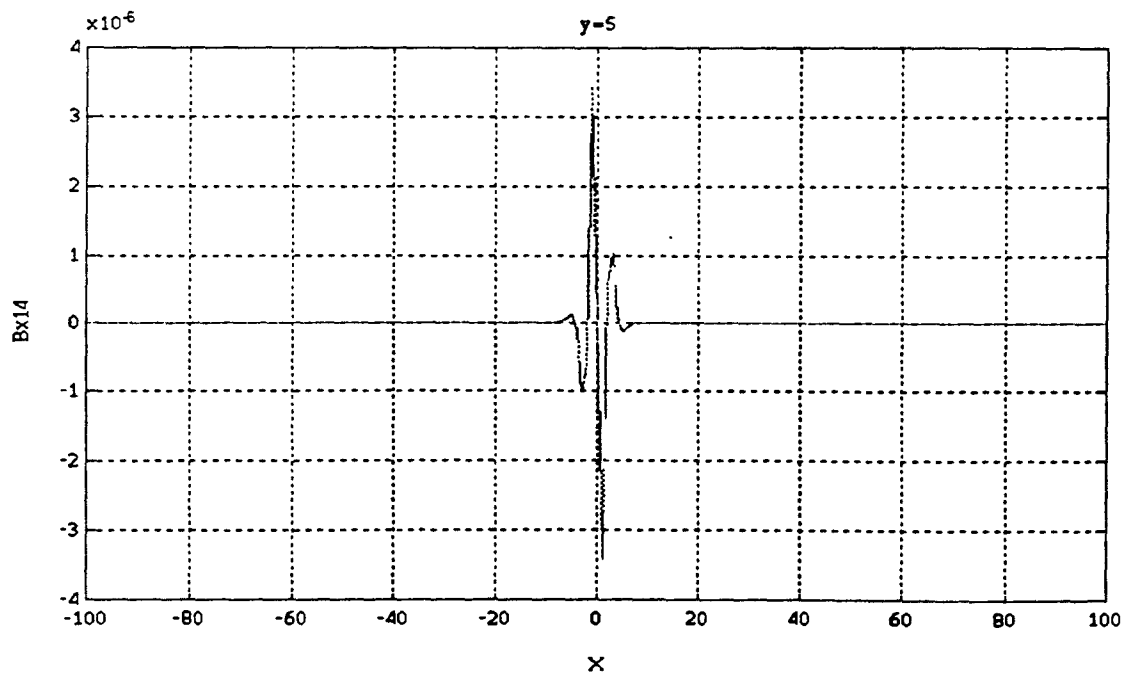


Figure 4-26a Axial component of induced magnetic field 4,  $y=5$ ,  $-100 < x < 100$

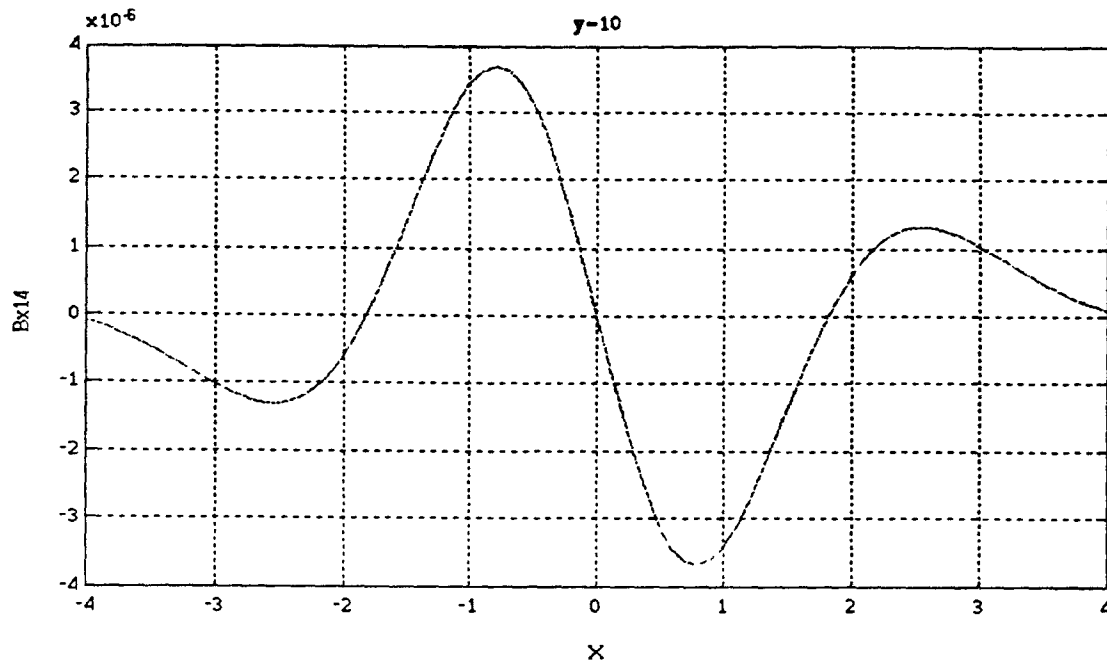


Figure 4-26b Axial component of induced magnetic field 4,  $y=5$ ,  $-4 < x < 4$

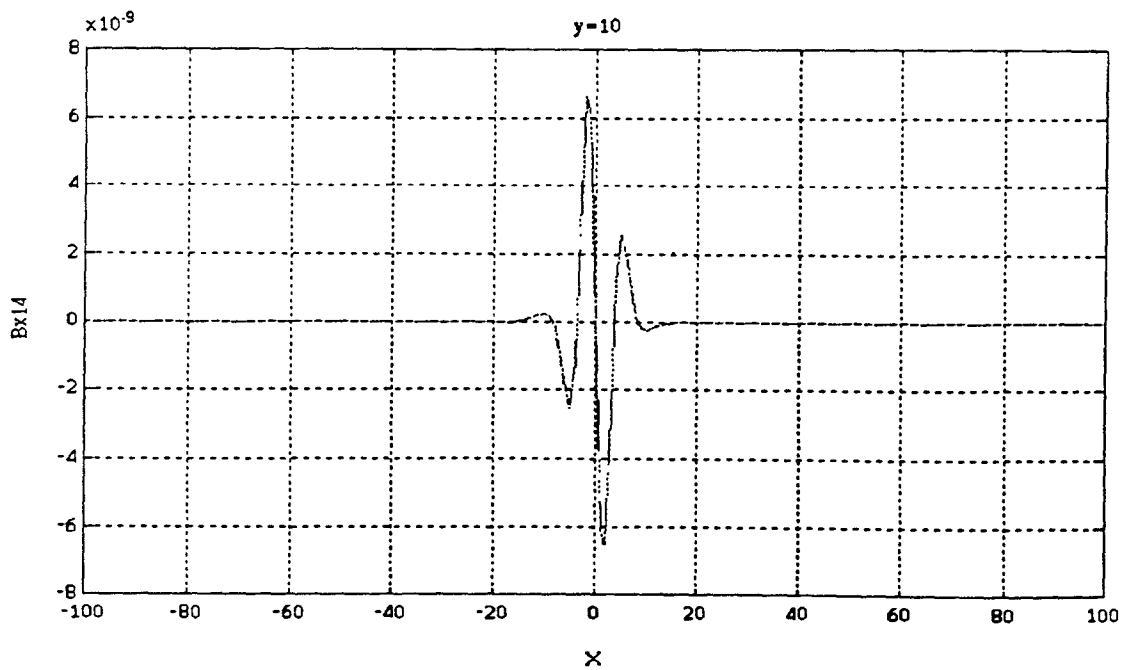


Figure 4-27a Axial component of induced magnetic field 4,  $y=10$ ,  $-100 < x < 100$

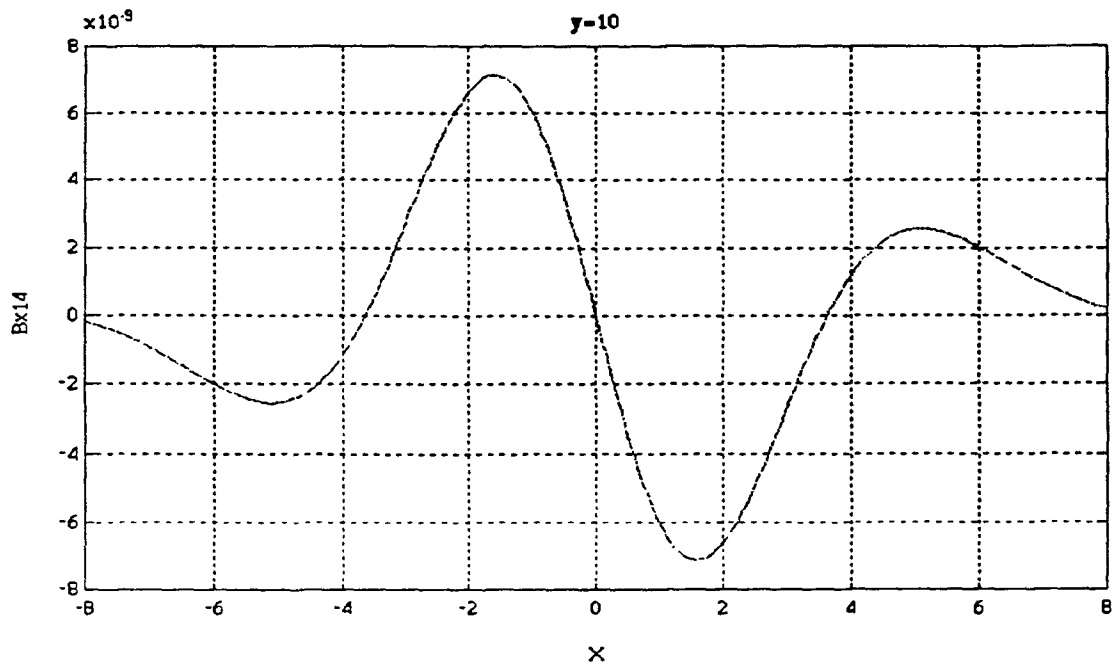


Figure 4-27b Axial component of induced magnetic field 4,  $y=10$ ,  $-8 < x < 8$

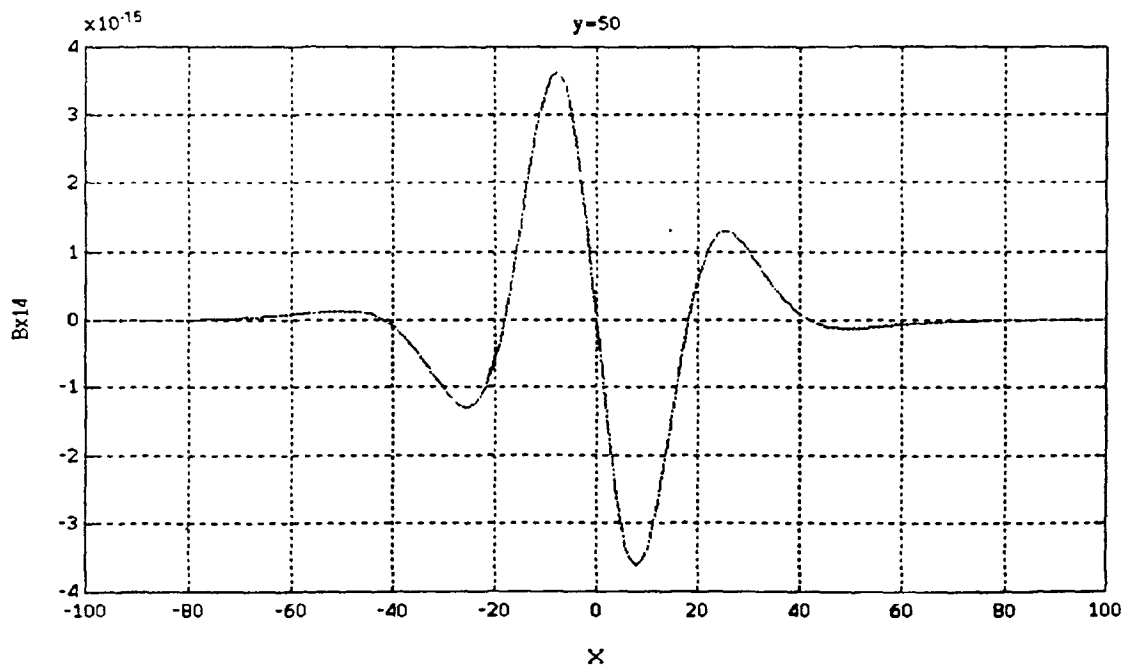


Figure 4-28a Axial component of induced magnetic field 4,  $y=50$ ,  $-100 < x < 100$

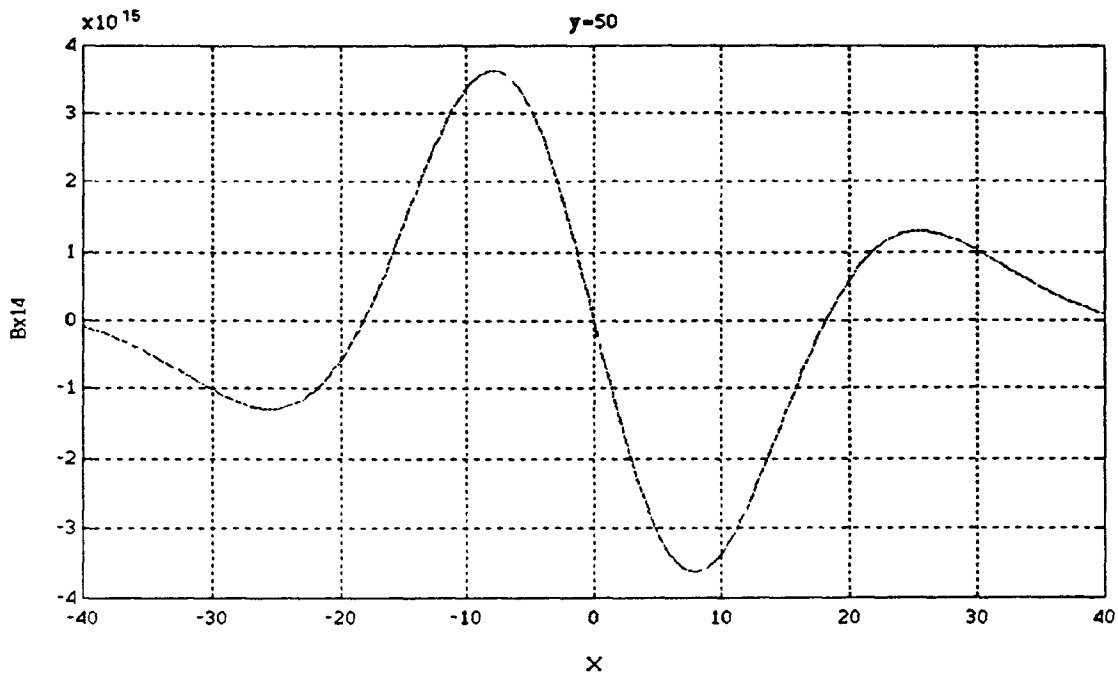


Figure 4-28b Axial component of induced magnetic field 4,  $y=50$ ,  $-40 < x < 40$

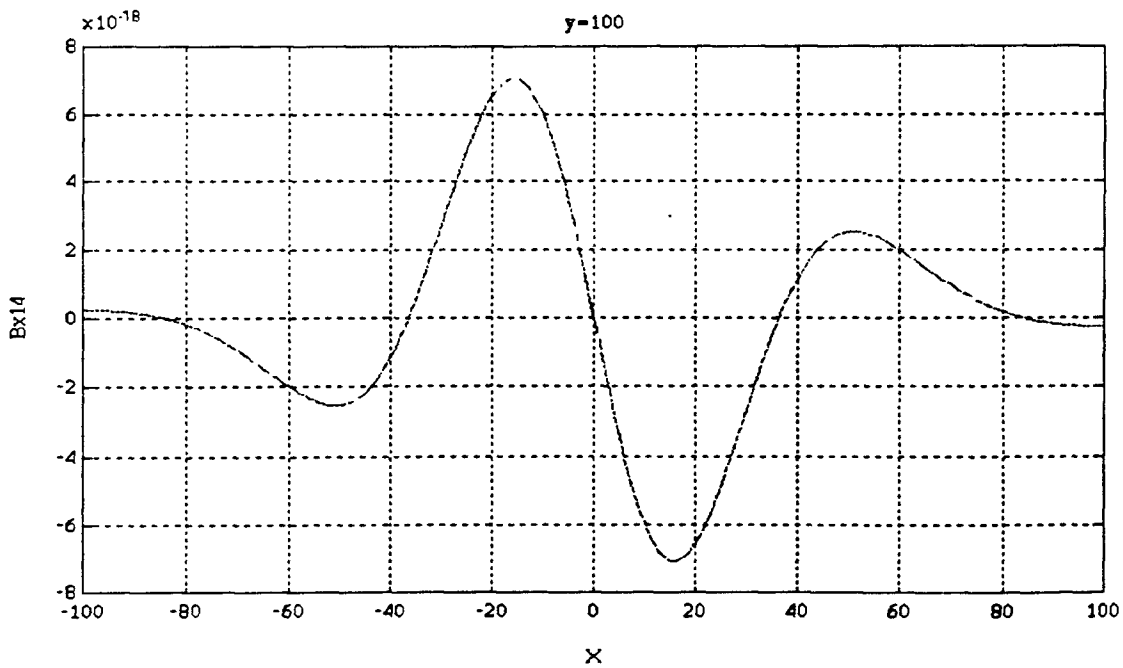


Figure 4-29a Axial component of induced magnetic field 4,  $y=100$ ,  $-100 < x < 100$

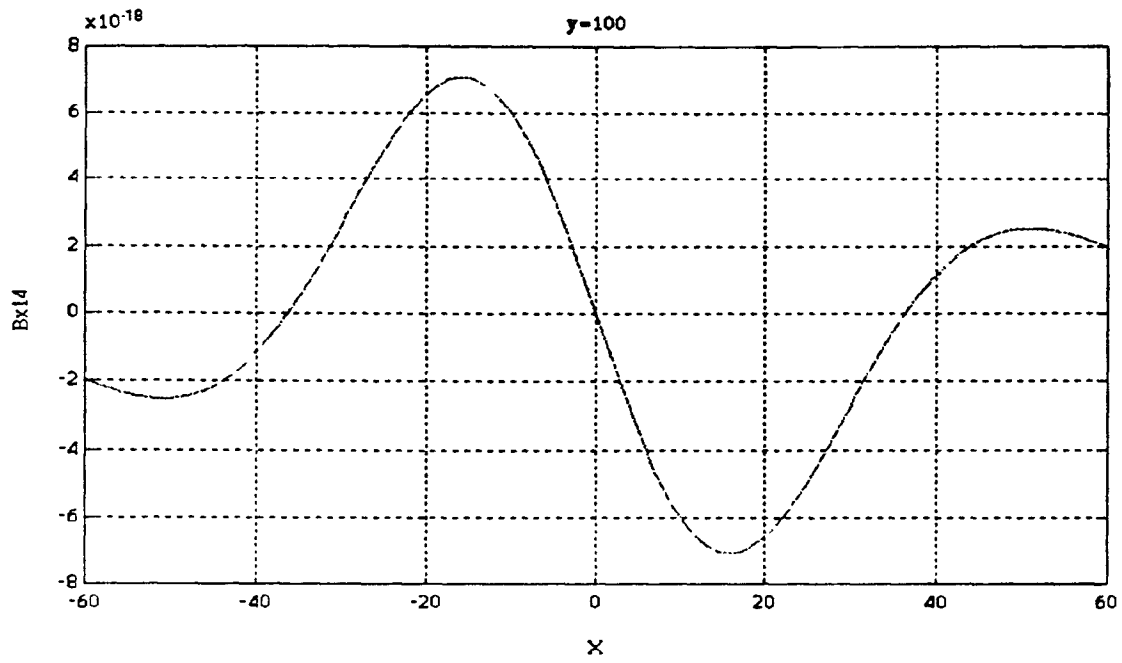


Figure 4-29b Axial component of induced magnetic field 4,  $y=100$ ,  $-60 < x < 60$

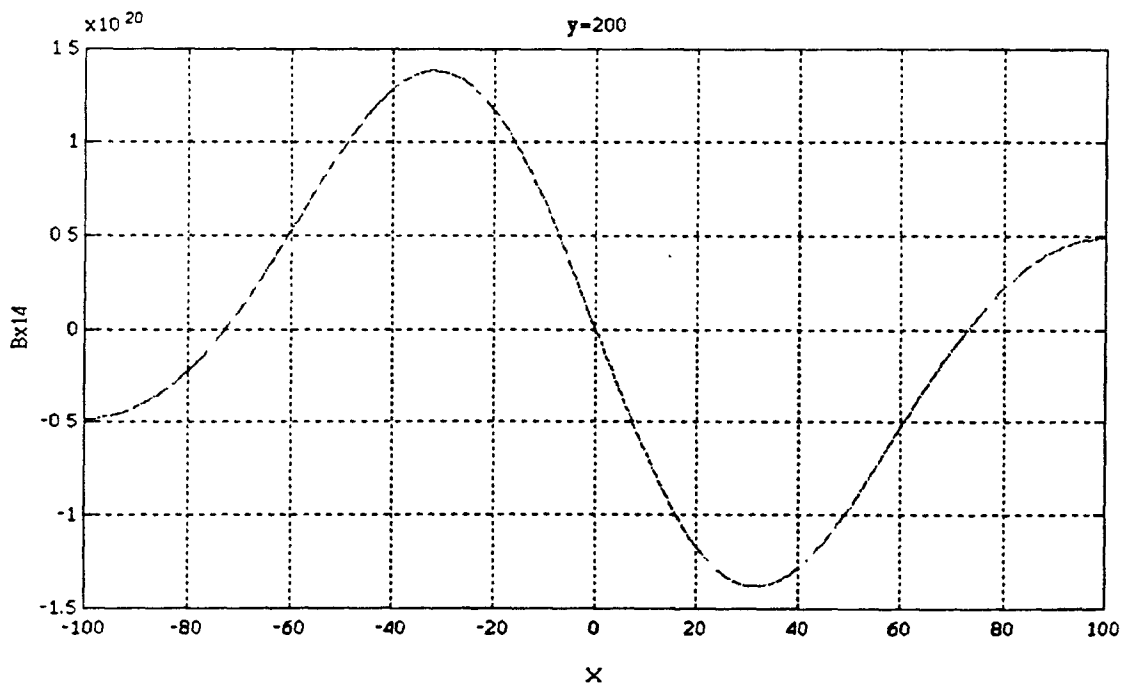


Figure 4-30a Axial component of induced magnetic field 4,  $y=200$ ,  $-100 < x < 100$



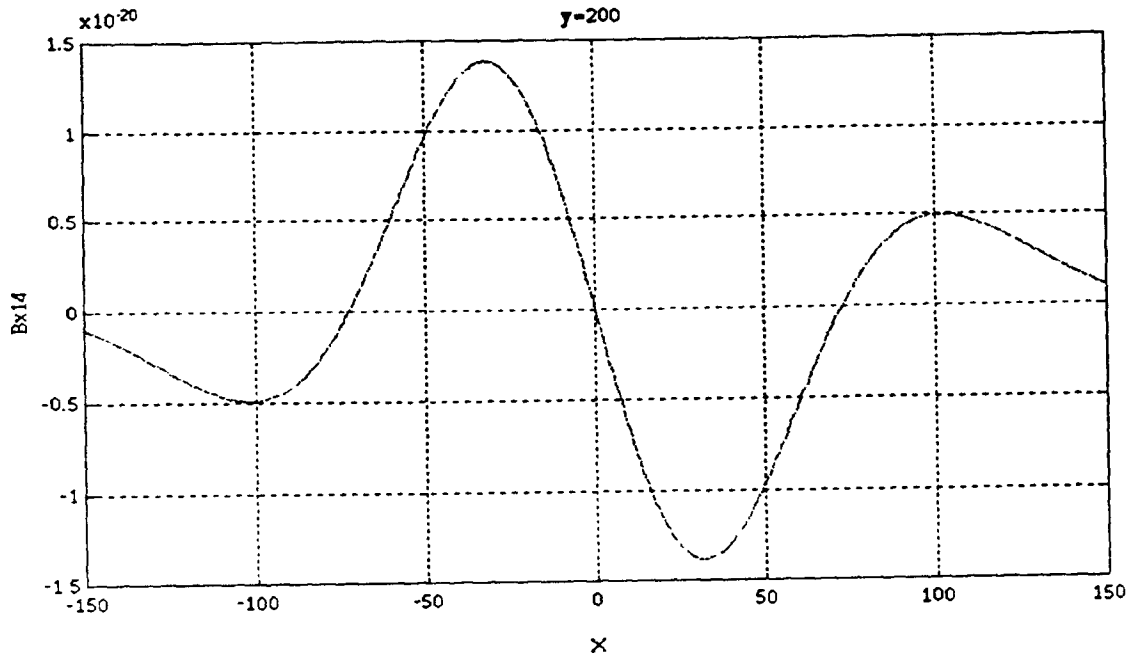


Figure 4-30b Axial component of induced magnetic field 4,  $y=200$ ,  $-150 < x < 150$

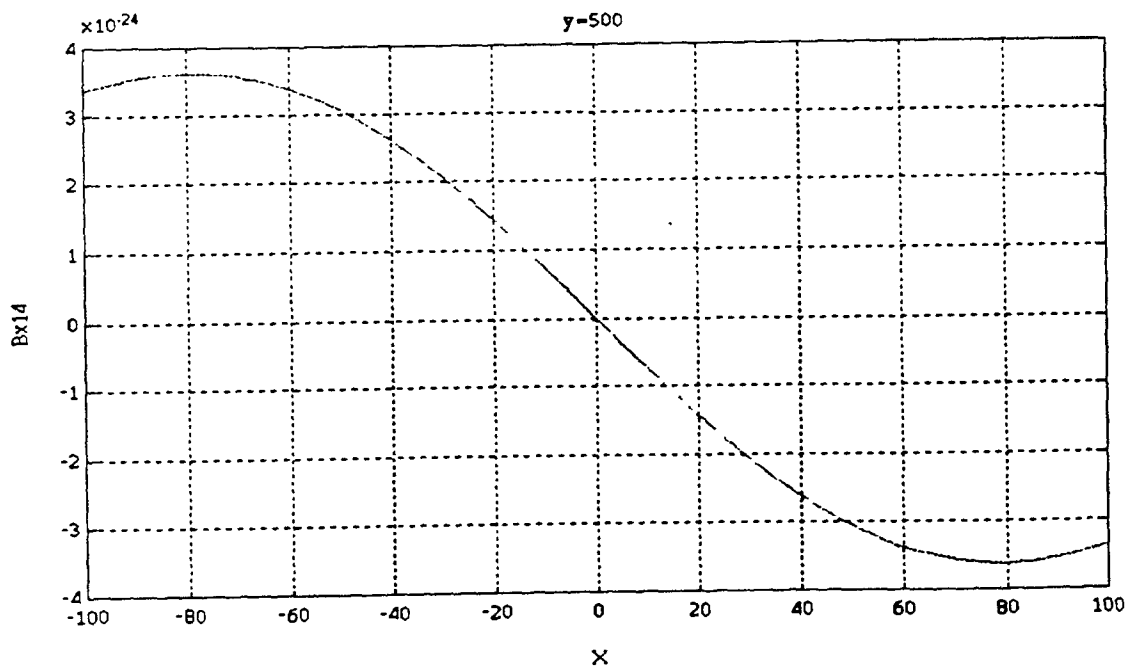


Figure 4-31a Axial component of induced magnetic field 4,  $y=500$ ,  $-100 < x < 100$

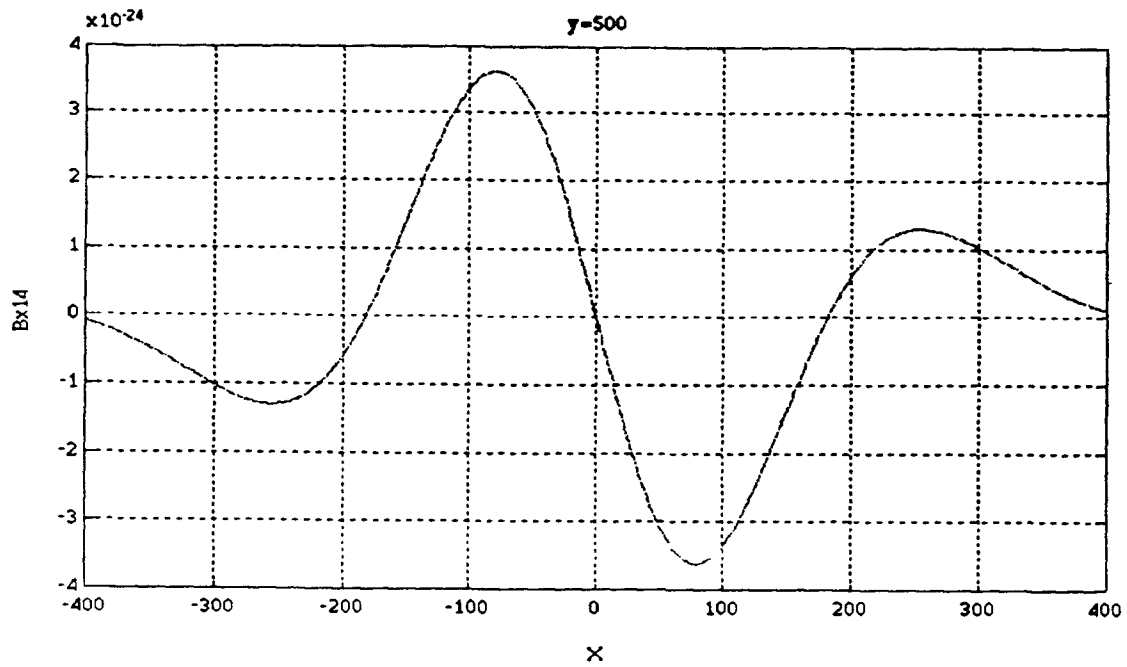


Figure 4-31b Axial component of induced magnetic field 4,  $y=500$ ,  $-400 < x < 400$

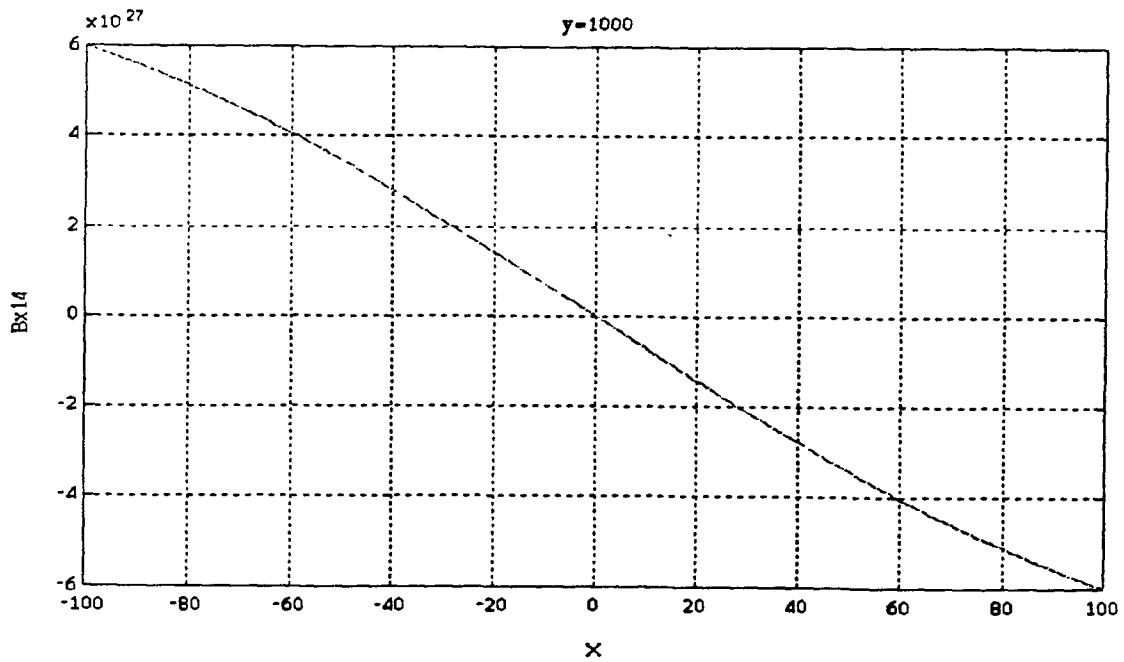


Figure 4-32a Axial component of induced magnetic field 4,  $y=1000$ ,  $-100 < x < 100$

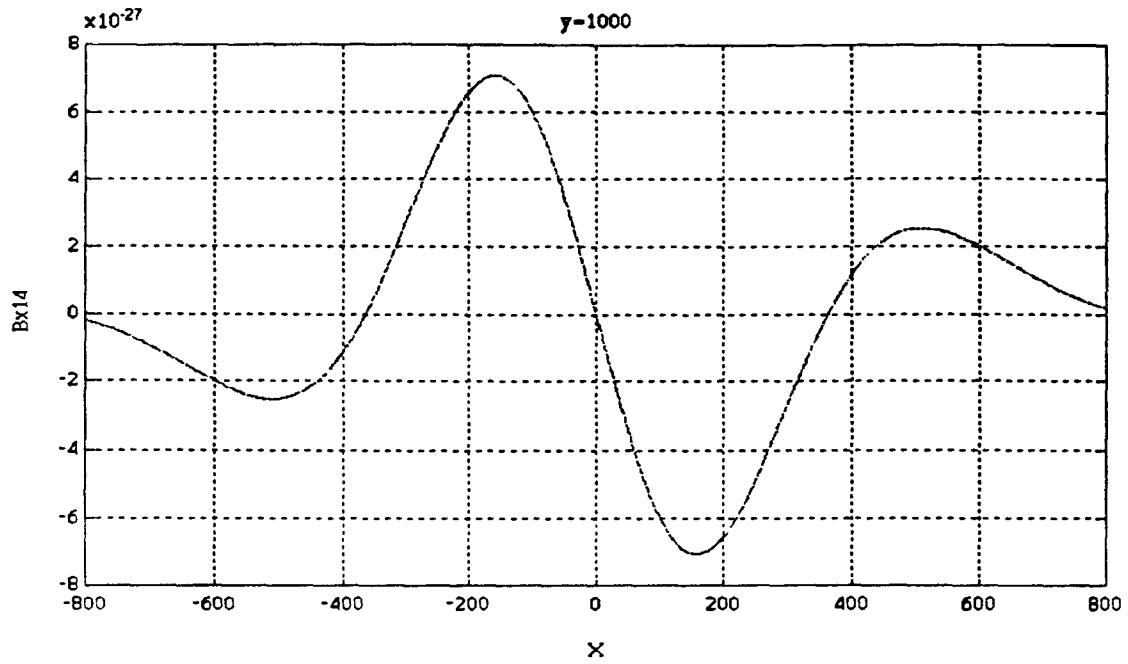


Figure 4-32b Axial component of induced magnetic field 4,  $y=1000$ ,  $-800 < x < 800$

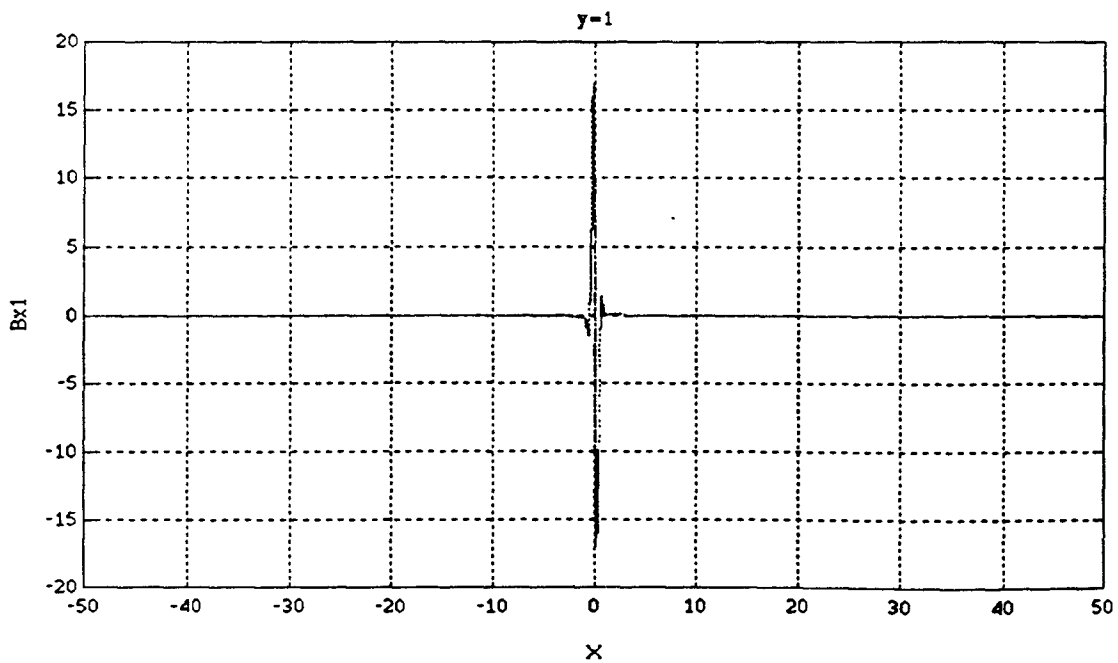


Figure 4-33a Axial component of total induced magnetic field,  $y=1$ ,  $-50 < x < 50$

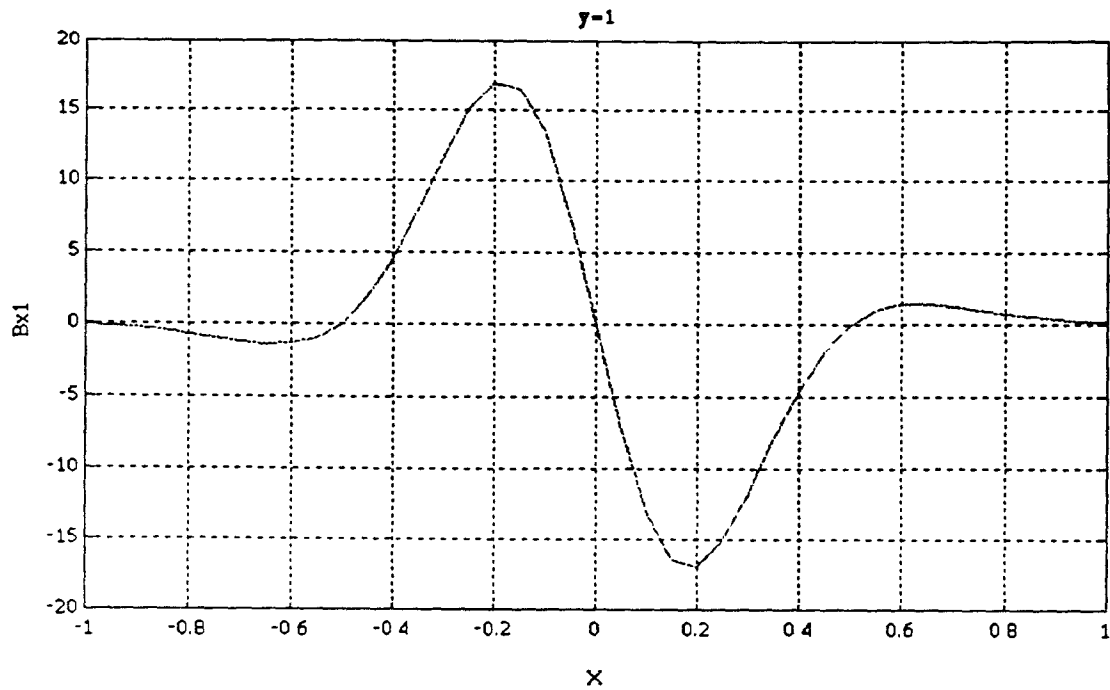


Figure 4-33b Axial component of total induced magnetic field,  $y=1$ ,  $-50 < x < 50$

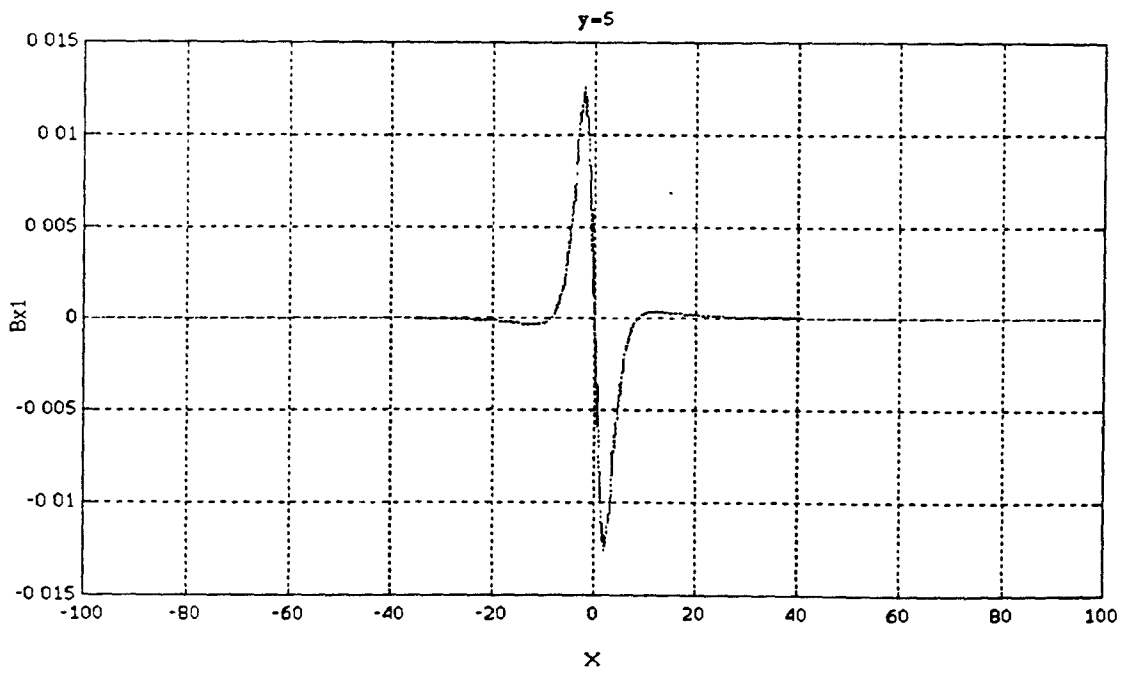


Figure 4-34a Axial component of total induced magnetic field,  $y=5$ ,  $-100 < x < 100$

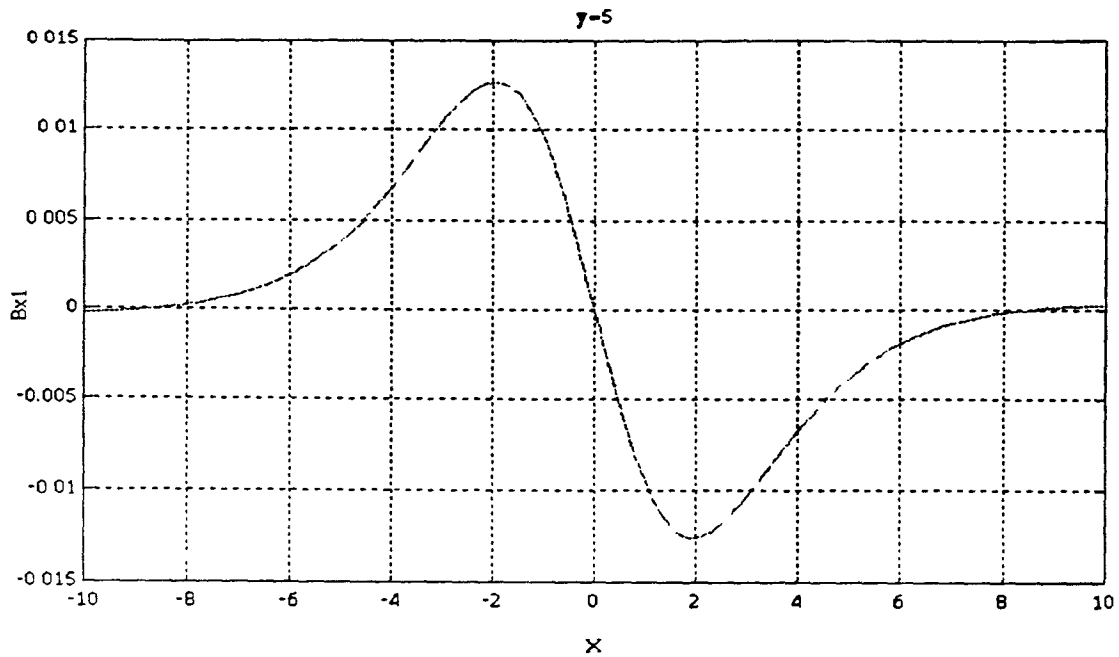


Figure 4-34b Axial component of total induced magnetic field,  $y=5$ ,  $-10 < x < 10$

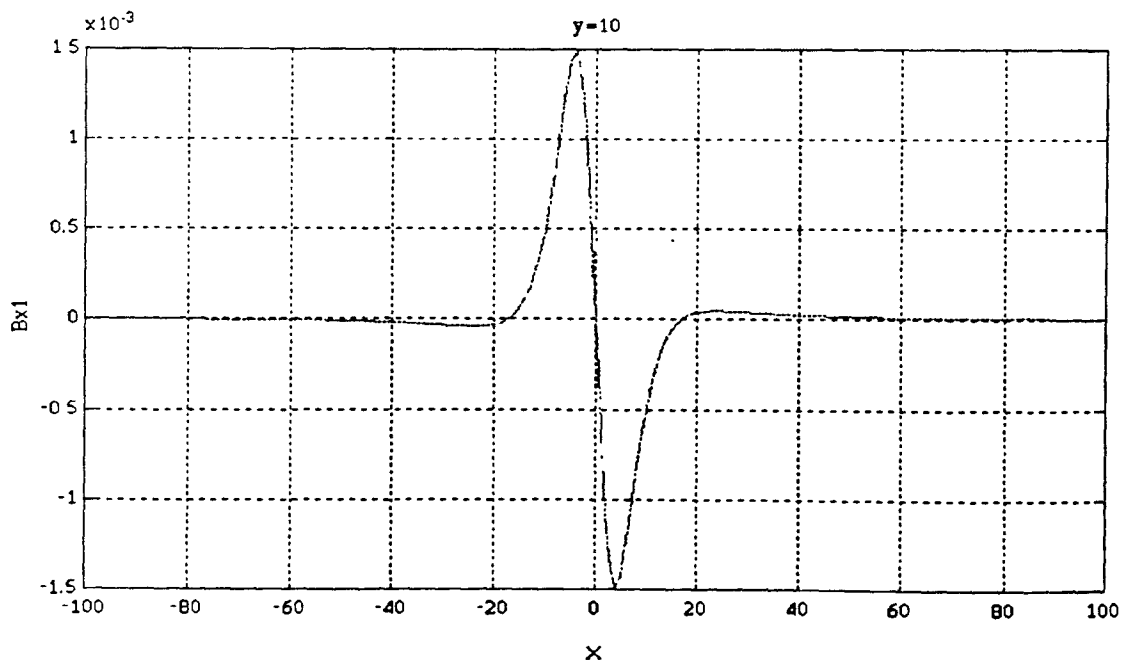


Figure 4-35a Axial component of total induced magnetic field,  $y=10$ ,  $-100 < x < 100$

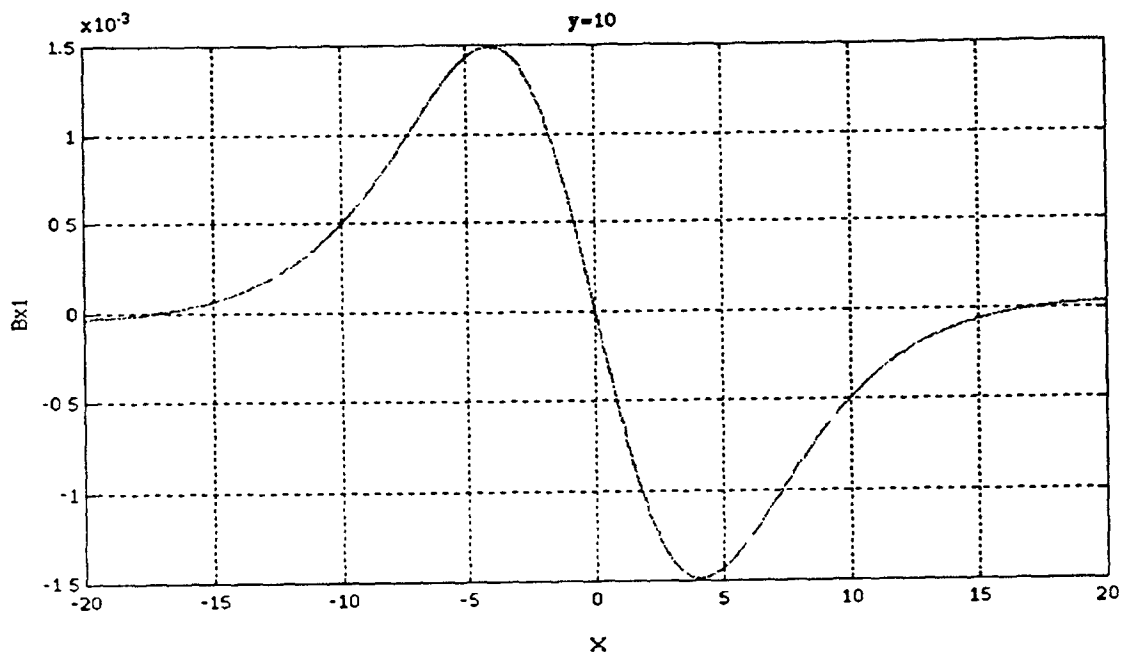


Figure 4-35b Axial component of total induced magnetic field,  $y=10$ ,  $-20 < x < 20$

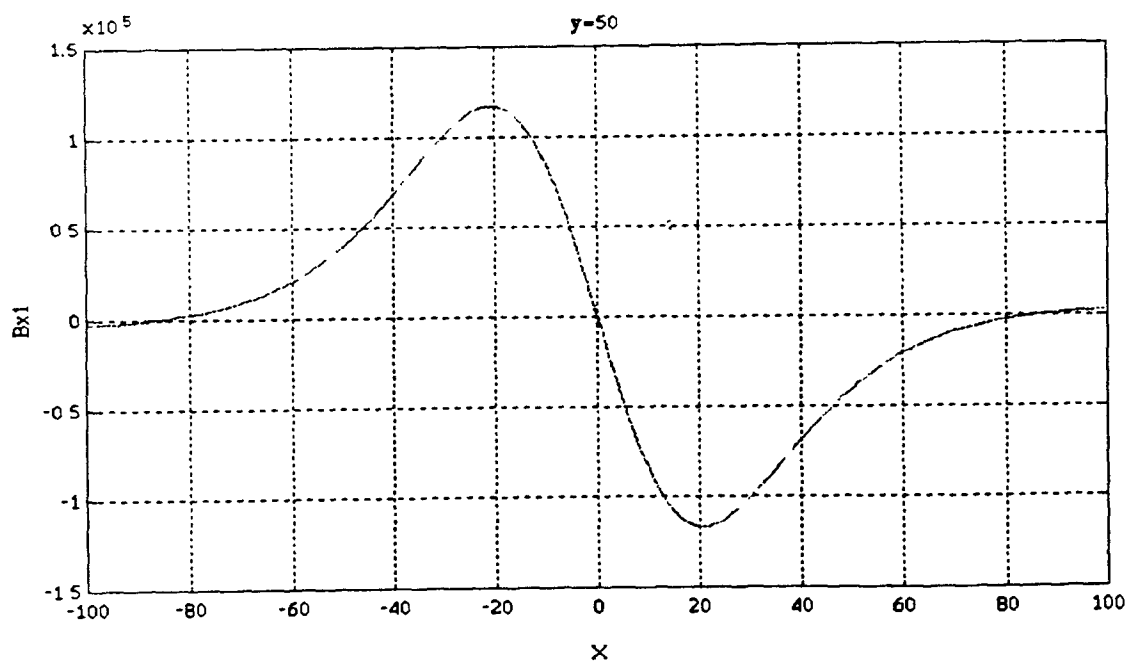


Figure 4-36 Axial component of total induced magnetic field,  $y=50$ ,  $-100 < x < 100$

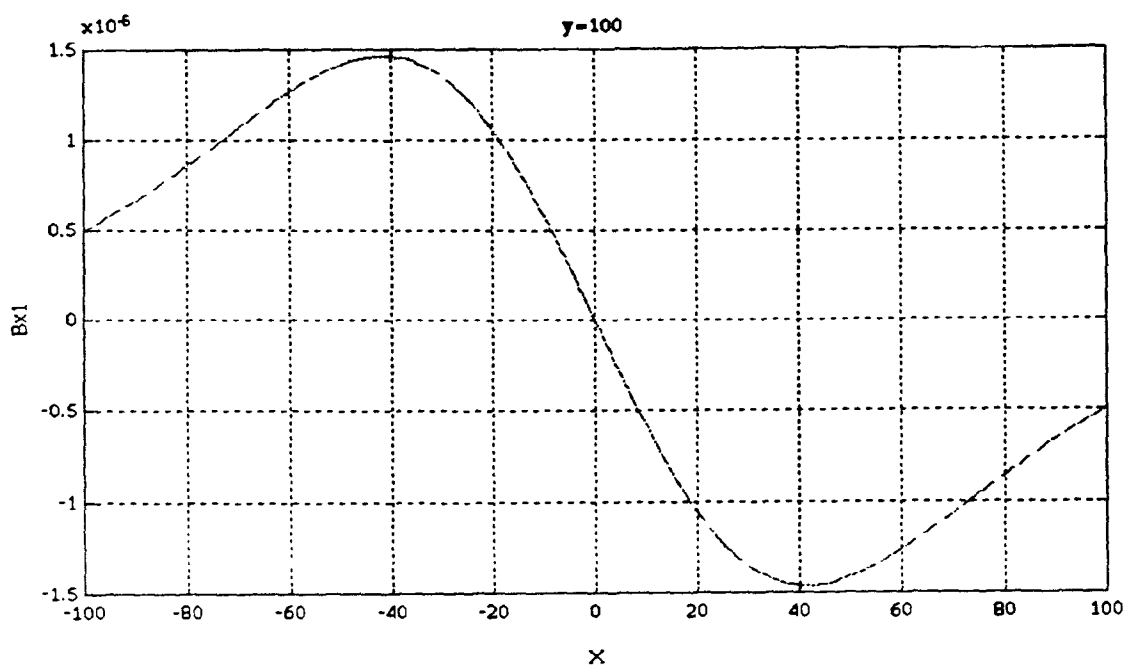


Figure 4-37a Axial component of total induced magnetic field,  $y=100$ ,  $-100 < x < 100$

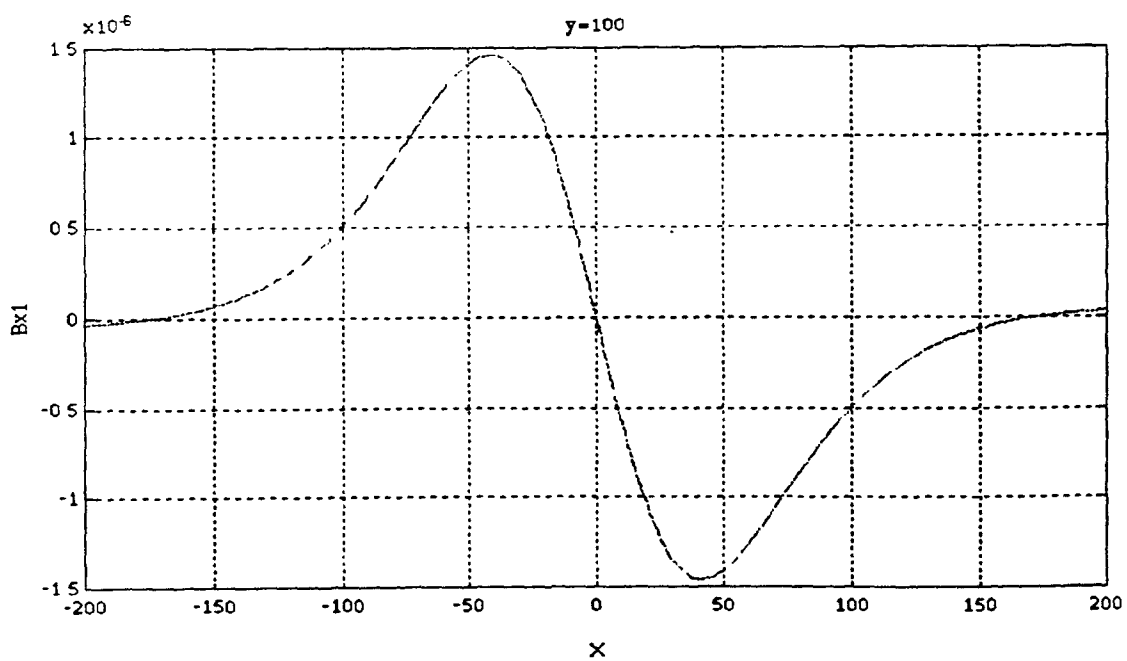


Figure 4-37b Axial component of total induced magnetic field,  $y=100$ ,  $-200 < x < 200$

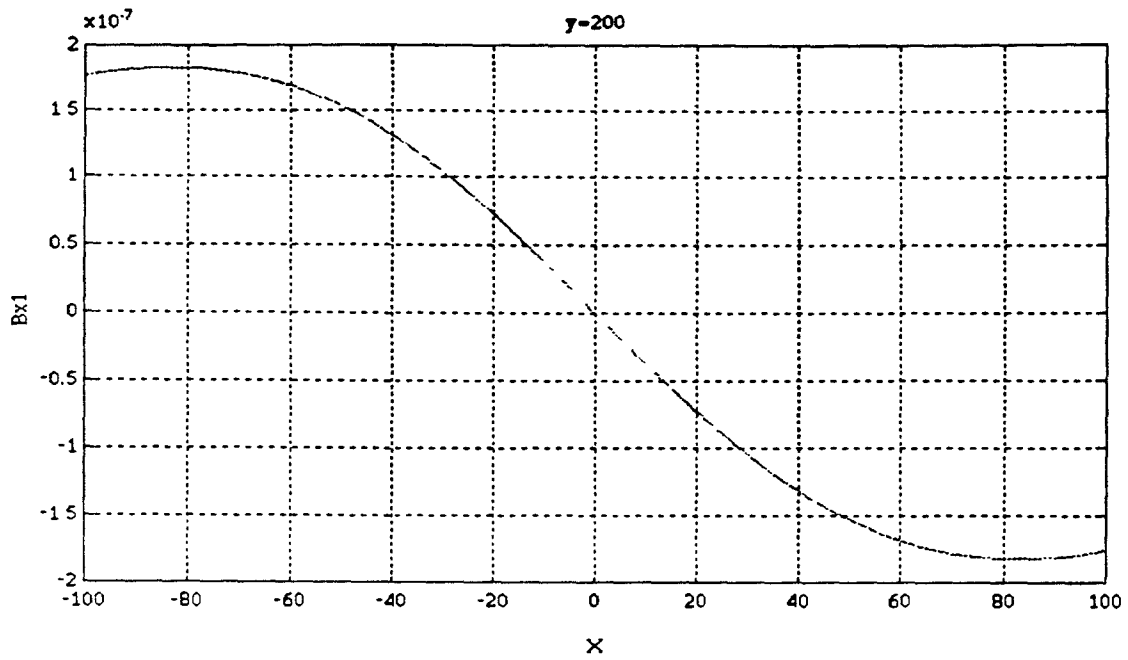


Figure 4-38a Axial component of total induced magnetic field,  $y=200$ ,  $-100 < x < 100$

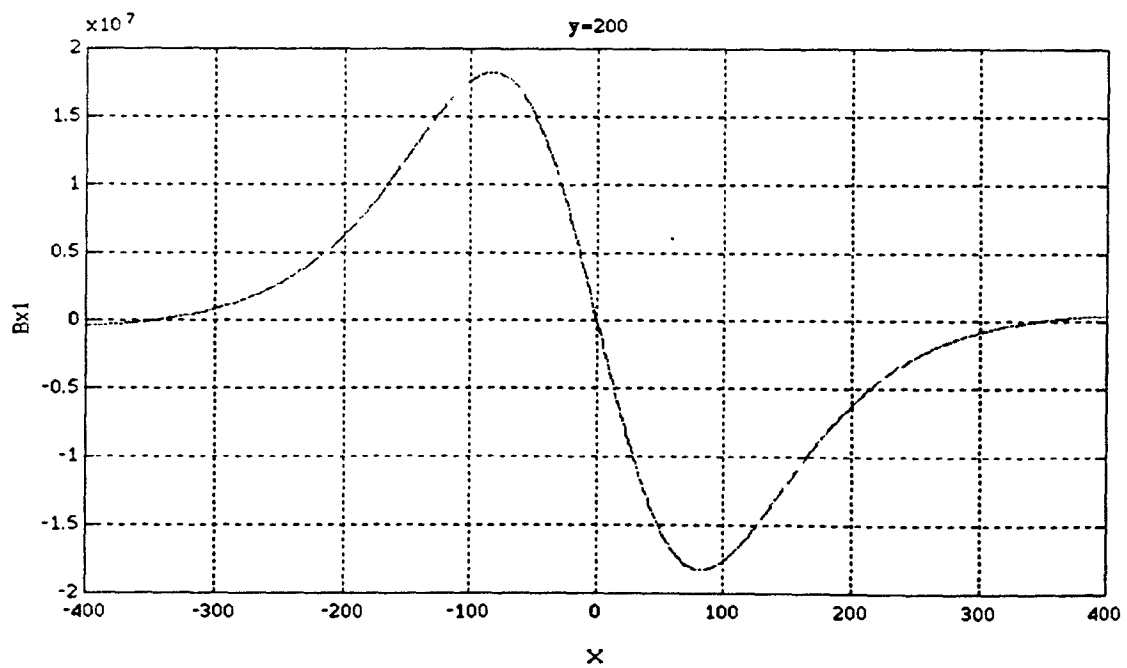


Figure 4-38b Axial component of total induced magnetic field,  $y=200$ ,  $-400 < x < 400$



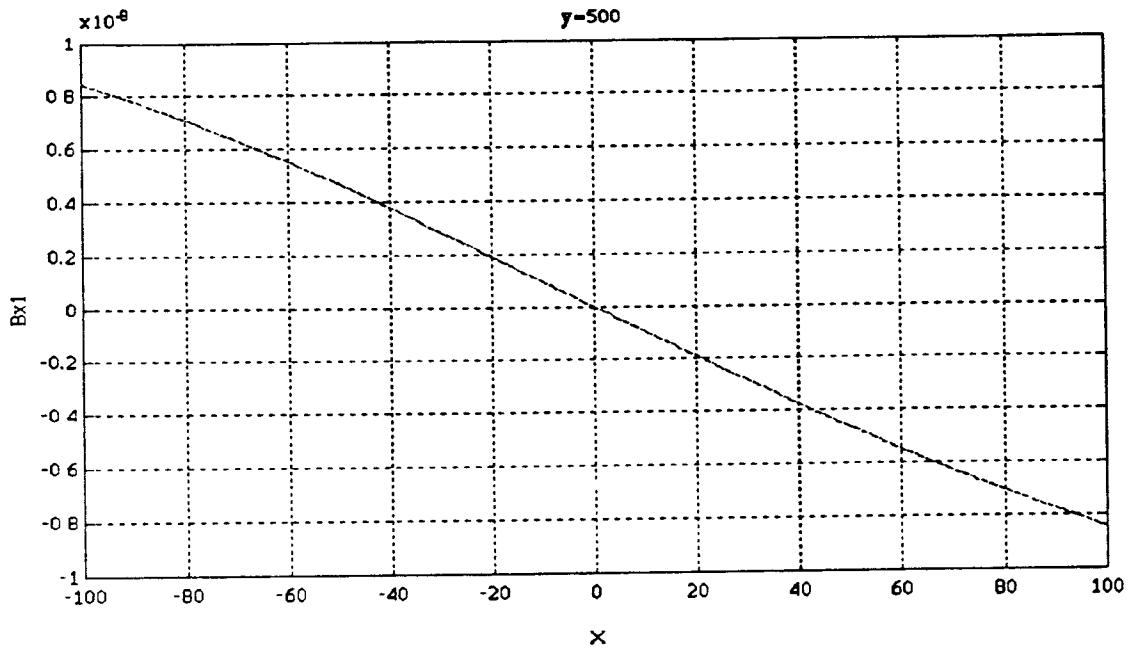


Figure 4-39a Axial component of total induced magnetic field,  $y=500$ ,  $-100 < x < 100$

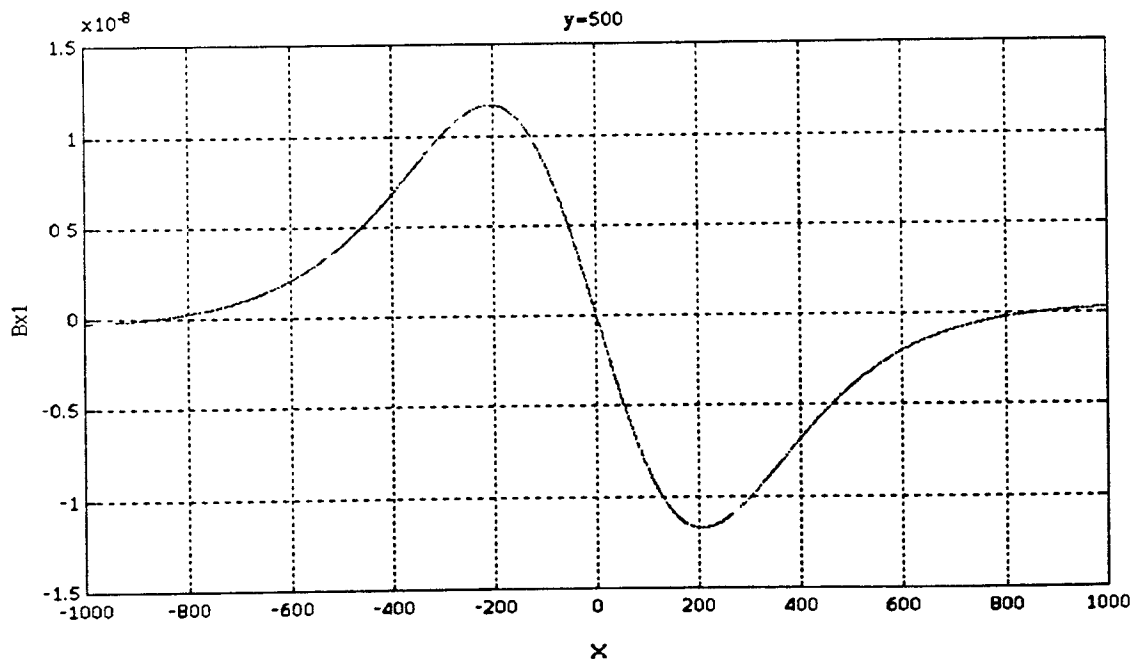


Figure 4-39b Axial component of total induced magnetic field,  $y=500$ ,  $-1000 < x < 1000$

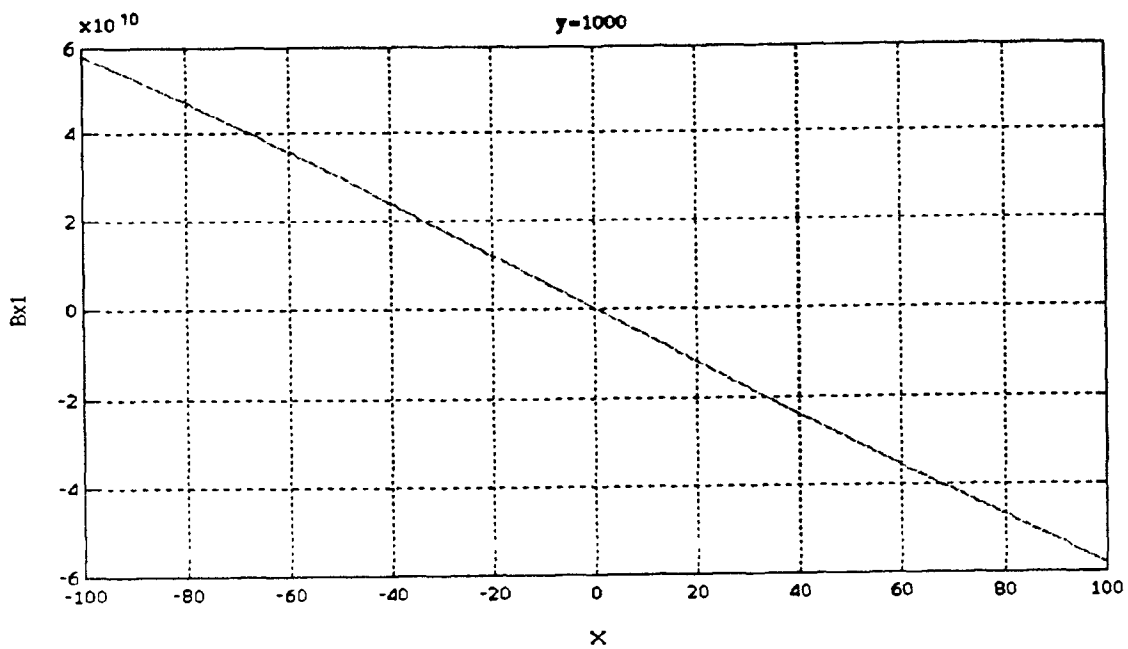


Figure 4-40a Axial component of total induced magnetic field,  
 $y=1000$ ,  $-100 < x < 100$

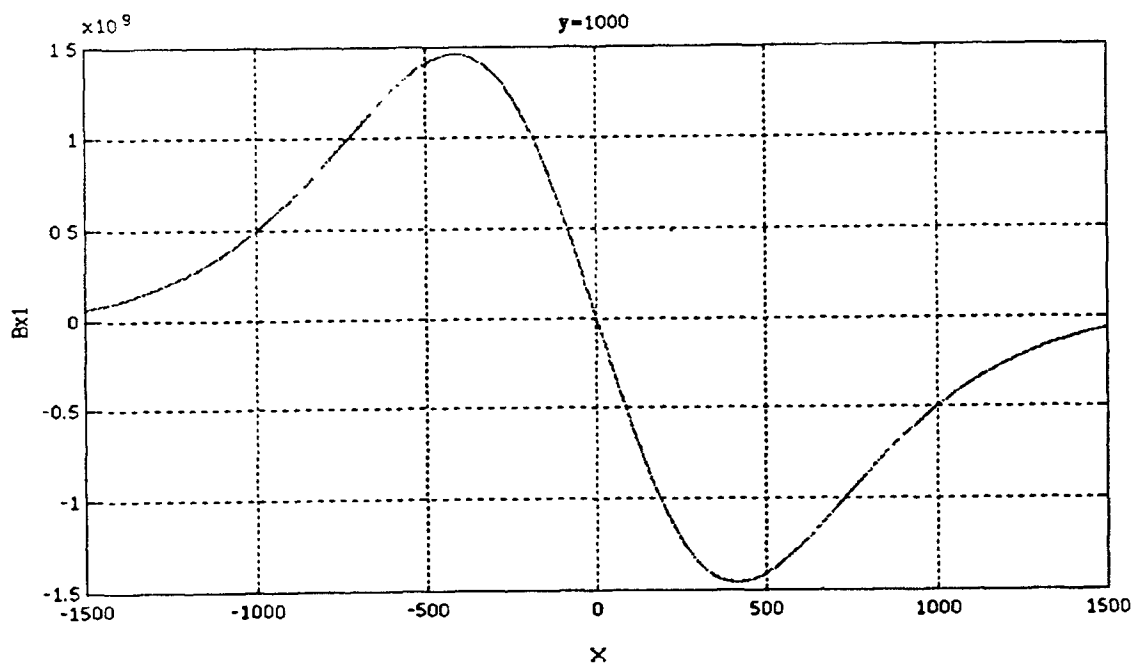


Figure 4-40b Axial component of total induced magnetic field,  
 $y=1000$ ,  $-1500 < x < 1500$

Missing Page